MECHANISTIC EVALUATION OF GRANULAR BASE STABILIZATION SYSTEMS IN SASKATCHEWAN

A Thesis Submitted to the College of
Graduate Studies and Research
In Partial Fulfillment of the Requirements
For the Degree of Master of Science
in the Department of Civil and Geological Engineering
University of Saskatchewan
Saskatoon

By
Jing Xu

PERMISSION TO USE

In presenting this thesis in partial fulfillment of the requirements for a Postgraduate degree from the University of Saskatchewan, the author has agreed that the Libraries of this University may make it freely available for inspection. The author has further agreed that permission for copying of this thesis in any manner, in whole or in part, for scholarly purposes may be granted by the professor or professors who supervised the thesis work or, in their absence, by the Head of the Department or the Dean of the College in which the thesis work was done. It is understood that any copying, publication, or use of this thesis or parts thereof for financial gain shall not be allowed without the author's written permission. It is also understood that due recognition shall be given to the author and to the University of Saskatchewan in any scholarly use which may be made of any material in this thesis.

Requests for permission to copy or to make other use of material in this thesis in whole or part should be addressed to:

Head of the Department of Civil Engineering

University of Saskatchewan

Saskatoon, Saskatchewan S7N 5A9

ABSTRACT

Saskatchewan Ministry of Highways and Infrastructure (MHI) is responsible for maintaining approximately 26,100 km of two lane equivalent highways network. Most highways in Saskatchewan are constructed primarily of granular materials. Granular materials serve various purposes in a pavement structure. In particular, granular materials distribute stress within the road structure and reduce the stress applied to the subgrade. Granular materials also mitigate pumping of subgrade fines into surfacing materials, as well as provide drainage for the pavement structure.

As a result of the rapid deterioration of roadways and the increasing highway traffic, a significant portion of the Saskatchewan highway system is in need of rehabilitation in the next couple of decades. However, increasing costs associated with road construction as well as budget constraints render many conventional rehabilitation solutions untenable in many applications. In addition, the depletion of quality aggregate also exists in many areas of Saskatchewan. Given that much of Saskatchewan granular pavement system will be in need of strengthening in the next few decades, there is a need to apply new cost-effective and aggregate-preserving pavement rehabilitation technologies such as cold in-place recycling and base strengthening.

The goal of this research is to improve the engineering design and performance of recycled and stabilized granular base systems under Saskatchewan field state conditions. The specific objectives of this research are to characterize the conventional laboratory behaviour, moisture sensitivity, and mechanistic behaviour of various granular base strengthening systems in the laboratory, to characterize the structural responses of various granular base strengthening systems in the field, and to evaluate the pavement thickness design and responses of various granular base pavement structures.

This research is based on a cold in-place recycling and base stabilization project undertaken by Saskatchewan MHI in fall 2006. Control Section (C.S.) 15-11 between km 5.0 and km 8.0 was selected as a typical thin granular pavement under primary weight loadings that required strengthening. Unstabilized granular base, cement stabilized

granular base, and cement with asphalt emulsion stabilized granular base were constructed and evaluated in this research.

Materials employed on C.S. 15-11 were sampled and prepared for the various laboratory tests performed in this research. Conventional tests performed included sieve analysis, Atterberg limits, sand equivalent, standard proctor compaction, and California bearing ratio strength and swell test. Advanced mechanistic and moisture sensitivity testing included indirect tensile strength, moisture capillary rise and surface conductivity, unconfined compressive strength, and rapid triaxial frequency sweep testing.

The cement and cement with emulsion asphalt stabilization of the granular base were found to improve the conventional, mechanical and moisture susceptibility properties of *in situ* C.S. 15-11 granular base materials. The cement stabilization applied on C.S. 15-11 provided a high degree of improvement relative to the cement with emulsion stabilization. The cement stabilization was found to be relatively easy to apply in construction, whereas the cement with emulsion stabilization was more difficult, particularly due to the problems associated with cold temperatures during late season construction.

The rapid triaxial tester (RaTT) was found to be a practical and useful apparatus to characterize the mechanistic constitutive behaviours of granular materials. The C.S. 15-11 *in situ* unstabilized base was found to have the poorest mechanistic behaviour among all three granular bases on C.S. 15-11, as expected. Cement stabilization improved the mechanistic behaviour of the *in situ* material significantly by providing the highest mean dynamic modulus, lowest mean Poisson's ratio, lowest mean radial microstrain, and the lowest mean phase angle. The cement with emulsion asphalt stabilization also provided a considerable improvement on mechanistic behaviour of C.S. 15-11 granular base materials. However, the degree of improvement was less than the cement stabilization system.

Non-destructive falling weight deflection measurements taken across the field test sections showed that the stabilization systems yielded a significant improvement of primary structural response profiles across the C.S. 15-11 test sections after stabilization. The cement stabilization system was found to yield the most significant structural

improvements among all the test sections constructed on the C.S. 15-11. The deflection measurements taken in 2007 after hot mix asphalt paving further identified that the unstabilized system is more sensitive to the freeze-thaw effects relative to cement stabilization and cement with emulsion stabilization systems.

This research also showed that the Saskatchewan MHI structural design system is not applicable to the design of stabilized granular base systems. Evaluation of the thickness design for C.S. 15-11 showed the unstabilized and the cement with asphalt emulsion stabilized test section met the criterion of fatigue cracking, but failed to meet the criterion of structural rutting in MHI design system. However, the cement stabilized section met both fatigue cracking and rutting criteria. The structural evaluation revealed that mechanistic pavement response analysis and validation are necessary in the thickness design of stabilized granular systems such as C.S. 15-11, where traditional MHI design system is not applicable.

This research employed finite element modeling and linear elastic pavement modeling software to determine the maximum shear stresses within granular base under typical Saskatchewan stress state conditions. The maximum shear stress values were found to locate on top of granular base courses under the applied circular loading edges ranging from 177 kPa to 254 kPa. These maximum shear stresses within the C.S. 15-11 test section granular base courses under field stress states were compared to maximum shear stresses occurring within samples measured by rapid triaxial testing performed in this research. The comparison showed that the ranges of shear stresses applied in the laboratory RaTT testing were close to shear stresses of granular bases in the field computed from modeling. Therefore, this research showed a good correlation of lab RaTT testing and field results for granular pavements.

In summary, this research met the objectives of mechanistically evaluating various granular base stabilization systems in Saskatchewan by means of various laboratory testing, non-destructive field testing, as well as mechanistic modeling and analysis. This research provided valuable data and showed considerable potential for improving design, construction, and QA/QC of conventional and stabilized granular base systems in Saskatchewan.

ACKNOWLEDGEMENTS

I gratefully wish to thank Dr. Curtis F. Berthelot for his guidance and support throughout my Master's program. He not only inspires me with his teaching but also sets an example of what an excellent civil engineer should be with his personality, hard work and discipline.

I also wish to thank my committee members: Dr. Dennis E. Pufahl, Dr. Leon Wegner, and Dr. Ian Fleming for their time and input into my program.

Thanks should also be given to Mr. Brent Marjerison for his encouragement and mentorship in pavement material class and throughout my Master's program.

I would like to give my sincere thanks to Mr. Allan Widger and Mrs. Darlene Cleven for their love, friendship and encouragement as I pursued my degree.

I also would like to thank Dr. Gordon Sparks, Dr. Jit Sharma, Dr. Lal Samarasekera, Mr. Joseph Chan, Ms. Debbie Forgie, Ms. Pella LeDrew, Mr. Alex Kozolow, Mr. Aziz Salifu, Ms. Ania Anthony, Ms. Diana Podborochynski, Mr. Kaki Fung for their help in my study. Due to limited space, I could not include all the names. However, I would like to thank my friends, especially those who have helped me during my study in Canada.

Acknowledgement is also given to the Civil and Geological Engineering Department and Saskatchewan Ministry of Highways and Infrastructure for the financial support.

Finally, I would especially like to specially thank my father Chengguo Xu, my mother Zaixiang Gao and my wife Xuan Wang for their love and unconditional support.

TABLE OF CONTENTS

LIST OF FIGURES

LIST OF TABLES

LIST OF ABBREVIATIONS

AADT – Average Annual Daily Traffic
AAPT – Association of Asphalt Paving Technologists
AASHTO – American Association of Highway and Transportation Officials
AMOS – Asphalt Mat on Subgrade
ASTM – American Society for Testing and Materials
AI – Asphalt Institute
CV – Coefficient of Variance
ESAL – Equivalent Single Axle Load
HMAC – Hot Mix Asphalt Concrete
IDT – Indirect Tension Test
ITS – Indirect Tensile Strength
LVDT – Linear Variable Differential Transducer
NCHRP – National Cooperative Highway Research Program
PI – Plasticity Index
QA/QC – Quality Assurance/ Quality Control
RAMS – Recoverable Axial Microstrain
RRMS – Recoverable Radial Microstrain
RAP – Reclaimed Asphalt Pavement
RaTT – Rapid Triaxial Tester
MHI – Ministry of Highways and Infrastructure
SHRP – Strategic Highway Research Program
SST – Superpave™ shear tester
TFHRC – Turner-Fairbank Highway Research Center
TMS – Thin Membrane Surface
TRB – Transportation Research Board
UCCS – Unconfined Compression Strength Test
VFA – Voids Filled with Asphalt
VMA – Voids in the Mineral Aggregate
VTM – Voids in the Total Mix

CHAPTER 1 INTRODUCTION

Saskatchewan's growing economic development and transportation rationalization have resulted in significant increases in both the volumes and load spectra of commercial heavy trucks. These factors are resulting in a need for strengthening many Saskatchewan roads (Berthelot et al. 2000). In order to promote the development of the provincial economy, there is a need to improve the field performance of several thousand kilometres of granular base systems which would provide higher load bearing capacity, improved performance and longer expected life.

Although conventional granular road systems are technically feasible in many applications, conventional thin granular pavement rehabilitation can be very expensive and exhibit numerous shortcomings with regards to long term performance. From an economic perspective, conventional granular pavement rehabilitation costs have increased significantly over recent years due to rising construction input costs such as fuel and labour, as well as depleting quality aggregates in many regions. Combined these effects have increased the cost of conventional road rehabilitation using conventional granular systems by up to 100 percent over the past three years. From a technical perspective, it has been witnessed that unmodified granular road base and subbase granular materials are limited in terms of strength under deviatoric stress states, and can have low climatic durability in the presence of moisture and freeze-thaw, particularly at low grade line applications. In addition, high plasticity and/or high contents of fines within granular base materials have been observed to increase the moisture and freeze-thaw sensitivity (Safronetz 2003; Berthelot et al. 2005). Additionally, high fine sand content reduces the shear strength, and therefore the field performance, of granular base pavements. Collectively, these effects can result in pavement deformation when subjected to freeze-thaw cycles and dynamic loadings (Saskatchewan MHI 1982; Berthelot et al. 2007), as shown in Figure 1-1.

In an attempt to improve the cost effectiveness of strengthening granular pavement and the field performance of granular pavements, granular stabilization technologies have been used in road construction for several years (G.Vorobieff and Wilmot 2001; Berthelot et al. 2007). Stabilization of granular materials often employs cement, fly ash, lime, asphalt emulsion, and foamed asphalt (Newman and Tingle 2004). With modern recycling equipment, these strengthening materials are now relatively easy to apply and can provide considerable benefits to many different granular material types, particularly the mechanical and climatic durability properties (Newman and Tingle 2004).

Figure 1-1 Typical Pavement Rutting Failure on C.S. 15-11 near Kenaston Saskatchewan

Recently, the Saskatchewan MHI has started applying cold in-place recycling and full depth strengthening to strengthen in-service thin granular pavements. However, there are no reliable mechanistic based characterization methods and specifications for the design and construction of granular base stabilization systems under Saskatchewan field state conditions. The design, construction, quality control and quality assurance are

still mainly based on few research initiatives and/or limited experience from other countries or areas. In addition, empirical experience from other places may pose significant problems when extrapolated to Saskatchewan conditions. Consequently, there is a need to evaluate the performance of alternative granular stabilization systems using more reliable, and scientific based evaluation methods, both in the laboratory and the field. As a result, the critical field performance parameters can be characterized and granular strengthening systems and specifications can be optimized for Saskatchewan field state conditions by this research.

1.1 Research Goal

The goal of this research is to improve the engineering design and field performance of recycled and stabilized granular base systems under typical Saskatchewan field state conditions.

1.2 Research Objectives

The objectives of this research are to:

- Characterize the conventional behaviour, mechanistic behaviour, and moisture sensitivity of a typical Saskatchewan poor performing granular base system, and of alternative stabilization systems for the poor performing granular systems, in the laboratory.
- Mechanistically characterize the field behaviour of various granular base stabilization systems using non-destructive testing techniques.
- Validate the pavement design systems employed and primary structural response of the various granular base stabilization systems applied in this research.

1.3 Research Hypothesis

It is hypothesized that stabilization can improve the laboratory and field performance of conventional Saskatchewan granular base systems, in terms of

mechanistic behaviour, resistance to moisture damage and field primary structural responses.

1.4 Scope

Control Section 15-11 *in situ* granular base, as a typical thin granular pavement requiring strengthening, was selected for this research, because the *in situ* granular base material of C.S. 15-11 is relatively high in fine sand fraction as well as plastic clay fines. These physical properties are believed to be the primary causes for marginal performance of granular base materials in the field, as illustrated in Figure 1-1.

In this research, test sections of granular base stabilization on C.S. 15-11 (km 5.0 to km 8.0) near Kenaston were constructed in October 2006. Three granular base stabilization test sections were evaluated in this research:

- Asphalt emulsion and cement stabilization (km 5.0 -km 6.0)
- Cement stabilization (km 6.0 -km 7.0)
- Remix and recompaction of *in situ* granular base control section (km 7.0 - km 8.0)

Remixed granular material from various test sections on C.S. 15-11 were sampled and transported to the laboratory for compaction and further laboratory characterization. Preliminary testing of the C.S. 15-11 granular base included grain size distribution, Atterberg limits, standard Proctor moisture density, California bearing ratio strength and swell, sand equivalent test.

The mechanistic laboratory characterization applied the rapid triaxial frequency sweep testing (RaTT) across various load frequencies and stress states representative of field state truck load spectra currently experienced. Moisture sensitivity testing samples were also subjected to moisture capillary rise, surface electric conductivity, indirect tensile strength (ITS), and unconfined compressive strength testing (UCCS).

Heavy weight deflectometer was used to characterize the *in situ* structural responses of various granular base stabilization systems constructed on C.S. 15-11, prior to construction, post base stabilization, and after hot mix asphalt placement.

1.5 Methodology

The following project elements and tasks were employed in this research:

- Project Element 1: Background Investigation and Literature Review
    - Task 1: Review literature of various granular pavement systems and general material property requirements from specifications, research reports and journal articles.
    - Task 2: Review literature of granular base stabilization and cold in-place recycling including design, construction processes, and quality control and assurance.
    - Task 3: Review literature pertaining to mechanistic laboratory tests and moisture sensitivity tests related to granular base materials characterization in this research.
    - Task 4: Review of various pavement analyses, design, and modeling systems.
    - Task 5: Review of non-destructive deflection testing technologies.
- Project Element 2: *In Situ* Material Sampling and Laboratory Sample Preparation
    - Task 1: Determine sampling plan.
    - Task 2: Sampling *in situ* and stabilized granular materials from C.S. 15-11 test sections during the construction pre-milling phase.
    - Task 3: Fabricate Marshall, CBR and gyratory samples in the laboratory.
    - Task 4: Store all samples in moist room at 25 °C for curing.

- Project Element 3: Conventional Laboratory Characterization of *In Situ* Granular Base Material

    - Task 1: Grain size distribution (STP 206-1 base on ASTM D422).
    - Task 2: Atterberg limits (ASTM D4318).
    - Task 3: Standard Proctor moisture-density test (ASTM D698).
    - Task 4: Sand equivalent test (ASTM D2419).
    - Task 5: California bearing ratio swell and strength test (ASTM D1883)

- Project Element 4: Climatic and Mechanistic Laboratory Characterization

Figure 1-2 illustrates the scheme of laboratory tests performed on materials from C.S. 15-11. Tasks performed included:

- Task 1: Indirect tensile strength (ITS) test was performed on 100 mm samples compacted by Marshall method (moist room cured and 24 hours soaked, ASTM D4123).
- Task 2: Indirect tensile strength (ITS) test was performed on 150 mm samples compacted by gyratory method (moist room cured and 24 hours soaked, ASTM D4123).
- Task 3: Moisture capillary rise test (Texas Transportation Institute & Pavement Scientific International protocol) was performed on 150 mm gyratory prepared samples.
- Task 4: Unconfined compressive strength (UCCS) test was performed on gyratory samples (moist room cured and 24 hours soaked, ASTM D5102).
- Task 5: Rapid triaxial frequency sweep characterization of samples was performed across various load frequencies and deviatory stress states (moist room cured of various stabilization systems).

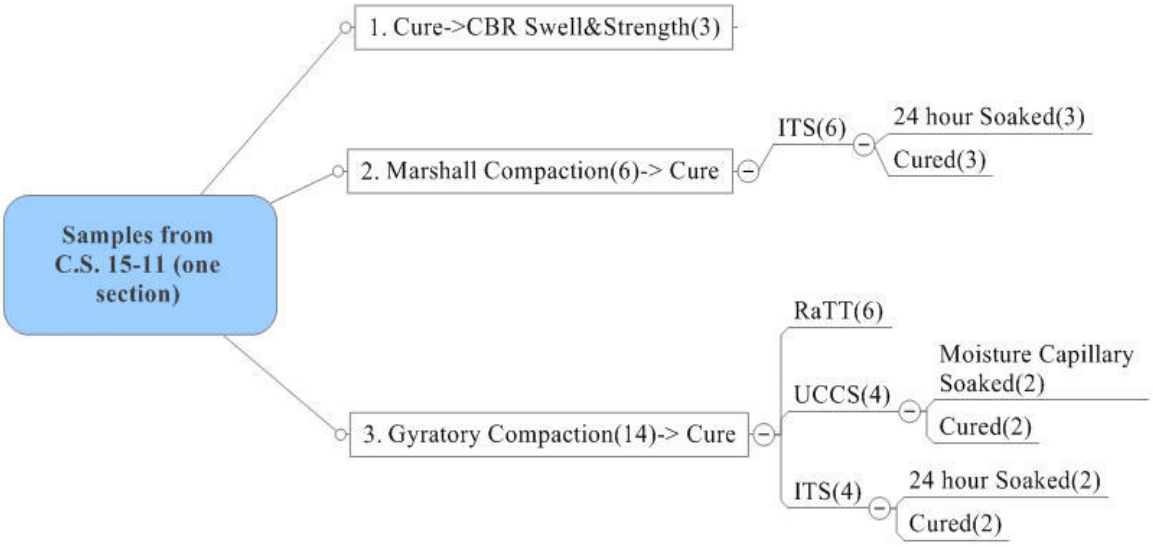

Figure 1-2 Laboratory Mechanistic Testing Framework

- Project Element 5: Field Non-destructive Deflection Testing

  - Task 1: Evaluate *in situ* structural properties using heavy weight deflectometer characterization of the C.S. 15-11 test sections prior to construction, post stabilization construction, and after asphalt surface paving.

- Project Element 6: Laboratory Characterization Data Analysis

  - Task 1: Quantify relationship of RaTT responses (dynamic modulus, Poisson's ratio, phase angle, recoverable radial strain) across various stress states, frequencies, and stabilization systems.
    - Graphical analysis
    - Analysis of variance
    - Tukey's pairwise comparison
  - Task 2: Quantify relationship of conventional laboratory testing results across stabilization system and climatic conditions.

- Project Element 7: Pavement Structure Design and Analysis

    - Task 1: Compare alternative strengthening system designs of C.S. 15-11 by conventional Saskatchewan MHI thickness design system.
    - Task 2: Compute critical strains within pavement structures of C.S. 15-11; evaluate the thickness design alternatives of C.S. 15-11 test sections with Saskatchewan MHI criteria.
    - Task 3: Compute field material responses in various granular bases of C.S. 15-11 test sections with finite element modeling and linear elastic modeling software. Accordingly, compare those results with responses of samples in laboratory RaTT testing.

- Project Element 8: Summary, Conclusions, and Future Recommendations

1.6 Layout of Thesis

Chapter 1 presents the background, goal, objective, scope, and methodology of this research. Chapter 2 introduces granular base stabilization systems, materials specifications, granular base stabilization and recycling construction processes. Chapter 2 also presents the mechanistic material characterization methods related to this research as well as pavement structure modeling systems. Chapter 3 summarizes the preliminary site survey results, the test section layout, the structure design, and construction records of the C.S. 15-11 granular strengthening test sections. Chapter 3 also presents the field material sampling process and non-destructive test results on C.S. 15-11 test sections. Chapter 4 summarizes the results and findings of conventional laboratory characterization across the various stabilization systems. Chapter 5 summarizes the results and findings of laboratory moisture sensitivity characterizations across the various stabilization systems. Chapter 6 summarizes the results and findings from the mechanistic RaTT characterization across different stabilization systems. Chapter 7 investigates the pavement structure design and pavement responses of C.S. 15-11. Chapter 8 presents the summary, conclusions and future recommendations based on the findings of this research.

CHAPTER 2 BACKGROUND AND LITERATURE REVIEW

Granular aggregate material is the primary structural member of flexible pavement systems, particularly for thin asphalt surfaced granular pavements which are commonly built in Saskatchewan. This chapter presents a summary of background information regarding granular pavements, including an introduction to granular materials and a summary of soil stabilization and cold in-place recycling systems. This chapter also summarizes the conventional and mechanistic laboratory characterization systems for granular pavement materials. The structural design and pavement modeling methodologies, as well as non-destructive deflection testing methods employed in this research, are also presented.

2.1 Introduction to Granular Pavement Materials

A typical flexible pavement structure consists of asphaltic concrete wearing surface course, the underlying base and subbase courses placed on a prepared subgrade. The asphaltic surface course is generally the stiffest layer and contributes the most to pavement integrity. The underlying granular layers distribute the load induced stresses throughout the granular pavement structure. Granular base material also contributes to drainage and frost resistance (MHI 1982; Muench 2004). The requirement of a satisfactory granular base material usually includes stability and resistance to moisture (Oglesby and Hicks 1982).

The granular base consists of a substantial layer of a properly proportioned blended mixture of soil and aggregate which is capable of supporting traffic in all weather conditions. Aggregates used in granular base and subbase applications generally consist of sand and gravel, crushed stone or quarry rock, slag, or other hard, durable material of mineral origin (Oglesby and Hicks 1982).

The gradation requirement of flexible granular pavements typically varies with granular layer type. For instance, Saskatchewan MHI specifies three bases (Type 31, Type 33, and Type 35) and three subbases (Type 6, Type 8, and Type 10) (MHI 2000), as listed in Table 2-1 and Table 2-2. The granular base is typically densely graded, with the amount of fines limited to promote drainage. The subbase, which is lower in the road structures, does not require such a high-quality material as granular base, as induced stresses are reduced considerably (Atkins 1997). Usually, the most suitable aggregates are those that are well graded from coarse to fine, to provide good stability. The common approach to achieve suitable aggregates is to establish limits for the various sizes of particles that will result in maximum dry density. For unbound granular material of a specific mineralogy, high stability in the field is generally associated with high density. However, many aggregates used in pavement structures are not well graded. Thus, specifications concerning gradation for this purpose are usually quite tolerant, with the idea, of making the best possible use of locally available materials (Wright 1996).

Table 2-1 Saskatchewan Base Course Gradation Requirements

Sieve Size	Percentage by Weight Passing Canadian Metric Sieve Series		
	MHI Type 31	**MHI Type 33**	**MHI Type 35**
31.5 mm	100	---	---
18.0 mm	75-90	100	100
12.5 mm	65-83	75-100	81-100
5.0 mm	40-69	50-75	50-85
2.0 mm	26-47	32-52	32-65
900 um	17-32	20-35	20-43
400 um	12-22	15-25	15-30
160 um	7-14	8-15	8-18
71 um	6-11	6-11	7-12
Plasticity Index	0-7.0	0-6.0	0-5.0
Fracture Face (%)	50.0 Minimum		
Light Weight (%)	5.0 Maximum		
Deleterious Materials (%)	2.0 Maximum		

Table 2-2 Saskatchewan Subbase Course Gradation Requirements

Sieve Size	Percentage by Weight Passing Canadian Metric Sieve Series		
	MHI Type 6	**MHI Type 8**	**MHI Type 10**
50.0 mm	100	100	100
2.0 mm	0 - 80.0	0 - 90.0	---
400 um	0 - 45.0	0 - 60.0	---
160 um	0 - 20.0	0- 25.0	---
71 um	0 - 6.0	0 - 15.0	0 - 20.0
Plasticity Index	0 - 6.0	0 - 6.0	0 - 6.0

The fine fraction of a granular material is the portion of the material passing the No. 200 sieve, comprising silt and clay sized particles. The function of this portion of the granular mixture is to act as filler for the remainder of the mixture and aid in the retention of stability during dry weather. The clay fraction contained in well graded bases also serves to retard the penetration of water in wet weather, as long as peak dry density is maintained. An excessive amount of silt and/or clay content may result in excessive volume change with change in moisture content. In areas where frost action is a factor, the percentage of material passing the No. 200 sieve may be reduced to prevent damage to a granular base or a subbase (Wright 1996). Base course with a high plasticity index has less strength than one without a high plasticity index (MHI 1982). Lowering the amount of soil passing No. 200 sieve should not have much impact on the base course stiffness which is more influenced by the confining pressure and the deviatoric stresses (MHI 1982).

The main specification of granular base is the grain-size distribution requirement. The shape of gradation curve is a good indication of strength (Atkins 1997). Many different specifications are used for these granular base mixtures by different highway agencies. For example, the American Association of State Highway and Transportation Officials (AASHTO) gradation requirements for base and subbase courses are listed in Table 2-3 (Wright 1996).

It should be noted that gradation requirements C, D, E, and F granular base are also suitable for surface courses. However, the plasticity characteristics of the granular systems are different. For base course, the fraction passing the 0.425 mm sieve shall have a maximum liquid limit at 25 and a maximum plasticity index at 6 (AASHTO 1986). The lower values of liquid limit and plasticity index indicate lower clay content. Based on local experience, the percentage passing the No. 200 sieve may be lowered to prevent frost damage for subbases (Oglesby and Hicks 1982).

Table 2-3 AASHTO Gradation Limits for Soil-Aggregate Subbase, and Base Course (AASHTO 1986)

Sieve Designation/Base Designation	Grading A	Grading B	Grading C	Grading D	Grading E	Grading F
50mm	100	100	----	----	---	---
25mm	---	75-95	100	100	100	100
9.5mm	30-65	40-75	50-85	60-100	---	---
4.75mm	25-55	30-60	35-65	50-85	55-100	70-100
2.0mm	15-40	20-45	25-50	40-70	40-100	55-100
0.425mm	8-20	15-30	15-30	25-45	20-50	30-70
0.075mm	2-8	5-20	5-15	5-20	6-20	8-25

Coarse aggregate shall not have over 50% loss in Los Angeles Abrasion Test

Amount passing 0.075 mm shall not be more that two thirds of the amount passing 0.425mm

Fraction passing 0.425 mm maximum W_l=25, maximum Ip=6

Agencies other than AASHTO have somewhat different specifications for granular bases. In general, grading requirements are about the same, but some lower the plasticity index to four or less to place a more stringent limit on troublesome fines. For instance, Alberta Infrastructure and Transportation required the fine contents in granular material to be nonplastic if used for asphalt stabilized granular base course (AIT 2003). Minimum fracture face percent is another commonly required parameter for granular base course, in order to get better deformation resistance and high stiffness for the material (Muench 2004). For example, Saskatchewan MHI requires a minimum 50 percent fracture face on the crushed coarse material (>5 mm) for all three types of granular bases (MHI 1996). Physical tests other than plasticity index and fracture face percentage may be used to control the properties of the soil mortar. For example, for California Department of Transportation class two granular base course, the minimum Hveem resistance values is 78 for a single test; minimum and running average Sand equivalent rating are 28 and 31 (Oglesby and Hicks 1982). In addition, the Alberta

Infrastructure and Transportation (AIT) specifies a maximum weight loss of 50 percent of granular materials in Los Angeles abrasion test for base courses (AIT 2003).

Granular base courses in Saskatchewan generally consist of well graded crushed gravel deposits which are typically stabilized with clay or silt binder materials. Saskatchewan Specification 3500 for granular base course and Specification 3300 for subbase course generally require base and subbase materials to be composed of sound, hard and durable particles of sand, gravel and rock free from elongated, soft or flaky particles, shale, loam, clay balls and organic or other deleterious material (MHI 2000). Cubical shaped particles are desirable, with a limited amount of flat or thin and elongated particles. The desired gradation and other physical requirements specified for Saskatchewan MHI bases and subbases by Saskatchewan MHI are listed in Table 2-1 and Table 2-2. The gradation curves are plotted in a semi-logarithmic scale as seen in Figure 2-1 and Figure 2-2.

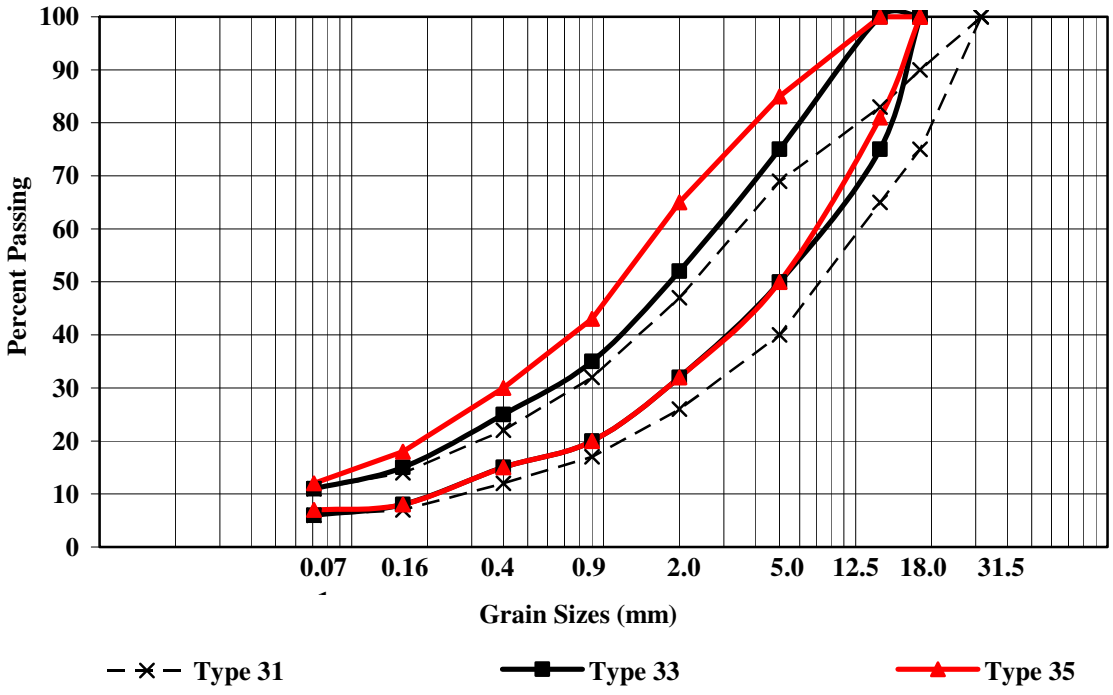

Figure 2-1 Gradation Envelopes of Saskatchewan MHI Base Courses

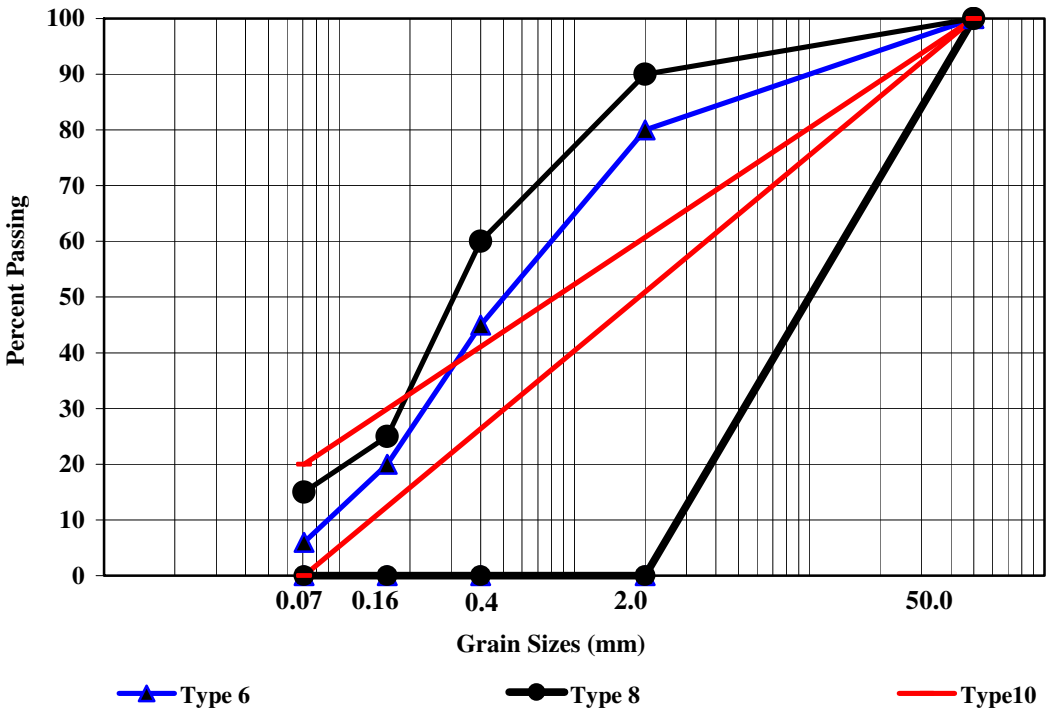

Figure 2-2 Gradation Envelopes of Saskatchewan MHI SubBase Courses

2.2 Conventional Granular Materials Testing

Granular material is a collective term for mineral materials such as sand, gravel, and crushed stone, which are used for granular base and subbase courses in both flexible and rigid pavements. Granular material can either be natural or manufactured. Natural aggregates are generally extracted from larger rock formations through an open excavation of bedrock deposits or glacial deposits. Extracted rock is typically reduced to usable sizes by mechanical crushing. Manufactured aggregate is often the by-product of other manufacturing industries.

Quality granular material is always desired for good performance of the granular pavement. This section will briefly discuss the conventional granular material tests to quantify the physical or engineering properties related to pavement.

2.2.1 Grain Size Analysis

The grain size distribution of a granular material is most often determined by sieve analysis. In a sieve analysis, a sample of dry granular material of known weight is

separated through a series of sieves with progressively smaller openings. Once separated, the weight of particles retained on each sieve is measured and compared to the total sample weight. Particle size distribution is then expressed as a percent passing each sieve size. Results are usually expressed in tabular or graphical format.

Granular gradation graphs are traditionally semi-logarithmic, while HMAC graphs often employ the standard 0.45 power gradation graph to emphasize the variance within a relatively small range of particle sizes. Typical semi-logarithmic graphs used for grain size analysis are presented in Figure 2-1 and Figure 2-2.

Standard sieve analysis test methods are:

- AASHTO T 27 and ASTM C 136: Sieve Analysis of Fine and Coarse Aggregates
- AASHTO T 11 and ASTM C 117: Materials Finer Than 75 mm (No. 200) Sieve in Mineral Aggregate by Washing
- Saskatchewan MHI Standard Test Procedure Manual 206-1: Sieve Analysis

2.2.2 Atterberg Limits and Plasticity Index

Soil plasticity is an important characteristic of the fines portion (<0.075 mm) within a granular material. In general, depending on its water content, a soil may exist in liquid, plastic, semi-liquid and solid states (Atterberg 1911). The upper and lower limits of the range of water content over which the soil exhibits plastic behaviour are defined as the liquid limits (W_L) and the plastic limits (W_P) respectively. The plasticity index (I_p), is:

$$I_P = w_L - w_P \quad \textbf{(2-1)}$$

Determination of limits is observed through two methods. The first method is based on the test procedures which Albert Atterberg developed (Atterberg 1911), but was refined by Arthur Casagrande for the use in civil engineering applications (Casagrande 1932, Codutto 2001). Two separate test apparatus and procedure are

required for the first method: one to find liquid limit and the other to find the plastic limit. The second method is the fall cone test developed by J. Olsson (Craig 2004). The falling cone apparatus is used to determine both Atterberg limits with slight variation in procedure, but with the use of only one apparatus.

Standard testing methods for limits and plasticity index are:

- AASHTO T 89, AASHTO T 90: Determining the Liquid Limit of Soils and Determining the Plastic Limit and Plasticity Index of Soils
- ASTM D 4318: Liquid Limit, Plastic Limit, and Plasticity Index of Soils
- British Standard 1377 (Part 2): Methods of Test of Soils for Civil Engineering Purposes
- Saskatchewan MHI Standard Test Procedure Manual 205-1: Atterberg Plasticity Index

2.2.3 Sand Equivalent Test

The sand equivalent value test provides a measure of the relative proportions of detrimental fine dust or clay-like material in soil or fine aggregates that pass the 4.75 mm sieve (ASTM 2003).

In this test, aggregate passing No.4 (4.76 mm) sieve is agitated in a water-filled transparent cylinder which is filled with a mixture of water and a flocculating agent (a combination of calcium chloride, glycerine and formaldehyde). After agitation and 20 minutes of settling, the sand separates from the flocculated clay, and the heights of clay and sand in the cylinder are measured. The sand equivalent value is the ratio of the height of sand to the height of clay times 100, as in the following equation 2-2. Cleaner aggregate will have a higher sand equivalent value. Specifications for aggregates in asphalt concrete often specify a minimum sand equivalent in the range of 25 to 35 (Roberts et al. 1996). However, Saskatchewan MHI requires a minimum sand equivalent value of 45 for asphalt concrete (MHI 1999).

$$SE = (sand\ reading \div clay\ reading) \times 100 \quad \textbf{(2-2)}$$

Standard testing methods for sand equivalent value are:

- AASHTO T 176: Plastic Fines in Graded Aggregates and Soils by Use of the Sand Equivalent Test
- ASTM D 2419: Sand Equivalent Value of Soils and Fine Aggregate
- Saskatchewan MHI Standard Test Procedure Manual 206-5: Sand Equivalent

2.2.4 Standard Proctor Moisture-Density Relationship

When soil is compacted, solid particles move together by mechanical means increasing the density of the soil. This action reduces the volume of air within the soil. The effectiveness of compaction is influenced by the moisture content of the soil. At low moisture contents, water acts as a lubricant allowing the particles to become more compacted. The addition of more water aids in expelling more air improving compaction. This trend continues until an apex where the water begins to displace the soil particles and begins to reduce the soil density (Head 1980).

The compaction characteristics of a soil can be assessed by the means of standard and modified laboratory Proctor compaction test (Proctor 1933). In the standard Proctor test, the soil is compacted in a cylindrical mould using a standard compaction effort, which uses a 24.4 N hammer dropping from a height of 305 mm. The mould can be 101.6 mm or 152.4 mm in diameter depending on the top size of the soil tested. A soil at selected water content is placed in three layers into the mould, with each layer compacted by certain blows at the standard compaction effort, the resulting dry unit weight is determined (ASTM 2003).

The procedure is repeated for a sufficient number of water contents. The dry density is then plotted against water content and the compaction curve is obtained, as shown in Figure 2-3. The optimal water content and the maximum dry density achieved

at the optimal water content can therefore be determined from the compaction curve (ASTM 2003).

If the soil contains more than five percent by mass of oversize fraction, an oversize correction shall be applied using ASTM D 4718 (ASTM 2003).

Standard testing methods for standard Proctor test are:

- AASHTO T 99: The Moisture Density Relations of Soils Using a 5.5-lb Rammer and a 12-in Drop
- ASTM D 698: Laboratory Compaction Characteristics of Soil using Standard Effort
- Saskatchewan MHI Standard Test Procedure Manual 206-5: Sand Equivalent

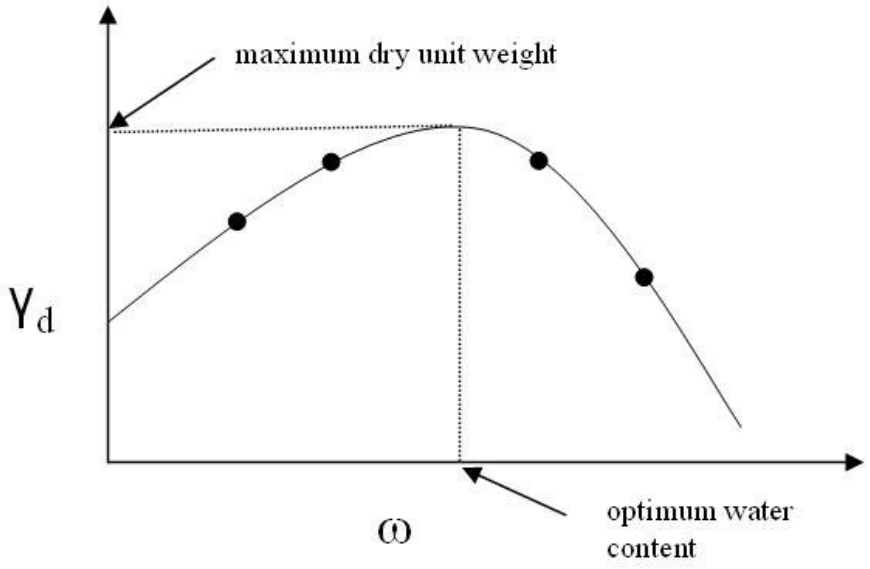

Figure 2-3 Moisture Density Relationship Compaction Curve

2.2.5 California Bearing Ratio

The California bearing ratio (CBR) test is a strength and swell potential test that compares the bearing capacity of a material with that of a well-graded crushed stone. The CBR test is primarily intended for, but not limited to, evaluating the strength

of cohesive materials having maximum particle sizes less than 19 mm. The CBR test was developed by the California Division of Highways in the 1930's and was subsequently adopted by numerous states, counties, U.S. federal agencies and international countries (Muench 2004)

The basic CBR test involves applying load to a small penetration piston at a rate of 1.3 mm (0.05") per minute and recording the total load at penetrations ranging from 0.64 mm (0.025 in.) up to 7.62 mm (0.300 in.). Figure 2-4 is a sketch of a typical CBR sample. Values obtained are inserted into the following equation to obtain a CBR value:

$$CBR(\%) = \frac{x}{y} \qquad \textbf{(2-3)}$$

Where:

x = the unit load on the piston (pressure) for 2.54 mm of penetration

y = standard unit load (pressure) for well graded crushed stone, for 2.54 mm penetration, y= 6.9 Mpa

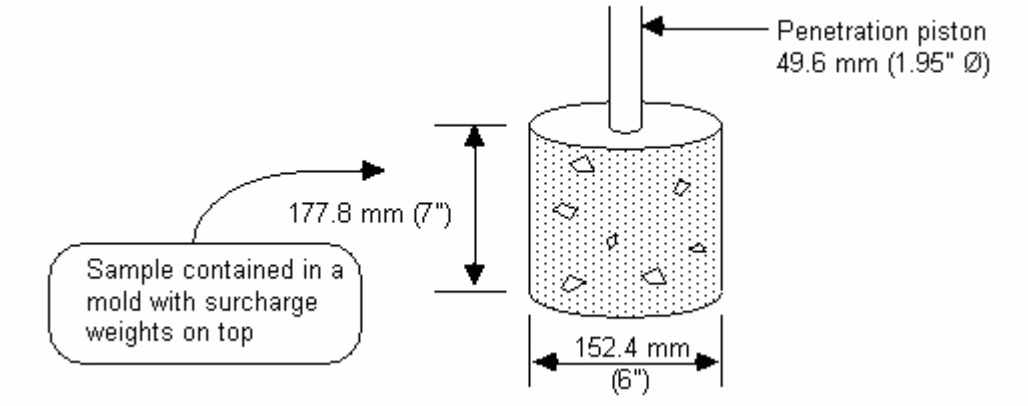

Figure 2-4 CBR Sample (Muench 2003)

Standard California bearing ratio test methods are:

- AASHTO T 193: The California Bearing Ratio
- ASTM D 1883: Bearing Ratio of Laboratory Compacted Soils

- Saskatchewan MHI Standard Test Procedure Manual 205-23: California Bearing Ratio

2.3 Stabilization of Granular Pavement Materials

Although conventional granular materials are both technically feasible and economically acceptable in pavement, they do exhibit shortcomings with regard to long term performance. Therefore stabilization is widely used to enhance granular material properties for pavement design purposes or to overcome deficiencies in available materials. Stabilization agents usually fall into a number of categories as follows (AAPA 1998):

- Lime-includes hydrated lime $Ca\ [OH]_2$, quicklime CaO and lime slurry
- Cement
- Blends incorporating supplementary cementitious material, for example, mixture of slag and lime, slag and cement, or lime and fly ash
- Bituminous-foamed asphalt, emulsion asphalt, cutback asphalt
- Chemical stabilization with proprietary chemicals
- Granular-the addition of natural materials to improve grading and other physical material characteristics

Climate and *in situ* soil type can have a significant effect on the choice of stabilization systems that will be employed. In wetter areas, it is important to ensure the wet strength of the stabilized material is adequate and susceptibility to moisture variation is low. Therefore the use of hydraulic binders is preferred. Lime is suitable for cohesive soils, when used as the agent to dry out the material. The use of bitumen emulsions is primarily employed to stabilized granular materials, particularly in hot, dry climates (AAPA 1998) .

To gain a preliminary assessment of the type of stabilization required for a particular pavement material, particle size distribution and Atterberg limits are

commonly used. The usual range of suitability of various types of stabilisation is based on the grain size distribution, the percentage of material passing 75 um sieve and the plasticity index of the soil. Figure 2-5 gives an initial guidance to select a stabilization type based on Australian experience (AAPA 1998) . The life-cycle costs of all feasible alternatives are usually compared between alternatives. The final decision on what alternative to choose is generally based on both engineering and economic concerns.

The advantages of stabilization and cold in-place recycling are as follows (AAPA 1998, Lay 1998):

- Reduce the pavement thickness by providing significant tensile strength with subsequent reduction in material quantities and costs.
- Reduce the moisture susceptibility of sub-surface structural layers.
- Enable the use of lower grade (marginal) materials in pavement construction, and preserve aggregates
- Improve the strength and stiffness properties of sub-specification material.
- Provide a working platform for construction equipment operating on soft material.
- Provide faster construction time and therefore less weather delays and detrimental effects of exposure to poor weather conditions.
- Reduce green house gas emission.
- Reduce energy consumption.

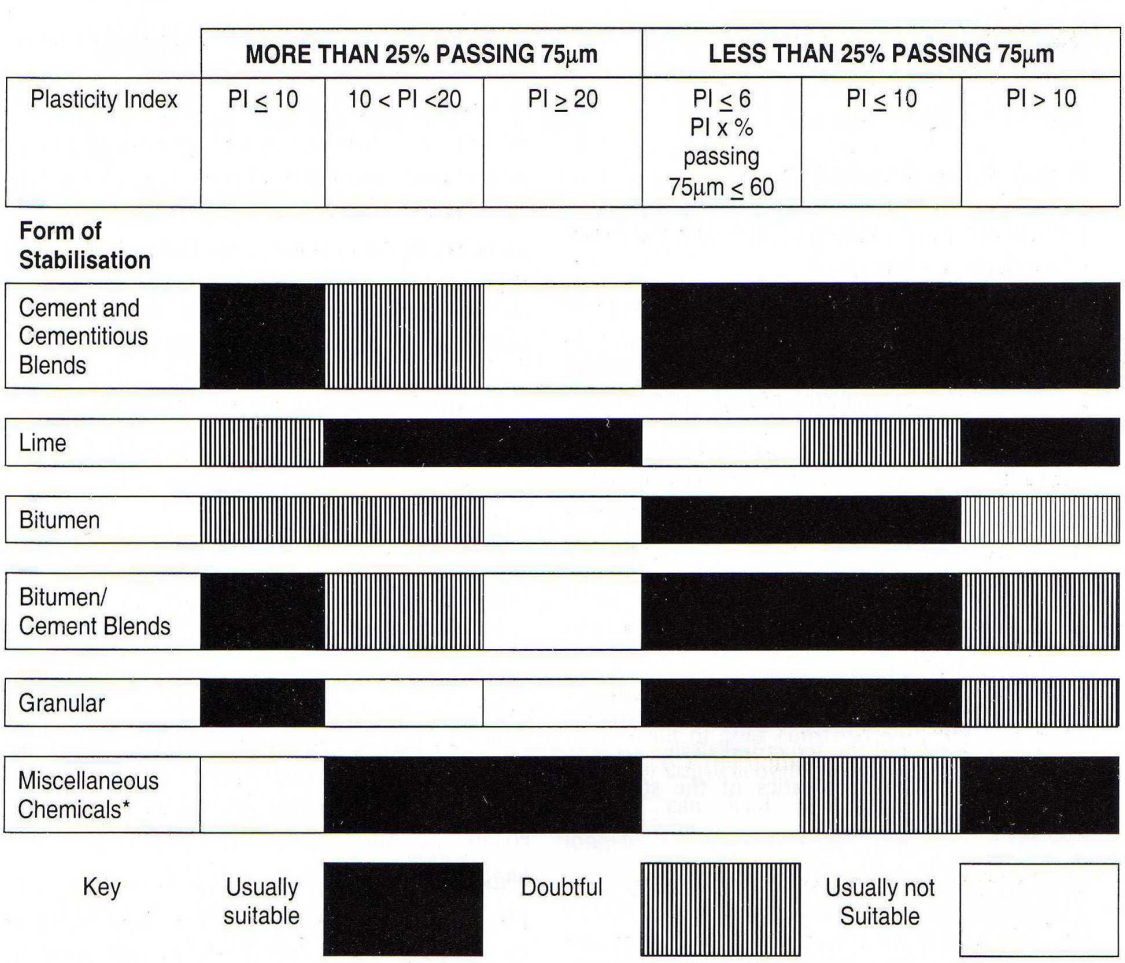

Figure 2-5 Selection of Method of Stabilization (AAPA 1998)

2.3.1 Cement Stabilization

Modern usage of cement for stabilization purposes dates back to 1917 when J. H. Amies took out a patent in the USA on soil and cement mixtures labelled “Soilamines” (O'Flaherty 1986) .

When water is added to neat cement, the major hydration products are calcium silicate hydrates, calcium aluminate hydrates, and hydrated lime. Cementation is primarily by means of adhesion bonding of the calcium silicate and aluminate hydrates to the rough mineral surfaces (O'Flaherty 1986) .

Experience shows that cement stabilization is best used for granular materials, particularly if they are well graded. Cement stabilization is thus a useful process to use when recycling a pavement. Cement stabilization can also be used for sand-clays and non-expansive clays with low plasticity, and with caution for heavy clays. Cement stabilization with heavy clays, high organic content clays, and soils with sulphate content may generate long term performance and problems in pulverizing, mixing and compaction. Depending on the specific project, cement content during stabilization varies from three to six percent by mass of dry soil. Material with six to fifteen percent cement by mass is known as lean concrete. Some typical cement contents for sandy clays and non-expansive clays with low plasticity are shown in Table 2-4 (Lay 1998).

Table 2-4 Cement Contents for Various Clay Type (Lay 1998)

Clay Type	Cement Requirement by Mass of Dry Soil (%)
Well graded sandy clay	2-5
Sandy clay	4-6
Silty clay	6-8
Heavy clay	8-12
Very heavy clay	12-15

The Portland Cement Association has published recommended cement stabilization levels for various soils (Portland Cement Association 1992). The cement content ranges can be selected by the AASHTO soil groups from the suggested cement content tables by Portland Cement Association. Samples at optimum moisture and maximum density are moist cured for 7 days and then subjected to either 12 cycles of wet/dry or freeze/thaw test. The percent loss by weight is required as in Table 2-5.

In flexible base courses, drying shrinkage can lead to both transverse and longitudinal cracks. Such cracks frequently reflect through to the pavement surface. Severe shrinkage cracking can have major detrimental effects on the stiffness of the cement-treated layer, and thus on its structural performance and should be mitigated in the design process (Lay 1998).

Table 2-5 FHWA Recommended Maximum Loss in Wet/Dry and Freeze/Thaw Test

AASHTO Soil Classification	Maximum Weight Loss in Test (%)
A-1,A-2,A-3	14
A-4,A-5	10
A-6,A-7	7

2.3.2 Bituminous Stabilization

Bituminous materials are believed to have been first used for modern stabilization purposes as dust palliatives on natural soil roads in Southern California in 1898 (O'Flaherty 1986). The process is more successful with granular material than with cohesive material. Bituminous stabilization is therefore primarily used on the granular base layer, and to a lesser extent, on the subbase layer (AAPA 1998).

Bituminous stabilization material acts as a waterproofing agent with fine grained soils, and thereby enhances soil strength. With coarse-grained soils, bituminous stabilization also acts as a cementing agent (lubricant/adhesive) and binds soil particles together. Obviously, in many soils, a combination of these mechanisms occurs (O'Flaherty 1986).

The type of bitumen stabilization method depends primarily on the soil characteristics and soil classification. Figure 2-6 summarizes the selection process to determine an appropriate bituminous stabilizing agent across the various types suitable for stabilization with bitumen and bitumen/cement blends (AAPA 1998).

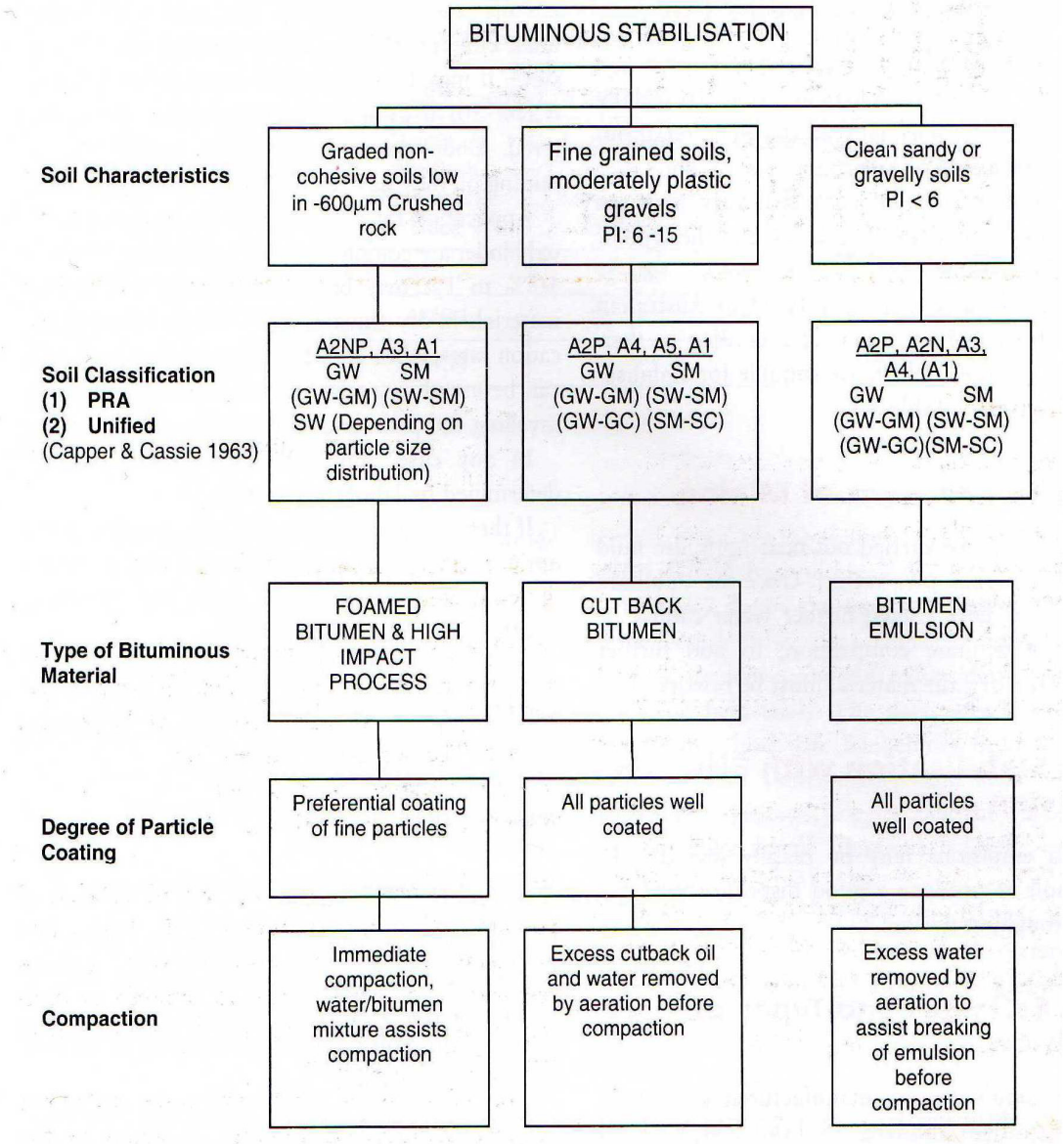

Figure 2-6 Guide to Selection of Bituminous Materials in Stabilization

Bituminous stabilization may be performed using any of the following bituminous binders with and without cement.

- Cut back asphalt
- Emulsion asphalt
- Foamed asphalt

As a guide to the selection of a suitable stabilizer type and amount for pre-design laboratory testing purposes, soils and granular materials normally require the addition of 2 to 5 percent by mass of residual bitumen, irrespective of whether the bituminous binder is added in the form of cutback asphalt, emulsion asphalt, or foamed asphalt (O'Flaherty 1986).

2.3.2.1 Cutback Asphalt Stabilization

Asphalt may be mixed with light cutter oils to produce binders which are fluid at ambient temperatures. In this form, materials may be sprayed cold or with slight heating and mixed with pre-moistened soil.

The cutback asphalt stabilization results in a material that gains strength slowly. The cutback asphalt has relatively large emissions, particularly volatile organic compounds (VOC). Due to the stringent air quality requirement, it is now rarely used (O'Flaherty 1986; AAPA 1998).

2.3.2.2 Emulsion Asphalt Stabilization

Emulsion asphalt is a mixture of asphalt binder and water that contains a small amount of emulsifying agent to cause the asphalt to become mixed with or suspended in the water (Asphalt Institute 1987). Emulsion asphalt may be either anionic emulsified asphalt with electro-negatively charged asphalt droplets or cationic emulsified asphalt with electro-positively charged asphalt droplets, depending on the emulsifying agent. Emulsion asphalts are further classified on the basis of how quickly the asphalt droplets will coalesce.

The terms RS (rapid setting), MS (medium setting), SS (slow setting), and QS (quick setting) have been used to standardize the classification of emulsion asphalt. A RS emulsion has little or no ability to mix with an aggregate. A MS emulsion is expected to mix with coarse but not fine aggregate, and SS and QS emulsions are designed to mix with fine aggregate, with the QS expected to break more quickly than the SS. ASTM D977 and D2397 or AASHTO M140 and M208 have developed standard specifications for the grades of emulsion (Asphalt Institute 1987).

Asphalt emulsion can be readily mixed with damp soil to produce a good dispersion of bitumen throughout the soil. Asphalt emulsion has been widely used as a stabilization agent in pavement rehabilitation projects for decades. Typically slow grade asphalt emulsion is suitable for use in stabilization to allow adequate mixing and placement time. Care should be taken if fines content of reclaimed material is greater than 15 percent because asphalt clay balls may form (Berthelot 2006). It is important that emulsion asphalt that is used in the field be subjected to laboratory testing programs first (AAPA 1998).

Application rates of two to three percent by mass of residual binder are commonly used (AAPA 1998). Lower rates of about 0.5 to 1 percent may be satisfactory for well-graded materials in dry climates with low fines content. Lower application rates, when added to granular base materials, can be useful as a construction expedient to reduce ravelling and the formation of pot holes under traffic. However, in any case, the application rate should be determined by laboratory testing (AAPA 1998).

If no other local data or testing information is available, a guide to the amount of emulsion to form a heavily bound material may be obtained from the following equation (Asphalt Institute 1983)

$$\text{Percentage of Emulsion} = 0.75(0.05\,A + 0.10\,B + 0.50\,C) \quad \textbf{(2-4)}$$

Where:

% of Emulsion = asphalt emulsion percent by dry weight of aggregate

A = % retained on 2.36 mm sieve

B = % passing the 2.36 mm sieve but retained on the 75 um sieve

C = % retained on 75 um sieve

Cement can be added with asphalt emulsion in the base stabilization. As a result, a highly-durable stabilized base course with rigidity of cement treated materials and the flexibility of asphalt concrete is obtained. Ordinary Portland cement is generally used for cement stabilization. However, Portland blast-furnace cement, silica cement, fly ash

cement or specific cement with added lime or gypsum may sometimes be employed in granular base stabilization (Collings 2001).

Portland cement and emulsified asphalt can increase the stiffness and reduce the permeability. Also, the addition of cement promotes the removal of excess water and assists the emulsion to break (Vuong et al. 1995). It is suggested that a modified material of this type could have a modulus of 500 to 1000 Mpa and a UCS< 1Mpa (AAPA 1998).

2.3.2.3 Foamed Asphalt Stabilization

Foamed asphalt is produced when water is added to hot bitumen, which has a temperature of approximately 180 degrees Celsius, to produce expansion of the hot asphalt which occupies ten to twenty times the volume of normal bitumen. In its short life span of just a few minutes, foamed asphalt will coat most surfaces of aggregates. As soon as the foam collapses, the mix should be compacted within 30 minutes (Kowalski and Starry 2007). Foamed asphalt can be used for spray and chip sealing when foamed asphalt has a expansion ratio of about eight and a half life of about 15 minutes are used.

The foamed asphalt stabilization is not useful with materials with a plasticity index of over 12, or with insufficient fines to form a well-graded end product (VicRoads 1993; Lay 1998). Research conducted by Wirtgen America Inc. (Kowalski and Starry 2007) showed that foam asphalt stabilization typically requires that the reclaimed material has a minimum 5 percent fines and a maximum of about 20 percent fines.

Mixing of foam asphalt should be carried out at or near optimum fluid (bitumen plus moisture) content. One of the physical attributes of foamed asphalt is that the fine aggregate particles are preferentially coated, leaving the coarse particles relatively uncoated with bitumen. Placement can be carried out immediately, but care must be taken with initial compaction to prevent instability (AAPA 1998).

Secondary additives such as fly ash, cement or quick lime are typically added to alter the characteristics of the finished product, or to make it more amenable to treatment with the bituminous binders. Cementitious additives should not exceed two percent by

mass, to avoid possible shrinkage cracking and/or rapid set of the foamed asphalt system (AAPA 1998).

The benefits of foamed asphalt stabilization include (Vorobieff and Wilmot 2001; Berthelot 2007; Kowalski and Starry 2007):

- Lower cost than full depth reconstruction.
- Has the ability to reopen to traffic immediately.
- Increase durability and waterproof ability to the pavement material.
- Has better resistance to pavement cracking.

While the limitations of foamed asphalt stabilization are identified to be (G.Vorobieff and Wilmot 2001; Berthelot 2007):

- Need suitable grading of fines in the pavement material.
- Special equipment and experienced operators are required.
- Need increased compactive effort to ensure fast compaction prior to setting of foamed asphalt stabilized material.

A recent pilot project in Ontario, Canada, used foamed asphalt in base stabilization, and has determined that the benefits of foamed asphalt stabilization also include a reduction in curing time and an extension to the construction season (Lane and Kazmierowski 2005).

2.3.3 Pavement Recycling

The engineering community's interest in recycling over recent decades has largely been based on economics. During the mid and late 1970s in the United States there were problems related to the reduced funding for transportation facilities, material supply, equipment availability, trained personnel, and energy awareness and availability. The recycling offered the solution to these problems. Specifically, recycling offered the following benefits (Epps 1990).

- Reduced costs (material, hauling, engineering et al.)
- Preservation of existing pavement geometrics
- Conservation of aggregates and binders
- Preservation of the environment
- Material and energy conservation

Commonly, flexible pavement recycling can be categorized into hot recycling and cold recycling. Cold recycling is the processing and treatment with bituminous and/or chemical additives of existing asphalt pavement without heating to produce a restored pavement layer. Cold recycling normally consists of milling an existing asphalt pavement to specified depth, mixing additives with Reclaimed Asphalt Pavement (RAP), spreading, and compacting the recycled mixture to a specified depth and cross slope. This is followed by placement of a new asphalt surface course, usually a hot mix asphalt overlay, but for some projects, an asphalt surface treatment only (AASHTO-AGC-ARTBA Joint Committee 1998).

Hot pavement recycling typically includes the heating of material during the recycling process. Depending on the recycling process requirements, hot recycling can be categorized into Hot In-place Recycling (HIR) and Hot Central Plant Recycling (HCRP). The HIR process consists of heating and softening the existing asphalt pavement to permit it to be scarified or hot rotary milled to a specified depth. The loosened pavement is then thoroughly mixed with "virgin" aggregate, new binder and/or recycling agents, then placed and compacted with conventional pavement equipment. The HCRP is the process of combining RAP with "virgin" aggregates, new asphalt binder, and/or recycling agents in a central plant to produce a recycled mix. Specially designed or modified batch or drum mix plants use the heat-transfer method to soften the RAP to permit its mixing (Kowalski and Starry 2007).

Figure 2-7 Wirtgen 2500 Recycler in Cold Recycling Process (Consedine 2002)

Figure 2-10 Hot in-Place Recycling Train (Courtesy of Martec)

According to the recycling depth, cold recycling can be categorized into full-depth and partial-depth. Full depth (reclamation/stabilization) cold recycling is a rehabilitation technique in which the full flexible pavement structure and predetermined portions of the base material are uniformly pulverized and mixed with a bituminous binder, resulting in a stabilized base course. Additional aggregate may be transported to the site and incorporated in the processing. This process is normally performed to a depth of 10 to 30 cm.

Partial-depth cold in-place recycling is a rehabilitation technique that reuses a portion of the existing asphalt-bound materials. Normal recycling depths are 5 to 10 cm. The resulting bituminous-bound recycled material is often used as a base course but can be used as a surface course on low to medium traffic volume highways (Epps 1990).

According to the recycling process requirements, cold recycling can be categorized into cold in-place recycling (CIR) and cold central plant recycling (CCRP). Generally cold in-place recycling is faster, more economical, and environmentally preferable because trucking and construction time is greatly reduced. Therefore energy consumption and haul road damage are significantly reduced. Also, cold in-place recycling conserves the aggregate as well as the asphalt materials as compared to "mill and fill" rehabilitation strategy. However, where surplus millings are available or an existing pavement has to be removed to allow stabilization, removal or some other treatment of underlying materials, central plant cold recycling is an excellent alternative (AASHTO-AGC-ARTBA Joint Committee 1998).

The following disadvantages have been identified for cold in-place recycling (O'Flaherty 1986; Epps 1990):

- Poorer control as compared to central plant mixing
- Traffic accommodation and disruption to process
- Relatively expensive pulverizing equipment, capital, maintenance, and operational costs
- Susceptibility to climatic conditions, including temperature and moisture

- Curing period needed for strength gain

Cold recycled materials have been used for subbases, bases, and surfaces. The most common use to date has been for base course. Most types of pavement distress can be rehabilitated by cold recycling. However, cracked pavements with structurally sound, well drained bases and subgrade are the best candidates (Epps 1990).

2.4 Mechanistic Laboratory Testing of Granular Pavement

Conventional phenomenological and empirical granular material testing methods characterize typical physical and strength properties of granular materials. However, conventional characterization methods cannot provide fundamental material constitutive relations which are related to pavement long term performance or mechanistic parameters which are useful for mechanistic road response modeling. Therefore, mechanistic laboratory testing is desired for further granular materials characterization in this research.

2.4.1 Unconfined Compression Strength Test

Unconfined compressive strength (UCCS) testing applies a vertical load at a fixed deformation rate to a cylindrical sample, as specified in ASTM D1074 for asphalt mixture, and ASTM D5102 for soil lime mixture. Unconfined compressive strength is the peak applied load divided by the original cross sectional area of the sample perpendicular to the direction of the load, as illustrated in Figure 2-8. Unconfined compressive strength is expressed as:

$$UCCS = \sigma_f = \frac{P_{11f}}{A_0} \quad \textbf{(2-5)}$$

Where:

σ_f = Peak stress at failure (Pa)

P_{11f} = Peak applied load at failure (N)

A_0 = Original cross section area (m^2)

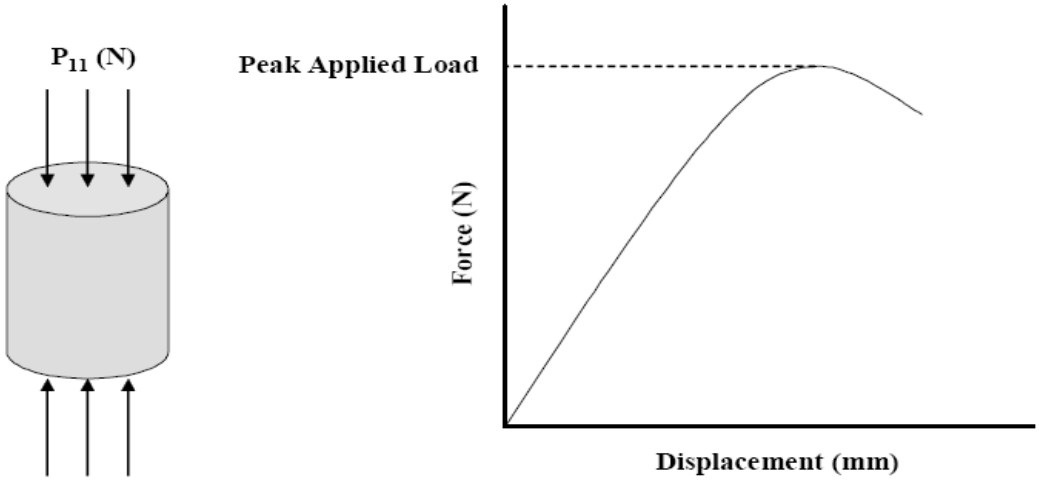

Figure 2-8 Unconfined Compression Test (Berthelot 2006)

Limitations of unconfined compressive strength characterization have been found to be as follows (Baumgarther 2005):

- The stress state generated during testing is highly deviatory in nature and unrepresentative of field state loading conditions.
- The results can be largely dependent upon load application rate.
- The UCCS does not provide feedback controlled multi-axial deflection measurements and, as a result, cannot be used to characterize the fundamental performance characteristics of asphalt concrete.

Standard testing methods for unconfined compressive strength for granular materials are:

- AASHTO 208 and ASTM D 2166: Unconfined Compressive Strength of Cohesive Soil
- ASTM D 5102: Standard Test Method for Unconfined Compressive Strength of Compacted Soil-Lime Mixtures

- Saskatchewan MHI Standard Test Procedure Manual 205-20: Sand Equivalent

2.4.2 Rapid Triaxial Frequency Sweep Test

The triaxial approach to determining material properties is useful for a variety of reasons. One of the important reasons to use the triaxial utility is its ability to properly handle the characterization of different types of materials, including materials that do not bind (e.g. unbound base and subgrade materials and asphalt concrete at high temperature) and/or those that are anisotropic (e.g. composites) (Crockford 1997). However, a standard geotechnical cell is not particularly attractive for production use because the standard cell and most standard geotechnical test procedures take significantly more time than would be accepted in a production pavement testing environment, especially for hot mix asphalt QC/QA. Also, drawbacks of traditional triaxial test apparatus include: limited stress state and test temperature testing capabilities; limited feedback control capabilities; limited dynamic testing capabilities; and direct measurement of Poisson's ratio is difficult (Berthelot et al. 1999).

The rapid triaxial testing system is a blend of traditional geotechnical cell sophistication, the simplicity of the Texas triaxial cell and Hveem stabilometer, and novel concepts in control, instrumentation and analysis that make it viable for obtaining engineering properties in a production lab environment (Berthelot 1999; Crockford et al. 2002).

The RaTT apparatus was first used in 1996, during the design and construction QA/QC of Saskatchewan's SHRP Specific Pavement Studies- 9A test sections (Berthelot et al. 1997, Berthelot 1999, Anthony 2007). Although RaTT is not yet widely implemented as part of conventional testing of pavement materials, RaTT is gaining understanding and acceptance in the pavement engineering community. The rapid triaxial frequency sweep testing has also been widely used on materials in the NCHRP 9-7 project and the Westrack project in the U.S. (Crockford 1997).

The RaTT cell consists of a cylindrical chamber with an aspect ratio of 1:1 to accommodate standard gyratory compacted samples. The RaTT cell employs a pneumatic confinement chamber with four linear variable differential transducers mounted axially around the sample. Axial tractions are applied by a standard servo-hydraulic test frame with two LVDTs mounted axially to measure vertical displacement. The RaTT cell can be operated in load or displacement control where the radial and axial loads or displacements are controlled independently (Berthelot et al. 2003).

One of the benefits of the Rapid Triaxial Testing over the conventional triaxial test apparatus is the ability to characterize samples prepared in the Strategic Highway Research Program (SHRP) gyratory compactor without the need to saw-cut or trim the test sample, which may introduce irregularities and damage in the form of micro-fracture in the sample The ability to use gyratory samples greatly expedites sample characterization and, therefore, facilitates mechanistic characterization of asphalt concrete mixes on a production scale (Anthony 2007).

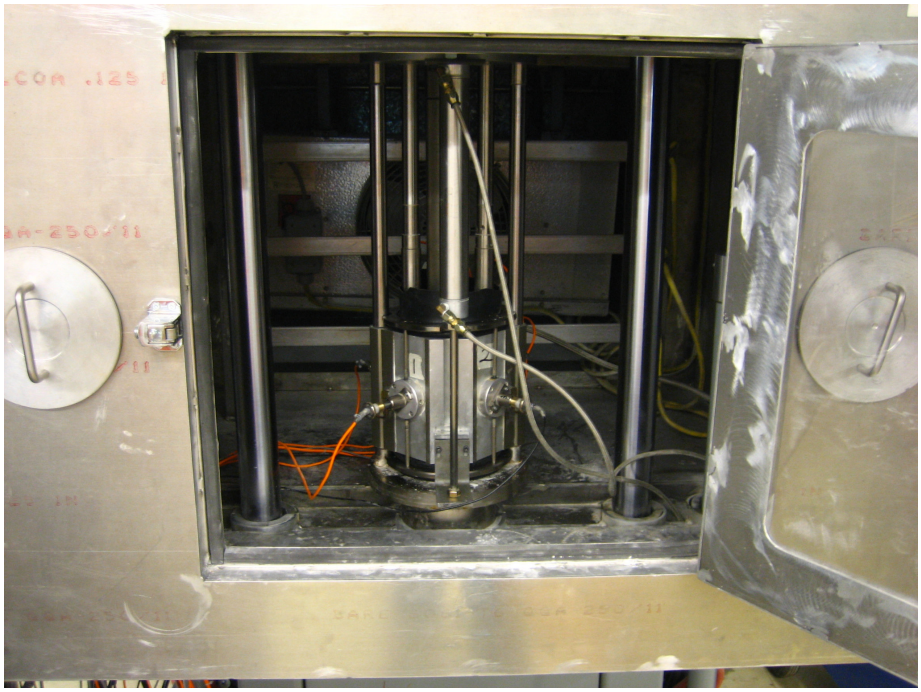

Figure 2-9 Rapid Triaxial Tester at University of Saskatchewan Transportation Centre

The RaTT apparatus has been proven to provide reliable information of mechanistic material properties of various pavement material types, such as asphalt concrete mixtures and granular materials (Berthelot 1999, Crockford et al. 2002, Berthelot et al. 2004, Baumgartner 2005, Anthony 2007), and is pictured in Figure 2-9.

The RaTT apparatus features independent closed-loop feedback control of the vertical and confining stresses exerted on the gyratory compacted samples of 150 mm height. The sample is inserted into a rubber membrane, which is used pneumatically to create radial confinement. Sinusoidal axial loading is applied at a specified frequency, and the resulting strains on the sample are measured by two axial and four radial linear variable differential transducers (Berthelot 1999).

The RaTT cell is capable of measuring the material constitutive relationships by simulating the following field conditions (Anthony 2007):

- Magnitude of axial load application (simulates varying vehicle loadings)
- Frequency of axial load application (simulates varying traffic speeds)
- Magnitude of radial confinement (simulates various locations within a pavement structure)
- Temperature (simulates various environment conditions)

Advantages of RaTT testing have been found to be as follows (Crockford et al. 2002; Berthelot et al. 2003):

- RaTT can be used for all flexible pavement materials including low cohesion base materials and hot mix at high temperatures.
- RaTT can provide both engineering properties and index properties. The properties may be used as index properties in QC applications and as engineering properties for structural design and performance prediction. Testing over the past five years from at least three different sources on a range of mix designs indicates good correlation with field rut measurements.

- Data analysis is embedded in the software so that the end result is immediately available with the computational details transparent to the user.
- RaTT can use gyratory samples as testing samples.
- The repeatability is proven to be good.

Rapid triaxial testing at University of Saskatchewan is proven to be capable of providing reliable mechanistic parameters of pavement materials. These parameters are (Anthony 2007):

- Dynamic Modulus
- Poisson's Ratio
- Phase Angle
- Recoverable Axial Microstrain
- Recoverable Radial Microstrain

2.4.3 Complex and Dynamic Modulus

The most comprehensive research effort of complex modulus started in the mid-1990s as part of NCHRP Projects 9-19 (Superpave Support and Performance Models Management) and NCHRP 9-29 (Simple Performance Tester for Superpave Mix Design). NCHRP Projects 9-19 and 9-29 document the development of a simple performance test for evaluating the resistance of asphalt mixtures to permanent deformation and fatigue cracking. The complex modulus test is the most promising test for both of NCHRP projects (Clyne et al. 2003).

The NCHRP projects 9-19 and 9-29 proposed new guidelines for the proper specimen geometry and size, specimen preparation, testing procedure, loading pattern, and empirical modeling. In these two projects the terminology was changed to dynamic complex modulus (Clyne et al. 2003).

For linear viscoelastic materials such as hot mix asphalt, the stress-strain relationship under a continuous sinusoidal loading is defined by its complex dynamic modulus (E*), as given in Equation 2-6. This is a complex number that relates stress to strain for linear viscoelastic materials subjected to continuously applied sinusoidal loading in the frequency domain. The complex modulus is defined as the ratio of the amplitude of the sinusoidal stress (at any given time, t, and angular load frequency, ω), $\sigma = \sigma_0 \sin(\omega t)$, and the amplitude of the sinusoidal strain $\varepsilon = \varepsilon_0 \sin(\omega t - \phi)$, at the same time and frequency, that results in a steady-state response, as shown in Figure 2-10 (Berthelot 1999, Witczak et al. 2002).

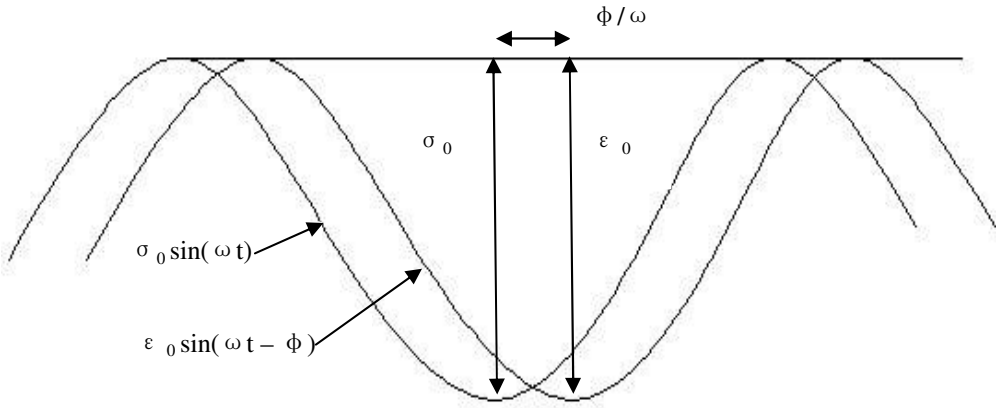

Figure 2-10 Dynamic Modulus Test Stress Input and Strain Response

$$E^* = \frac{\sigma}{\varepsilon} = \frac{\sigma_0 e^{i\omega t}}{\varepsilon_0 e^{i(\omega t - \phi)}} = \frac{\sigma_0 \sin(\omega t)}{\varepsilon_0 \sin(\omega t - \phi)} \quad \textbf{(2-6)}$$

Where:

σ_0 = peak (maximum) stress

ε_0 = peak (maximum) strain

ϕ = phase angle, degrees

ω = angular velocity

t = time, seconds

The real and imaginary portions of the complex modulus (E*) can be written as:

$$E^* = E' + iE'' \quad \textbf{(2-7)}$$

Where the E' value is generally referred to as the storage or elastic modulus component of the complex modulus, while E" is referred to as the loss or viscous modulus.

The dynamic modulus is defined as the absolute value of the complex modulus, or

$$E_d = \left|E^*\right| = \frac{\sigma_p}{\varepsilon_p} \quad \textbf{(2-8)}$$

Where:

σ_p = peak (maximum) stress

ε_p = peak (maximum) strain

Dynamic modulus of asphalt concrete is known to be dependent upon voids in total mix (VTM), temperature, and stress state (Cragg and Pell 1971, Shook 1984, Chehab et al. 2000). Research of Minnesota Road Research Project (MnROAD) found that under a constant load frequency, the dynamic modulus decreases with the increase in test temperature for the same mixture, while the phase angle increases with the increase in test temperature from -20°C to 20°C. However, at 40°C and 54°C the phase angle decreases with the increase in test temperature, as expected. Under a constant test temperature, the dynamic modulus increases with the increase of test frequency and the phase angle generally shows the opposite trend, as expected (Clyne et al. 2003).

The NCHRP 9-29 will finalize testing equipment and develop testing procedures for the dynamic modulus test (Witczak 2005). The new dynamic modulus test can be used in asphalt pavement thickness design software, or to gauge which mixture is appropriate for a given application. Usually the applied loads are relatively lower than for the repeated load deformation test. With the repeated load deformation test, a loading

head applied a load of 500 pounds to a cylindrical specimen at a rate of ten times per second (Brown 2006).

2.4.4 Phase Angle

The phase angle (δ), is the angle at which the strain response lags behind stress, and is an indicator of the viscous properties of the material being evaluated. Mathematically, this is expressed as (Witczak et al. 2002):

$$E^* = \left|E^*\right|\cos\delta + i\left|E^*\right|\sin\delta \quad \textbf{(2-9)}$$

$$\delta = \frac{t_i}{t_p} * 360 \quad \textbf{(2-10)}$$

Where:

t_i = time lag between a cycle of stress and a cycle of strain (sec)

t_p = time for a stress cycle (sec)

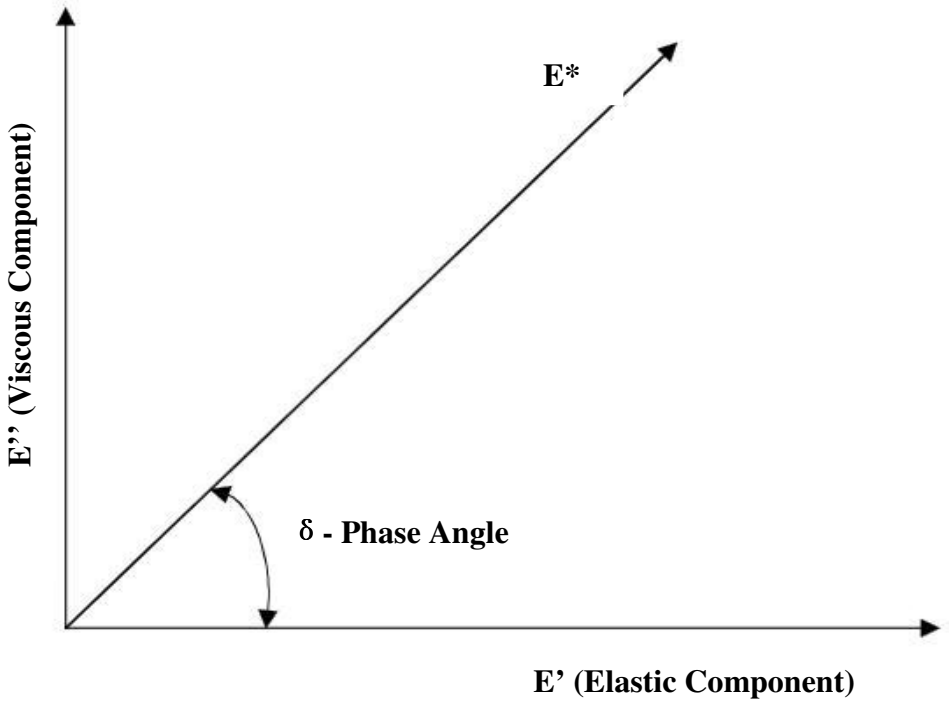

Figure 2-11 Phase Angle and Complex Modulus in Polar Coordinates

For a purely elastic material, $\delta = 0$, and the complex modulus (E*) is equal to the absolute value. For pure viscous materials, $\delta = 90°$ (Muench 2004). This relationship is shown in Figure 2-11.

2.4.5 Poisson's Ratio

In a triaxial test, Poisson's ratio is the relationship of the radial strain to the axial strain, resulting from an applied load in the axial direction. When continuous radial confinement is applied to a sample in triaxial testing, radial and axial strains are monitored directly, and Poisson's ratio can be expressed as (Berthelot 1999):

$$\nu(t) = \frac{\varepsilon_{22}(t)}{\varepsilon_{11}(t)} = \frac{\varepsilon_{33}(t)}{\varepsilon_{11}(t)} \quad \textbf{(2-11)}$$

Where:

ν = Poisson's Ratio in radial versus axial directions

$\varepsilon_{11}(t)$ = Strain in axial coordinate direction

$\varepsilon_{22}(t)$ = Strain in radial coordinate direction

$\varepsilon_{33}(t)$ = Strain in radial coordinate direction

Because particulate composite materials are capable of generating significant ranges in Poisson's ratio, Poisson's ratio can be a critical measure of mechanistic behaviour of road materials and can significantly influence the behaviour of road structures (Berthelot 1999).

2.5 Moisture Sensitivity Testing of Granular Pavement

Moisture has been a significant problem affecting granular pavement performance, especially for areas with free-thaw cycles and/or high ground water table. As a result, the moisture sensitivity of granular materials is of great engineering interest with regard to design and construction of granular pavement systems.

2.5.1 Indirect Tension Test

Indirect tension test was initially used in Superpave™ to determine the creep compliances and indirect tensile strengths of asphalt mixtures at low and intermediate pavement temperatures. These measurements can be used in performance prediction models to predict the low-temperature thermal cracking potential and intermediate-temperature fatigue cracking potential of asphalt pavements (FHWA 2006).

Procedures for conducting indirect tensile strengths and resilient modulus of asphalt mixture is described in AASHTO T322 (AASHTO 1996) and ASTM D4123 (ASTM 1982). The specimen should have a minimum height of 5 cm and a minimum diameter of 10 cm for aggregate up to 25.4 mm maximum size, or, a height of at least 7.62 cm and a minimum diameter of 15 cm for bigger aggregate up to 38.0 mm maximum size (ASTM 1982). The apparatus is shown in Figure 2-12.

Figure 2-12 Indirect Tensile Strength Testing Apparatus at PSI Technologies Inc.

The indirect tensile strength is calculated as the following equation:

$$S_t = 2P_{ult} / \pi DT \quad \textbf{(2-12)}$$

Where:

D = the diameter of the specimen

P = the ultimate applied load

T = thickness of specimen

The vertical dimetral tensile and compressive stresses may be expressed mathematically for plane stress and plane strain as follows (Berthelot 2006). The stress state is illustrated in Figure 2-13. The equations of strains under plane stress condition are shown as follows:

Plan stress (Dimetral Axis):

$$\sigma_{11r} = \frac{2P}{\pi td} \quad \textbf{(2-13)}$$

$$\sigma_{22c} = -\frac{2P}{\pi t}\left(\frac{2}{d-2y} + \frac{2}{d+2y} - \frac{1}{d}\right) \quad \textbf{(2-14)}$$

Where:

d = the diameter of the specimen

P = the ultimate applied load

t = thickness of specimen

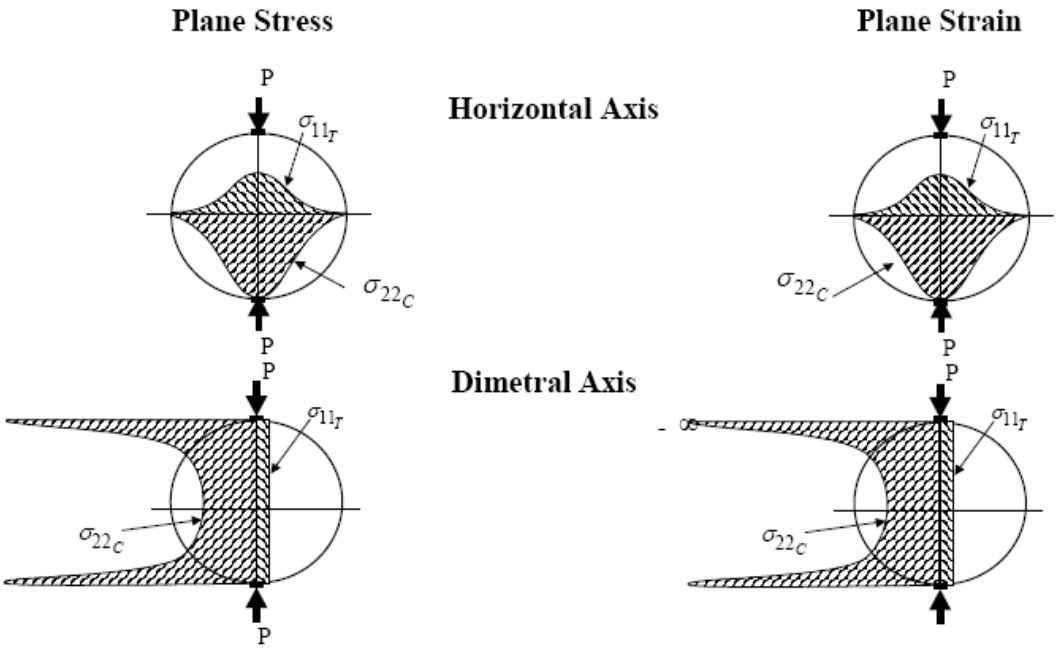

Figure 2-13 Stresses of Indirect Tension Test under Plane Stress and Plane Strain Conditions

Australian Asphalt Pavement Association (AAPA) recommends a minimum indirect tensile strengths of 100 KPa for various stabilized base materials in Australia (AAPA 1998).

Many laboratory tests have been employed to evaluate moisture susceptibility of pavement materials. However, no test to date has attained wide acceptance (Roberts et al. 1996). In fact, just about any performance test that can be conducted on a wet or submerged sample can be used to evaluate the effect of moisture on pavement materials by comparing wet and dry sample test results. Superpave™ recommended the modified Lottman Test as the current most appropriate testing for asphalt concrete (TRB 2007).

Modified Lottman test is documented in AASHTO T 283 (AASHTO 1986). This test compares the indirect tensile strength test results of a dry sample and a sample exposed to water/freezing/thawing. The test sample is subjected to saturation, an optional freeze cycle, followed by a freeze and a warm-water cycle before being tested for indirect tensile strength. Test results are reported as a tensile strength ratio as follows:

$$TSR = \frac{S_2}{S_1} \quad \textbf{(2-15)}$$

Where:

TSR = tensile strength ratio

S_1 = average dry sample tensile strength

S_2 = average conditioned sample tensile strength

Typically, a minimum TSR of 0.70 is recommended for the modified Lottman method, which should be applied to field-produced rather than laboratory-produced samples (Roberts et al. 1996). For laboratory samples produced in accordance with AASHTO TP 4 (Method for Preparing and Determining the Density of Hot-Mix Asphalt Specimens by Means of the Superpave Gyratory Compactor), AASHTO MP 2 (Specification for Superpave Volumetric Mix Design) specifies a minimum TSR of 0.80 (Muench 2004).

Typically, indirect tension testing is employed on hot mix asphalt samples. However, as long as the sample is cohesive and sticks well during testing, the indirect tension test can also be used to characterize the granular materials.

2.5.2 Tube Suction Test

Climatic resistance to moisture and freeze-thaw cycles is a very important performance indicator of stabilized granular base materials. It is paramount to evaluate granular material climatic durability in the design and evaluation of granular pavement stabilization.

The tube suction test was one of the tests developed to evaluate aggregate climatic durability. The tube suction test was developed by Saarenketo and Scullion at the Texas Transportation Institute (TTI) for investigating the suction properties of various base course aggregates in 1994 and 1995 (Berthelot et al. 2007). The tube suction test was further refined and used at the Tampere University of Technology, the Lappi Region of Finland, and at the University of Saskatchewan (Saarenketo 2006, Berthelot et al. 2007).

The tube suction test monitors the capillary rise of moisture within a cylinder compacted soil, assessing the material's moisture susceptibility. The dielectric value and surface conductivity value at the surface of the sample are measured with a probe, providing an estimation of the free or unbound water within the soil specimen, as seen in Figure 2-14 and Figure 2-15 (Barbu et al. 2003).

The dielectric value is a measure of the volumetric moisture content and the state of molecular bonding in a material. Low dielectric values indicate the presence of tightly absorbed and well arranged water molecules. Granular bases or stabilized bases with low dielectric values normally have better strength properties (Little 2000).

The electrical conductivity indicates the material ability to conduct an electric current. The electrical conductivity is an indication of the amount of ions dissociated from the free water. A higher electrical conductivity is associated with more ions present in the pore water system, which may indicate less climatic durability (Little 2000).

In the tube suction test, base aggregate samples are compacted at optimum moisture with a gyratory compactor into a 305 mm high and 152 mm diameter plastic tube. After compacting, a perforated cover is placed on the bottom of each tube. The samples are dried in an oven at 45 °C until significant changes in mass are no longer observed. The samples are then allowed to cool at room temperature for at least two days. When their temperature has stabilised, the samples are placed in a dish containing about 20 mm of deionised water as seen Figure 2-16 (Saarenketo 2006). The samples are left absorbing water and the surface dielectric and conductivity value are monitored by the probe at certain time intervals.

A plot of surface dielectric values versus time provides the basis for performance classification, as seen in Figure 2-17. The poorest performing materials exhibit final dielectric values higher than 16, which is considered to be a threshold value (Barbu et al. 2003).

Figure 2-14 Tube Suction Test Devices (Courtesy Roadscanners)

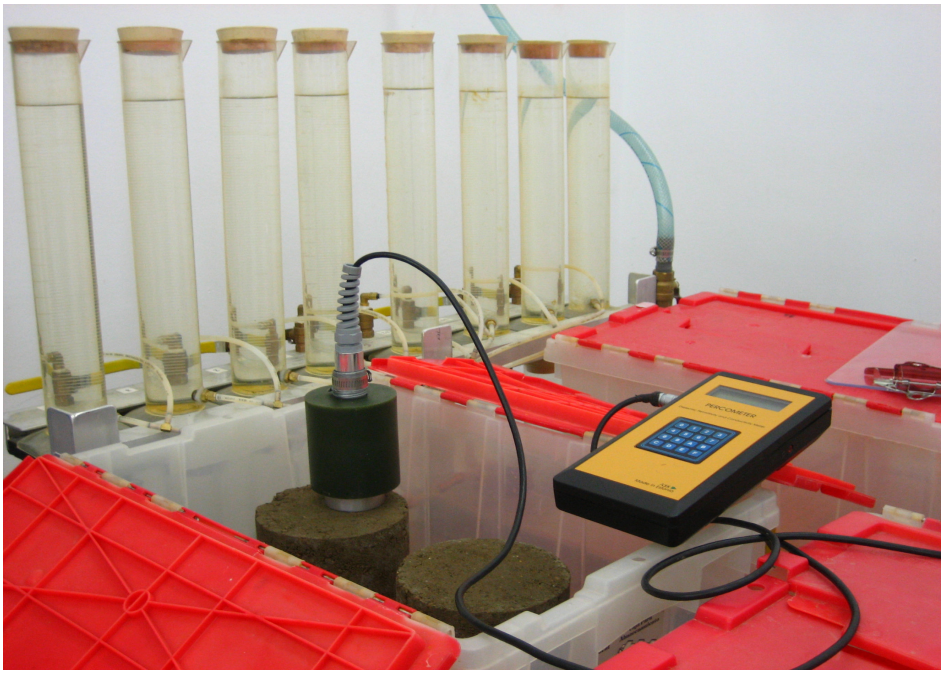

Figure 2-15 Tube Suction Test Devices (Courtesy PSI Technologies Inc.)

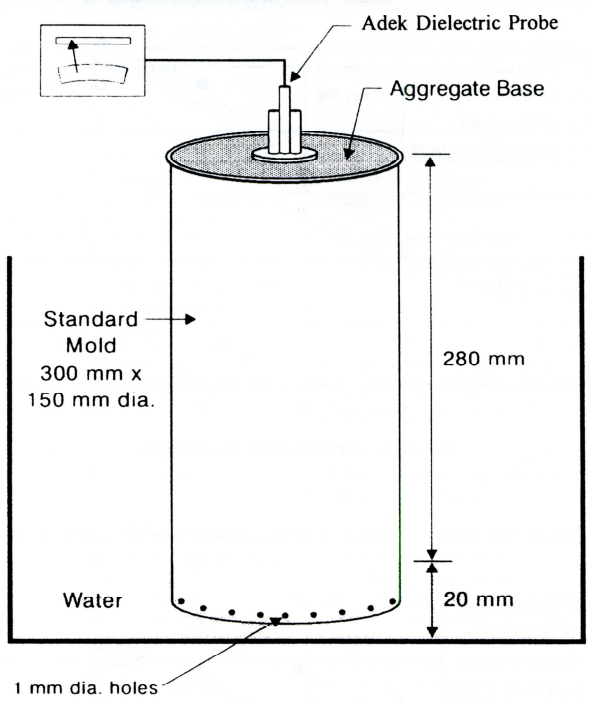

Figure 2-16 Illustration of Tube Suction Test (Scullion and Saarenketo 1997)

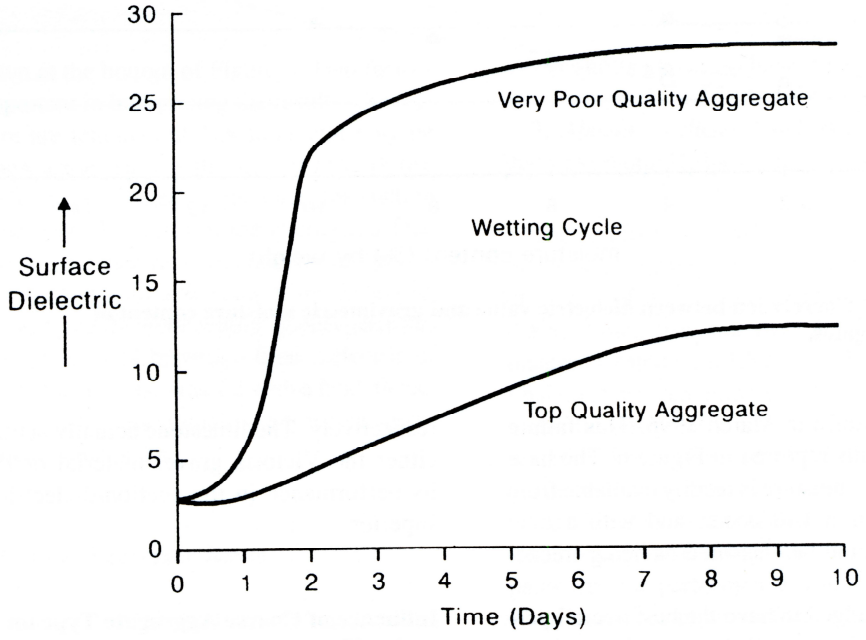

Figure 2-17 Typical Plots of Tube Suction Test (Scullion and Saarenketo 1997)

The tube suction test was found to be adequately repeatable at higher dielectric values (greater than 10) while the test is relatively not repeatable at dielectric values generally below 10 (Guthrie et al. 2001). Therefore, the maximum dielectric value should be chosen to include the categorical moisture susceptibility rankings of interest (Guthrie et al. 2001). Moreover, different conditions for conducting the tube suction test were evaluated, such as the tube diameter, the effect of compaction energy and size of clods. The results from the tests conducted using smaller tube diameters are similar to those provided from tests using "classic" tubes. In the range of compaction energies used, the final dielectric values were similar for samples compacted at the Proctor optimum moisture content (Barbu et al. 2003).

The University of Saskatchewan has been using the tube suction test to rate aggregate moisture susceptibility since the late 1990's. Tube suction tests conducted at the University of Saskatchewan were generally modelled after the tube suction test developed by TTI with the exception that the moisture conditioned samples were not confined, to allow the samples to expand freely as they do in the field. The tube suction test has been successfully employed to evaluate the climatic durability of various Saskatchewan granular pavement materials (Berthelot et al. 2005, Berthelot et al. 2007)

2.6 Structural Design and Analysis of Stabilized Granular Pavements

Pavement structural design, including granular base thickness design, is a comprehensive and iterative process. Due to the large number of required design inputs, as well as the number of potential solutions, pavement design involves the selection of an optimum design under a given inference of field performance and cost. Figure 2-18 illustrates the general pavement design procedure.

There are numerous methods of measuring the imposed traffic loading including Average Annual Daily Traffic (AADT) with a factor for percent trucks, maximum wheel loads allowed, number of trucks and buses using roads, Equivalent Single Axle Load (ESAL). Methods used to measure soil and aggregate quality includes those based on soil classification, soil index properties, and soil strength test of various types. For example, the methods used to estimate soil strength include: Group Index (GI), California bearing

ratio (CBR), Modulus of Subgrade Reaction (K), Resistance Value (R), and Resilient Modulus (Mr).

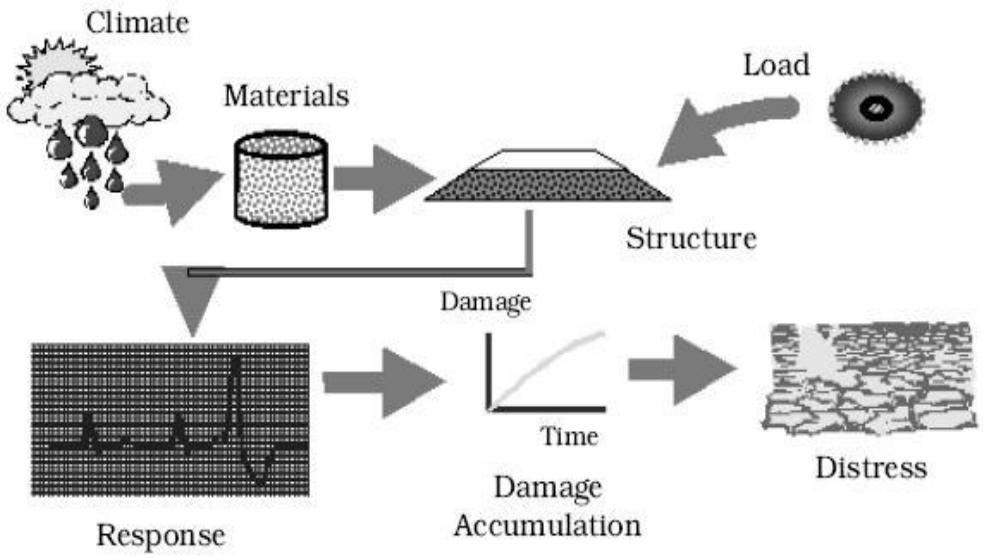

Figure 2-18 General Pavement Design Procedure (C-SHRP 2002)

2.6.1 Introduction to Structural Design across Canada

Currently, the primary methods to perform pavement structural design are stated below (Berthelot 2005).

- Empirical based layer equivalents
- Surface deflection methods
- Elastic theory based methods (Shell and Asphalt Institute Method)
- AASHTO method
- Mechanistic-empirical method

Across Canada, transportation agencies have developed standard pavement thickness equivalencies based on years of experience. Unlike the Federal Highway Administration (FHWA) in the United States, there is no single agency responsible for funding pavement construction and rehabilitation or setting pavement design standards in

Canada. Pavement design for the primary highway network in Canada is under provincial jurisdiction with the federal government responsible for national parks roadways. Each agency is free to use whatever design procedure they choose for pavement design and rehabilitation (C-SHRP 2002). A summary of the general pavement design methods and parameters used by the provinces and the Federal Government are given in Table 2-6.

2.6.2 Saskatchewan MHI Modified Shell Method

Shell International Petroleum published the Shell Pavement Design Manual (SPDM) in 1978 based upon a multi-layer linear elastic analysis (Whiteoak and Read 2003). The Shell Pavement Design Manual was presented in the forms of graphs, charts, and tables. The theory behind the Shell nomographs is based upon a three layer structure consisting of an asphalt layer on a base of unbound granular base overlaying the existing subgrade (Whiteoak and Read 2003).

Table 2-6 General Pavement Design Methods across Canada (C-SHRP 2002)

Agency	Subgrade Soil Classification	Subgrade Soil Adjustments for Strength	Method of Thickness Design	Layer Thickness Adjustments for Moisture/Frost
British Columbia	Drilling Unified Soil FWD	---	AASHTO 93 FWD	AASHTO guidelines
Alberta	Resilient Modulus-based on back-calculated value from adjacent section	Modulus correction value of 0.36	AASHTO 93	Drainage Coefficient
Saskatchewan	CBR (from G.I.)	Soaked CBR	Shell	Modify Subgrade Support Value CBR
Manitoba	Group Index Mr	---	AASHTO 93	Frost Susceptible soil adjustment
Ontario	Mr CBR K-value	OPAC Effective Mr	AASHTO 93 Adapted for local conditions	Drainage Coefficient
Quebec	Mr	Effective Mr	AASHTO	MTQ frost protection curve
New Brunswick	---	---	Shell used originally to determine basic strength	---
Prince Edward Island	CBR	Soaked CBR	Benkelman Beam	---
Nova Scotia	CBR Mr	Soaked CBR	AASHTO 93	---

Subgrade soil adjustments compensate for the seasonal variance of subgrade strength parameter

Saskatchewan MHI uses a series of surfacing thickness design charts commonly called the Saskatchewan Thickness Design Curves to estimate the surfacing structure thickness. The design charts were first developed by Shell Research. The charts were modified for Saskatchewan conditions, and exist for a range of subgrade CBR 2.5 to 20 (MHI 1981).

In Saskatchewan, the traffic evaluation is the estimation of the number of equivalent 80 kN single axle passes per lane which is expected to occur over the design life of the highway. The design life for new highway and rehabilitation projects is typically 15 years. Therefore the N_{15} is a design parameter which is calculated as the number of equivalent 80 kN single axle passes and the subscript 15 means the passes are occurring over 15 years. The information required to perform a traffic evaluation is as follows (MHI 1981).

- AADT-average annual daily traffic
- % commercial- percentage of AADT that is commercial truck traffic
- Growth rate-the rate at which traffic will increase over 15 years
- Directional split- the percentage of traffic in each of the design lanes
- Equivalency factor-the equivalent single axles per commercial vehicle

The design criteria of Saskatchewan methods are to control the horizontal tensile strain at the bottom of asphalt layer and the vertical compressive strain at the top of subgrade. Various combinations of asphalt concrete and granular base course will result in the same vertical compressive strain for a given traffic loading as shown in Figure 2-19. In the design chart, the subgrade design CBR value is specified in the upper left-hand corner. Each chart displays asphalt concrete thickness on the vertical axis and granular thickness on the horizontal axis. Each chart contains a series of curves representing various levels of design traffic loadings in terms of the number of 80 kN axle passes expected in the design lane during the life of the structure. Each curve represents the surfacing thicknesses which will meet the criteria of limiting the horizontal tensile and vertical compressive strains in the asphalt-bound layers and in the subgrade respectively.

Any combinations of structure below the ESAL profile will result in premature subgrade rutting and any combination above the curve will delay in subgrade rutting at given traffic loading. The design charts assume that various combinations of asphalt concrete and granular base course for a given traffic loading will give the same horizontal

tensile strain at the bottom of the asphalt concrete layers as shown in right of Figure 2-19. Both the requirements in Figure 2-19 must be met; the curves from each of the figures can thus be combined as shown in Figure 2-20. Any point to the left and below the point of the intersection does not meet both criteria (MHI 1981). As seen in Figure 2-21, each Saskatchewan curve is divided into three zones by vertically-oriented lines. The zones are designated, from right to left as CBR 80, 40, 20 (MHI 1981). Given the subgrade CBR and the design traffic loading, a series of equivalent structures can be selected from the appropriate design thickness chart. The optimal alternative will meet the minimum thickness and be most cost effective.

A typical granular base pavement for Saskatchewan MHI commonly consists of 50 to 100 mm of asphalt concrete, 100 to 180 mm of granular base and 50 to 250 mm of granular subbase. A typical standard pavement structure is illustrated in Figure 2-22 (MHI 1982).

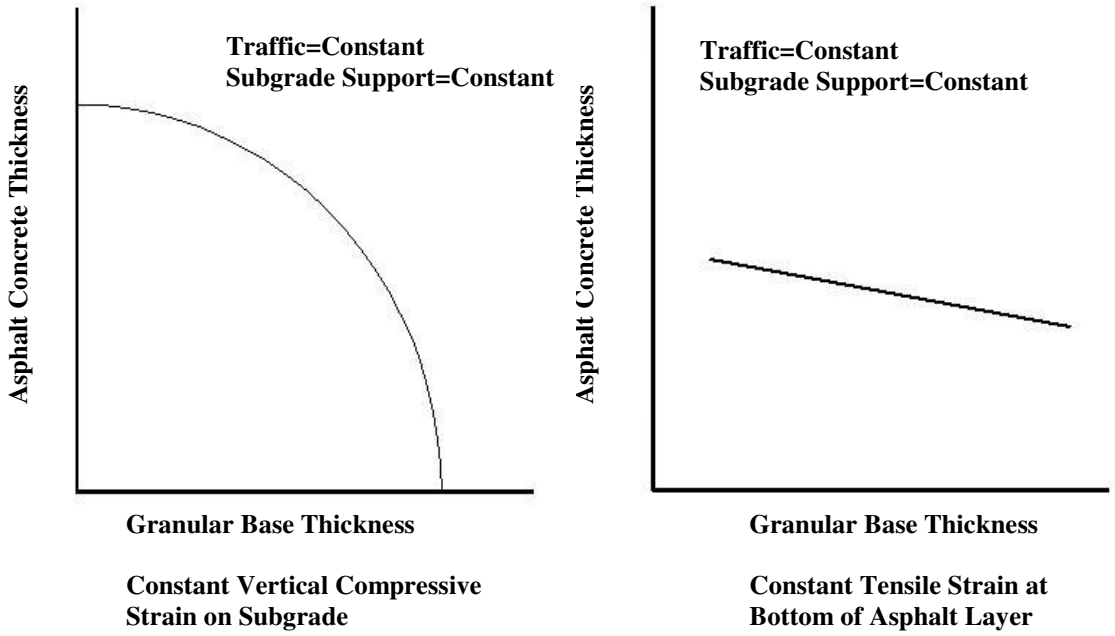

Figure 2-19 Thickness Curves for Constant Vertical and Horizontal Strain (after MHI 1981)

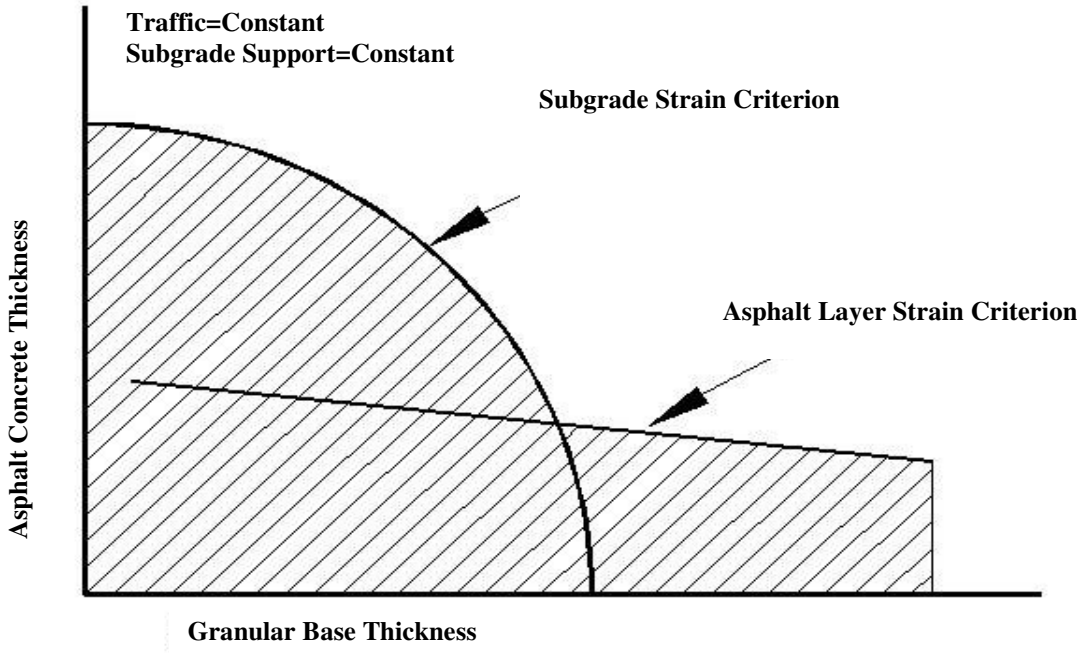

Figure 2-20 Simplified Saskatchewan Design Curve (after MHI 1981)

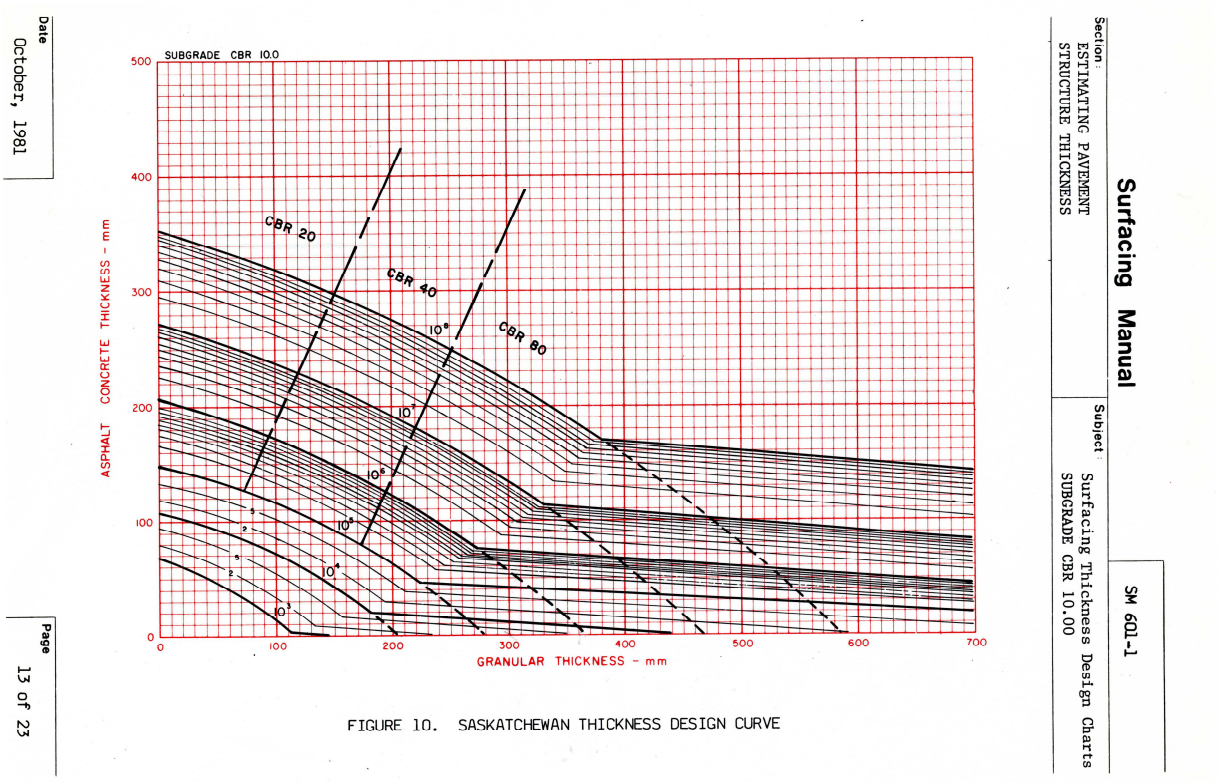

Figure 2-21 Saskatchewan Thickness Design Curve (after MHI 1981)

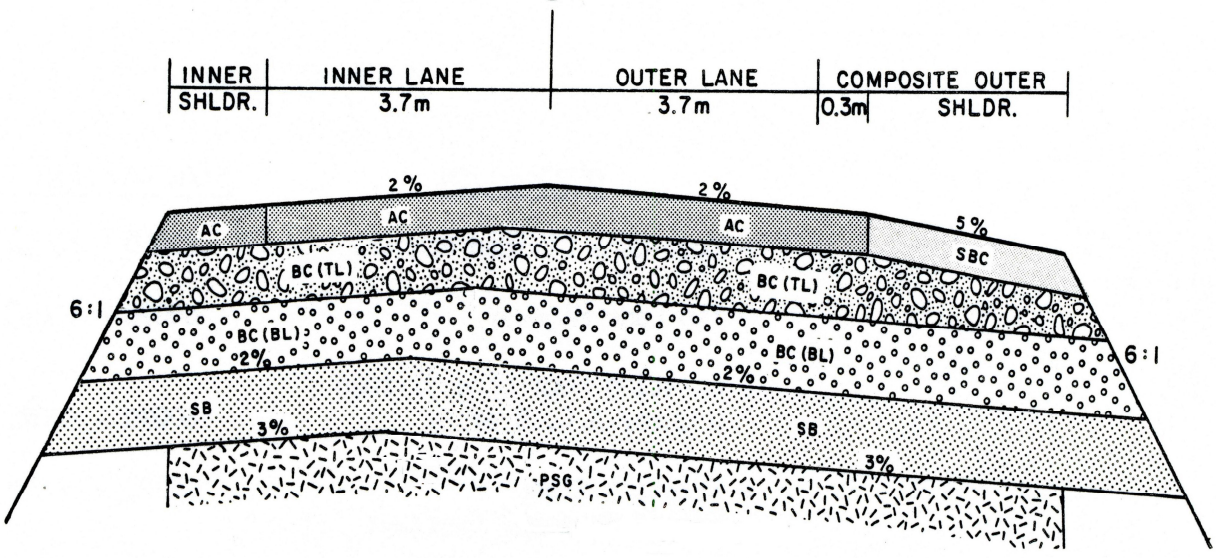

Figure 2-22 Typical Four Lane Divided Highway Standard Pavement Using Granular Base (after MHI 1982)

Limitations of Saskatchewan MHI pavement thickness design curves include (Marjerision 2005; Berthelot 2007):

- Asphalt stiffness is equivalent to a 150-200 A penetration grade asphalt.
- The options for type of pavement structure are limited only in CBR 20, CBR 40 and CBR 80 material.
- Structural design assumes a high dry newly prepared subgrade.
- MHI system is not calibrated for recycled systems.
- The base of MHI design system is AASHO road test which employed 5-6 axle trucks instead of B-train trucks.

Also, the Saskatchewan MHI pavement thickness design system is based on multi-layer elastic theory and two critical strain criterions. The pavement structure is actually not linear elastic material and the failure mechanism is not simply limited to the two critical strains.

In summary, the Saskatchewan MHI modified Shell design methodology is not appropriate for the design of thin granular pavement systems. The Saskatchewan MHI protocol is also not appropriate for pavement rehabilitation design using recycled and/or stabilized road material systems.

2.6.3 Mechanistic Based Structural Design of Granular Pavement Stabilization and Recycling

Until now, few thickness design guides have been published specifically for stabilization and/or cold in-place recycling. Some agencies assumed that the structural capacity of the recycled and/or stabilized material is equal to that of conventional materials. Conventional material is replaced with an equal thickness of recycled and/or stabilized material without a formal structural design (Epps 1990).

Due to the limitations of the assumption of equivalent strength of recycled materials and conventional materials, a structural evaluation is strongly recommended

prior to cold in-place recycling and stabilization thickness design. Besides the laboratory preparation and testing of recycled/stabilized mixtures for the structural design, non-destructive deflection testing of existing pavement should be used to determine the overlay or surface course thickness required when cold recycling (AASHTO-AGC-ARTBA Joint Committee1998).

Wirtgen is a pioneer firm in stabilization and recycling worldwide. Wirtgen has developed three methods as guidance for cold recycling and stabilization structural design in its Cold Recycling Manual in 2004 (Wirtgen 2004). Namely the structural number approach, mechanistic analysis and the stress ratio limit method. The design manual suggests that the design methods should be selected in accordance with increasing structural capacity requirements, as illustrated in Figure 2-23.

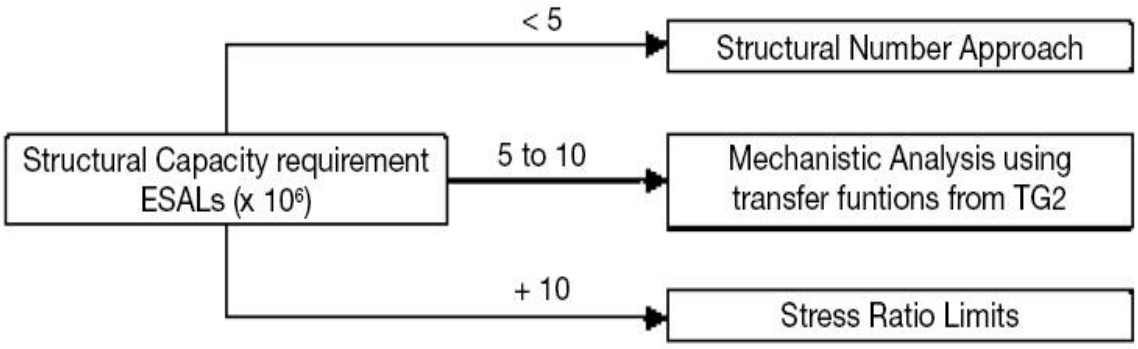

Figure 2-23 Guidelines for Selecting the Appropriate Design Method

Indirect tension test is typically used to determine the resilient modulus of samples of stabilized materials, and the modulus is used to determine a structural coefficient, a_2, for overlay design with the AASHTO guide. No figures exist in the AASHTO 1993 guide specifically for cold recycled mixtures and determining an a_2. However a_2 is determined in some instances using the recommendations in the AASHTO guide covering bituminous-treated bases. The a_2 values normally being used for cold recycled layers with asphalt emulsion as the additive range from 0.25 to 0.35 (AASHTO-AGC-ARTBA Joint Committee1998) Another research on the foamed asphalt stabilized base calculates a_2 to be 0.18 for foamed asphalt stabilized base by falling weight deflectometer (FWD) testing and backcalculation (Romanoschi *et al.* 2003).

The Asphalt Institute and Chevron methods are also available as the form of design charts for cold in-place recycled materials, depending on gradation (Asphalt Institute 1983; FWHA 2007). However, these methods are limited to certain gradation by experience, which are hard to apply when the design inputs vary from place to place.

2.6.4 Structure Analysis and Modeling

Engineers have always been interested in the behaviour of the materials of pavement structures. However, the exact analytical solution for an elastic continuum was not developed until the1940s. Burmister presented the first solution for two elastic layers in 1943 and then expanded his theory to three layer elastic systems for representative loading conditions in 1945. A Burmister two layer pavement structure is illustrated in Figure 2-24. Burmister developed and presented the general equations and obtained the solutions by assuming a stress function involving Bessel functions and exponentials (Burmister 1943; Burmister 1945).

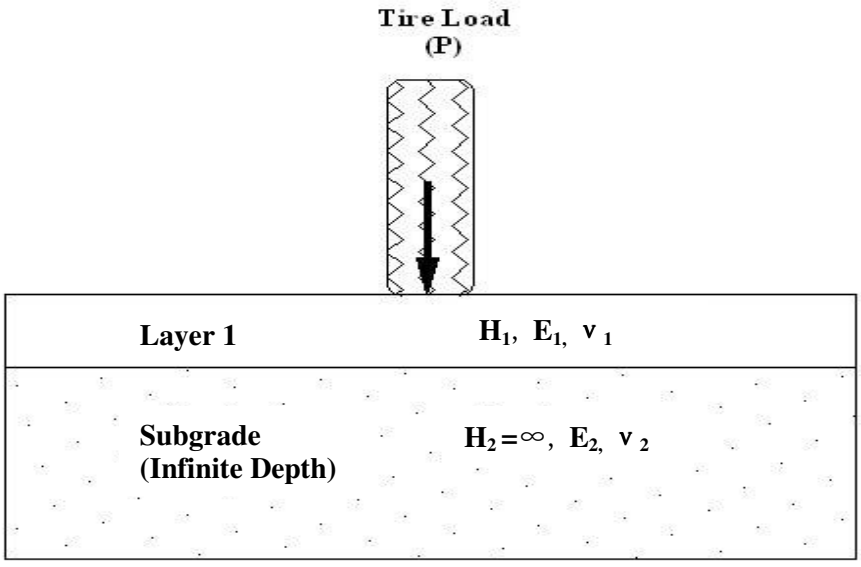

Figure 2-24 Burmister Two Layers Linear Elastic Model (Berthelot 1999)

Burmister's layered linear elastic pavement analysis requires several simplifying assumptions in order to satisfy the requirement of calculation:

- Each layer is homogeneous, isotropic, and linear elastic.
- Each layer is weightless.
- The pavement structure has a semi infinite subgrade layer and finite thickness layers above.
- Continuity exists throughout the road structure and across the boundaries.
- There are no applied tractions outside the applied wheel loads.

Acum and Fox (1951) extended the theory to a three layer system based on a wide range of pavement parameters. Shiffman (1962) published the solutions for multilayered systems. Whiffin & Lister (1963) and Skok & Finn (1963) illustrated how layered elastic analysis could be used pavement design. Peattie and Dorman presented several concepts, which later became a part of the Shell pavement design methodology (Peattie 1963; Monismith 2004). Many other researchers had also contributed to the developing of using linear elastic analysis to analyze pavement structures.

Given the improved computation capacities, many computer programs like ELSYM and BISAR have been developed based on linear elastic layered pavement theory. ELSYM was developed at University of California, Berkeley by G. Ahlborn (Ahlborn 1972). BISAR developed by Shell, which considers not only vertical loads but also horizontal loads, is another widely used program (Shell 1978). Other widely used compute programs based on linear elastic theory include CHEV (Warren and Dieckmann 1963) and CIRCLY (Wardle 1977).

Although the multilayered elastic system is widely used and accepted; it is, at best, a rather poor approximation of the actual pavement system. Most pavement materials are not linear elastic. Many experience elastic deformations for some range of loading, and then viscous, plastic, and visco-elastic deformations occur with increased stress levels. The rates of these deformations are stress dependent. The material properties often change with time, temperature and moisture levels. Furthermore, the material properties are neither isotropic nor uniform because the material is often particulate in nature. The pavement layers are also not infinite in horizontal extent (Rohde and R.E.Smith 1991).

To overcome the limitations of linear elastic programs, two solutions of linear viscoelastic materials pavement structures were developed: VESYS (Kenis 1978) and VEROAD (Nilsson et al. 1996).

The finite element technique has been applied to pavement systems since the 1960s as another powerful tool to over come the limitations of linear elastic systems (Wilson et al. 1967; Barksdale 1973). The finite element methods allow for the nonlinear elastic modeling of pavement materials. Each element in the pavement system is assigned an independent anisotropic material property thus modeling the pavement more realistically than the purely linear elastic layered model. For granular and fined-grained materials, stress dependent material models and failure criteria are used to define the structural properties of each element in the grid. The structural stiffness properties of each element are obtained using energy principles, approximate displacement functions. The analysis of each load deformation problem is based on an iterative process (Zienkiewicz and Taylor 2000). A summary of current available solutions for asphalt concrete pavement analysis is shown in Table 2-7 (Monismith 2004).

Table 2-7 Summary of Available Computer Programs for Pavement Analysis

Program	Theory	Number of Layers (max)	Number of Loads (max)	Program Source
BISAR	MLE	5	10	Shell
ELSYM	MLW	5	10	FHWA
PDMAP	MLW	5	2	NCHRP I-10
JULEA	MLE	5	4+	USACE WES
CIRCLY	MLE	5+	100	MINCAD, Australia
VESYS	MLE or MLVE	5	2	FHWA
VEROAD	MLVE	15	/	Delft Technical University
ILLIPAVE	FE	/	1	University of Illinois
FENLAP	FE	/	1	University of Nottingham

MLE – multilayer elastic, MLVE - multilayer viscoelastic, FE – finite element

2.7 Field Non-destructive Deflection Testing of Granular Pavements

Non-destructive deflection testing of pavements has gained acceptance and popularity since the first Benkelman Beam was developed at the Western Association of State Highway Organizations (WASHO) road test in 1954 (TRB 1954). By measuring the pavement response induced by this load, the structural integrity or stress-strain properties of pavement structure can be determined (Rohde and R.E.Smith 1991). Deflection testing has become popular because it is rapid, relatively inexpensive, and the pavement materials are tested in a truly undisturbed state. Three distinct types of measuring devices were developed.

2.7.1 Static Deflection Equipment

Static deflection equipment is used to measure pavement surface deflections under static or slow moving loads. The most commonly used static equipment includes the Benkelman Beam. This provides deflection measurements at any number of points under a non-moving or slow moving load. This device was developed at WASHO Road Test in 1952 and was the most widely used device until recently (Bandara and Briggs 2004). A common characteristic of these devices is the relative horizontal motion between the load and the testing point during the time of testing. The vehicle velocity during these tests is generally less than 3 mph, resulting in loading time much greater than typically found with moving wheel loads (Hudson et al. 1987). The significantly long time needed for testing also results in a potential safety issue for the testing equipment and crews.

The main advantages of these static/slow moving deflection testing devices are simplicity, low instrument cost and the possibility of utilizing realistic load levels. The disadvantages of these devices are that they are slow, labour intensive, do not provide a "true" deflection basin and suffer relatively poor precision and bias (Bandara and Briggs 2004).

Figure 2-25 Benkelman Beam Testing (Courtesy of Dr. Curtis Berthelot)

2.7.2 Steady State Deflection Equipment

Steady state equipment uses a relatively large static preload and a sinusoidal vibration to the pavement with a dynamic force generator. With some devices, it is possible to change the magnitude and the frequency of the applied load (Bandara and Briggs 2004). These devices, like the Dynaflect, the Road Rater, and the Cox Device, firstly apply a static preload to the pavement. Counter-rotating masses or an eletro-hydraulic system then generates a steady-state harmonic vibration in the pavement.

The steady state deflection equipment is stationary when measurements are taken with the force generator (counter rotating weights) operating and the deflection sensors (transducers) lowered to the pavement surface. A major problem with this equipment is that the relatively large static preload may adversely affect the accuracy of the test (Bandara and Briggs 2004). The large preloads required to keep such a device in contact

with the pavement surface have been found to stiffen the pavement system (Hoffman and Thompson 1981).

2.7.3 Impulse Deflection Equipment (FWD)

The Dynatest, KUAB, and Phoenix Falling Weight Deflectomers are included in the third group called the impulse devices. They produce a transient load to the pavement by dropping a load from a predetermined height onto a base plate sitting on the pavement surface. By changing the drop height or weight of the load, the magnitude of the impulse can be adjusted (Little 1999). The advantage of an impact load response measuring device over a steady state deflection measuring device is that it is quicker, the impact load can be easily varied and it more accurately simulates the transient loading of traffic (Muench 2004).

The FWD is popular because of its technical suitability. It is reported that among the different devices and methods analyzed, it appears that the FWD best simulates pavement under a moving truck load (Hoffman and Thompson 1981). Based on measured responses of an instrumented pavement section, it's found that the pavement's stress and strain conditions during an FWD test are very similar to the conditions under a heavy vehicle load (Ullidtz 1987).

All impulse type non-destructive testing devices produce a transient load to the pavement surface typically lasting 25 to 30 ms. The impulse load is generated by a falling mass from one or more predetermined heights. The resulting load pulse is transmitted to the pavement as a half sine wave. The peak deflections and load magnitude are captured, reported and automatically stored. Testing procedures with impulse load devices are documented in ASTM 4694 and ASTM D4695.

Deflections are most commonly measured with velocity transducers (seven or more) which are mounted on a bar and automatically lowered to the pavement surface with the loading plate. One transducer is located in the center of the loading plate and others are located at different distances from the loading plate. (Bandara and Briggs 2004).

The analysis of deflection data has gone through continuous improvements during the last few decades. Most techniques developed fall into two categories: deflection parameters and backcalculation of layer moduli.

Figure 2-26 Dynatest HWD (Courtesy of PSI Technologies)

In Saskatchewan, FWD has been adopted and employed for decades. FWD was successfully used to measure the pavement structural integrity of Saskatchewan's road network at both project and network levels (PSI 2006). Most of the applications in Saskatchewan thus far are pavement evaluation for design and quality assurance purposes. However, falling weight deflectometer is also gaining more and more applications in research activities in Saskatchewan, such as developing asset management for municipal road networks and for developing mechanistic based ESAL factors for local roads (Berthelot et al. 2007, Thomas et al. 2007).

2.8 Chapter Summary

Chapter two summarizes the findings of a literature review performed to evaluate state of the art technologies and research results related to this research. The findings and conclusions of this chapter are described below.

The requirements for satisfactory granular base materials typically are stability (strength) and climatic durability (moisture and freeze-thaw). The main specification for the granular base is the gradation requirement. In order to provide a satisfactory granular pavement material, laboratory tests have been adopted and traditionally used for characterizing the properties of the granular material. Chapter two contains a selection and investigation of several laboratory tests such as gradation, CBR, et al., which are considered as conventional granular material characterization methods. The testing procedures, specifications, advantages, and disadvantages are summarized.

Stabilization and recycling technologies of granular pavement are introduced in this chapter. The two most common types of stabilization, hydraulic and bituminous stabilization, were investigated and discussed. Stabilization and cold in-place recycling systems for granular pavements have shown remarkable advantages such as pavement thickness reduction, energy and material conservation, and significant strength improvement as compared to traditional granular pavement rehabilitation methods.

Moisture has been a significant problem affecting granular pavement performance, especially for areas with freeze-thaw cycles and/or a high ground water table. As a result, moisture sensitivity of granular materials is of great interest for the engineers in the design and construction of granular pavement systems. Indirect tension test and tube suction test have been proven to be two tests which can effectively characterize the moisture sensitivity of granular materials applied in this research.

Other than conventional testing methods, rapid triaxial testing is capable of characterizing mechanistic constitutive relations of granular materials. The main outputs of the RaTT testing are Poisson's ratio, dynamic modulus and phase angle. RaTT is

found to be a time efficient and pragmatic tool to characterize the mechanistic constitutive relations of granular material. As a result, it is proposed to apply RaTT testing to evaluate various stabilized granular materials in this research.

Based on research of pavement design systems across Canada, it is found that the Saskatchewan MHI Shell pavement design system is not appropriate for pavement rehabilitation design using recycled and/or stabilized road material systems. Several innovative design methodologies, particularly for stabilized pavement structure, were briefly introduced and summarized.

Although elastic theory is a simplification of real field material constitutive conditions, linear elastic theory has been the most widely used technology in pavement design and analysis so far. Viscoelastic theory and finite element analysis add more strength and accuracy to the pavement modeling. However, these two modeling techniques are more complex and difficult to apply without the aid of a high performance computer.

The FWD is becoming increasingly popular in pavement evaluation due to its technical suitability. The advantages of the FWD device are that the FWD quickly simulates the transient loading of traffic, as well as providing relatively accurate mechanistic parameters of the pavement structure. As a result, the FWD is proposed to be used in this research to evaluate the pavement integrity of various stabilized structures. The FWD will be used prior to construction to determine the condition of old pavement structures in the design phase. Also, the FWD will be used to evaluate the field performance of stabilized pavement structures after stabilization construction.

CHAPTER 3 PRELIMINARY SITE INVESTIGATION, DESIGN AND CONSTRUCTION

Saskatchewan Ministry of Highways and Infrastructure (MHI) is responsible for maintaining approximately 10,000 km of low traffic volume roads, which accounts for more than one-third of the provincial highway system. Many low traffic volume roads, such as thin membrane surface (TMS), asphalt mat on subgrade (AMOS), and thin granular pavement structures, are rapidly deteriorating due to increasing truck traffic resulting from transportation rationalization, as well as economic development and expansion within the province. As a result, a large portion of the Saskatchewan low volume road system, particularly those roads identified as economic corridors, needs to be strengthened in the next couple decades (Baker et al. 2000; Berthelot et al. 2007).

However, budget constraints render conventional strengthening solutions untenable in many applications. Also, the depletion of aggregate in Saskatchewan is a major problem in many areas of the province. It is estimated that the total gravel demand by MHI is projected to be at 193,289,000 cubic metres by 2049. This gravel demand correlates to an estimated shortage of 45 million cubic metres by 2049. For every 10 km increase in haul there would be an increase of approximately $125,000 per kilometre for a TMS upgrade project (subbase/base/seal) and $73,000 per kilometre for the TMS base overlay project (150 mm plus seal) in Saskatchewan (Marjerison 2004).

Cold in-place recycling and base stabilization are believed to conserve aggregate and offer a more cost effective strategy than conventional upgrade methods. Due to these advantages, cold in-place recycling has served as an economical and conservative solution for structural upgrading of low volume Saskatchewan road network since late 1990s (Baker et al. 2000; Berthelot et al. 2000; Berthelot et al. 2001).

C.S. 15-11 *in situ* granular base between km 5.0 and km 8.0 was selected as a typical thin granular pavement economic corridor recently upgraded to primary weight load rating that is requiring structural strengthening (PSI 2006).

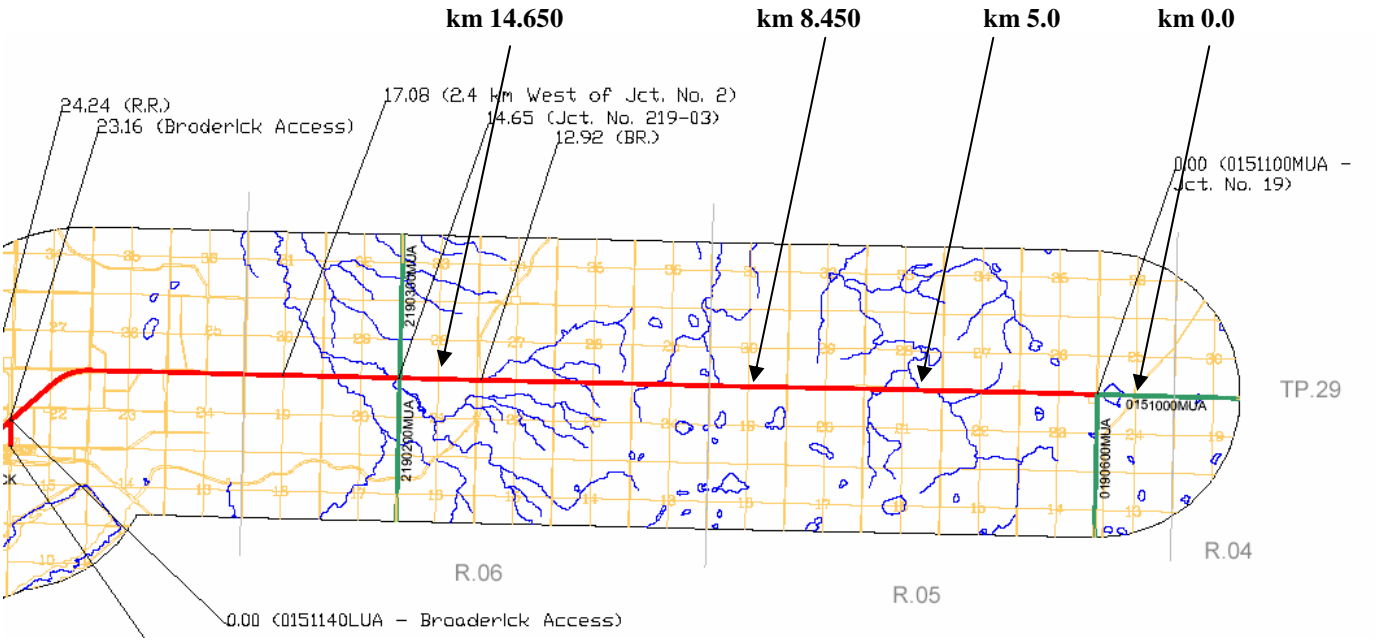

Figure 3-1 C.S. 15-11 Map and Control Limits

This chapter summarizes the visual condition survey prior to construction, the granular base stabilized systems applied, test section layout, and construction process of the C.S. 15-11 test sections. As well, quality control/quality assurance and non-destructive deflection test results across the test sections constructed are presented.

3.1 *A Priori* Pavement Condition Survey

Over recent years, increased commercial transportation has resulted in accelerated pavement deterioration, which has reduced the level of service of C.S. 15-11. The pavement condition of C.S. 15-11 prior to construction was determined to be generally intact with minor potholes, moderate severity rutting, severe shoving, and seal bleeding. A typical photo of the pavement conditions before construction is illustrated in Figure 3.2.

Figure 3-2 Rutting on C.S. 15-11 Pavement Prior to Stabilization Construction

3.2 Test Section Layout

Given the deterioration of C.S. 15-11, Saskatchewan MHI identified the need to rehabilitate C.S. 15-11 using cold in-place recycling and full depth reclamation technologies. The preliminary site investigations with ground penetrating radar and falling weight deflectometer characterization were performed by PSI Technologies Inc**.** Based on visual condition survey as well as non-destructive structural assessment, C.S. 15-11 was found to be relatively structurally sound. However, the double seal surface and granular base were observed to be showing rutting and shear failures, as illustrated in Figure 3.2.

The limits of the test sections proposed were from km 5.0 to km 8.0 (PSI 2006). In addition, as built records show that km 5.0 and km 8.0 on C.S 15-11 is comprised of a relatively uniform granular base thickness, and relatively sound substructure (PSI 2006). According to these factors, Saskatchewan MHI decided to construct C.S. 15-11 test section for research of cold in-place recycling systems in Saskatchewan.

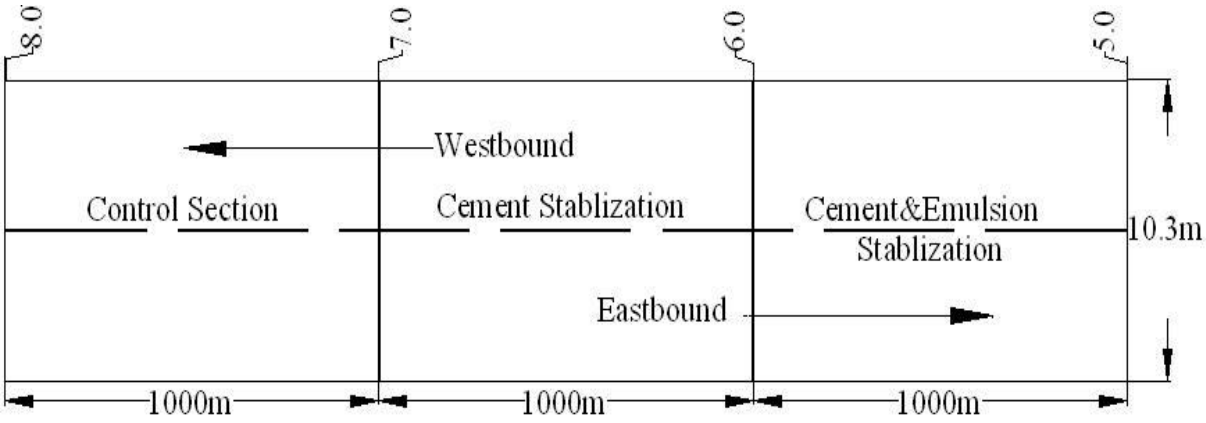

Figure 3-3 C.S. 15-11 Test Section Layout

The test sections constructed on C.S. 15-11 located between Kenaston and Outlook from kilometre limit 5.0 to 8.0. The test site comprises three granular base stabilization test sections. Each test section is one kilometre long. The layout of the test section can be seen in Figure 3-3. Three different granular base rehabilitation/stabilization systems applied were:

- Asphalt emulsion with cement stabilization (km 5.0 ~km 6.0).
- Cement stabilization (km 6.0 ~km 7.0).
- *Remix* and recompaction (km 7.0 ~km 8.0).

3.3 Test Section Structure Design

C.S. 15-11 was initially built as a thin granular base with a double surfacing layer. The as-built record of the Highway 15-11 pavement structure prior to rehabilitation is illustrated in Figure 3-4.

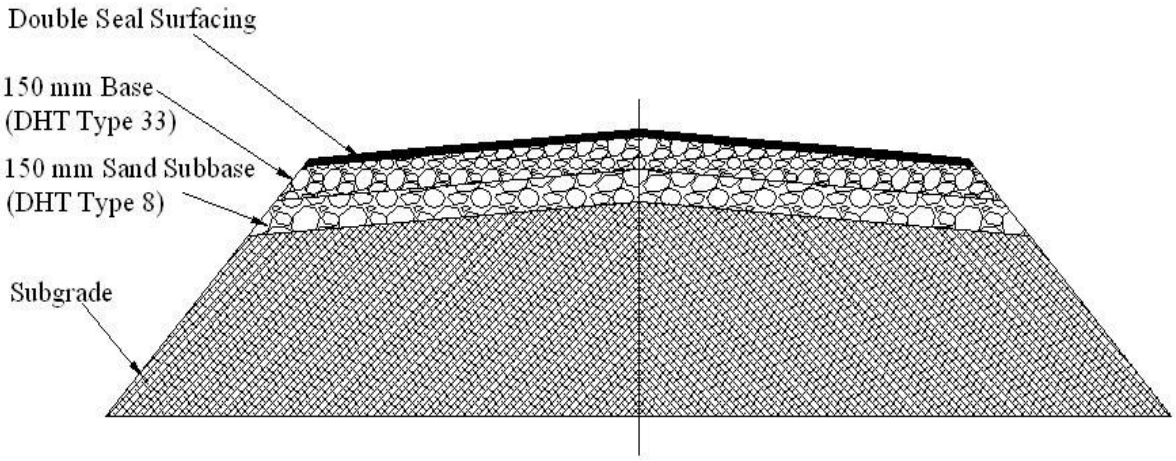

Figure 3-4 C.S. 15-11 Pavement Structure Prior to Construction

As shown in Figure 3-4, the C.S. 15-11 as-built structure was composed of a prepared *in situ* subgrade, 150 mm MHI Type 11 sand subbase, 150 mm Type 33 granular base, and the double seal surfacing. Given the preliminary field investigation, the strengthening thickness is recommended to be 150 mm for two different strengthening systems on C.S. 15-11 test sections. The proposed strengthened structure was recommended to comprise an *in situ* subgrade, 150 mm *in situ* subbase granular, 150 mm strengthened granular base and 40 mm hot mix asphaltic surfacing, as illustrated in Figure 3-5. The details of structure and mix design criterion and considerations can be found in the C.S. 15-11 Design report (PSI 2006).

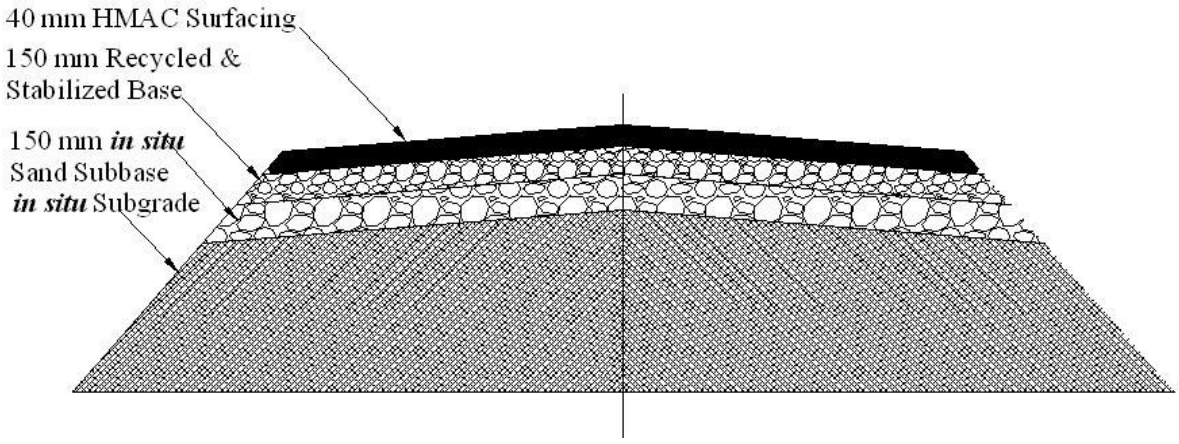

Figure 3-5 C.S. 15-11 Rehabilitation Structural Design Cross-Section

3.4 Test Section Construction Process

Construction of the C.S. 15-11 test sections began on September 25, 2006 and was completed in middle of October, 2006. Saskatchewan MHI conducted all construction operations including milling of the old pavement, incorporating the stabilizers into the recycled material mixture, mixing, compaction, and placing of the asphaltic surfacing. The asphalt surface placement was not completed until August 2007 due to the difficulties in construction and quality control under poor weather conditions in October 2006.

The construction process applied on C.S.15-11 began with pre-milling the existing road structure to the design depth (150 mm). The double seal asphalt surfacing of C.S. 15-11 test section was pre-milled at each construction segment prior to the addition of PSI Cem™ with and without asphalt emulsion, as shown in Figure 3-6. Pre-milling and rotomixing of the deteriorated double seal asphalt surface into the underlying *in situ* granular base layer was performed to achieve a homogeneous rotomixed material before stabilization.

The C.S 15-11 pilot project employed a small rotomixer for milling of old pavement, as shown in Figure 3-6. It was found that the small rotomixer was adequate for rotomixing and reclaiming approximately 5000 m^2 per day. However, the production rate of the small rotomixer, as compared to larger commercial systems, was observed to be much slower, as anticipated. Nevertheless, the Saskatchewan MHI crews were able to incorporate dry cement powder for full depth stabilization and achieved moderate compaction within the daily time limit.

The full depth strengthening process of cement stabilization involved spreading the design quantity of PSICem™ over the pre-rotomixed material, as shown in Figure 3-7. The PSICem™ was then rotomixed into the recycled material, as shown in Figure 3-8. Rotomixing of the PSICem™ into the pre-rotomixed material ensures a uniform blend throughout the upper granular base.

Figure 3-6 Premilling and Rotomixing the Deteriorated C.S. 15-11 Pavement

Figure 3-7 Truck Spreading Cement on C.S. 15-11

Figure 3-8 Rotomixing Cement with Reclaimed Materials on C.S. 15-11

During the full depth strengthening process of cement with emulsion stabilization, the rotomixed material was windrowed into the middle of the road by the motor grader, as shown in Figure 3-9. An asphalt distributor truck then distributed the modified asphalt emulsion onto the road surface in three passes, until it reached the design quantity of asphalt, as shown in Figure 3-10 and Figure 3-11. The rotomixer was used to rotomix the stabilized system to achieve the homogeneity.

After rotomixing the stabilizer to the specified depth, a motor grader was used to cross blade and shape the reclaimed material, as shown in Figure 3-12 . The reclaimed material was then compacted by the pneumatic rollers to obtain a smooth surface with the designed cross slopes gradelines and the required density, as illustrated in Figure 3-13.

Figure 3-9 Motor Grader Windrow Strengthened Material on C.S. 15-11

Figure 3-10 Asphalt Emulsion Spreading Truck with Asphalt Tank on C.S. 15-11

Figure 3-11 C.S. 15-11 Pavement after Spreading Asphalt Emulsion

Figure 3-12 Cross Blading and Shaping of C.S. 15-11

Figure 3-13 Pneumatic Roller Compaction Train

3.5 Construction Quality Control and Quality Assurance Testing

PSI Technologies Inc. performed the on site construction quality control and assurance measures of the full depth reclamation test sections. The quality control and assurance tests included *in situ* density measurements, *in situ* moisture content measurements, and final cross slope measurements.

A full depth nuclear gauge (150 mm direct transmission) was used to characterize the *in situ* density and moisture content of the reclaimed and full depth granular strengthened system.

In situ nuclear-density quality assurance test results obtained during construction of the C.S. 15-11 full depth granular strengthening test sections are presented relative to the optimum standard Proctor moisture-density profile (PSI 2006). The quality control results obtained during construction are summarized in Table 3-1.

Table 3-1 Test Section *In Situ* Dry-Density Quality Control Measurements Summary

Chainage (km)	Stabilization Type	Average Dry Density Measurements (kg/m^3)	Average % of Standard Optimum Dry Density	Average Individual Dry Density Measurement Pass/Fail
5.0 ~6.0	Cement-Asphalt Emulsion	2199	99.1	Pass (75 %) Fail (25 %)
6.0 ~7.0	Cement	2120	98.6	Pass (70 %) Fail (30 %)
7.0 ~8.0	Unstabilized	2151	99.1	Pass (95 %) Fail (5 %)

The dry density criterion established for the C.S. 15-11 project was a minimum average of 100 percent standard Proctor density with no individual measurement below 98 percent of standard Proctor dry density. As shown in Table 3-1, the average daily *in situ* dry density measurements ranged from 98.6 percent to 99.1 percent. As also shown in Table 3-1, the percent failed *in situ* dry density measurements ranged from 5 percent to 30 percent of the total measurements taken.

In situ moisture content quality control measurements were obtained during construction of C.S. 15-11 full depth strengthening test sections and were compared to the standard Proctor optimum moisture content of the full depth strengthened system (PSI 2006). *In situ* moisture measurement results are summarized in Table 3-2. It was shown that stabilized systems were installed slightly dry of optimum content. The reason for this was due to late season construction and poor weather conditions.

The moisture content criterion specified for the full depth strengthened reclaimed material was ±1.5 percent of standard Proctor optimum moisture content by dry weight of soil. As shown in Table 3-2, the average daily *in situ* moisture measurements by section ranged from 5.6 percent to 6.3 percent. Table 3-2 shows that the daily section percent failed *in situ* moisture measurements ranged from 5 percent to 45 percent of the total measurements taken.

Cross slope measurements were obtained on the finished surface of the completed stabilized layer on C.S. 15-11 as summarized in Table 3-3.

Table 3-2 Test Section *In Situ* Nuclear Moisture Quality Control Measurements

Chainage	Stabilization Type	Average Individual Nuclear Moisture Measurements (% Moisture)	Average Difference from Optimum Standard Moisture Content	Average Individual Moisture Measurement Pass/Fail
5.0 ~6.0	Cement-Emulsion	6.3	-1.3	Pass (70 %) Fail Dry (30 %)
6.0 ~7.0	Cement	6.3	-0.7	Pass (95 %) Fail Dry (5 %)
7.0 ~8.0	Unstabilized	5.6	-1.4	Pass (55 %) Fail Dry (45 %)

Table 3-3 Test Section Cross Slope Quality Assurance Measurements Summary

Chainage	Stabilization Type	Target Cross Slope (%)	Average Cross Slope (%)	Average Individual Cross Slope Measurement Pass/Fail
5.0 ~6.0	Cement-Emulsion	3.0	3.2	Pass (50 %) Fail (47.5% Low, 2.5% High)
6.0 ~7.0	Cement	3.0	3.4	Pass (47.5%) Fail (45.0% Low, 7.5% High)
7.0 ~8.0	Unstabilized	3.0	3.9	Pass (85 %) Fail (12.5% Low, 2.5% High)

As shown in Table 3-3, the average daily cross slope measurements by section ranged from 3.2 percent to 3.9 percent. The percent failed cross slope measurements ranged from 15.0 percent to 52.5 percent.

It was observed from the measurements that a significant amount of individual measurements at C.S. 15-11 test section failed the quality control tests requirements. It is

believed that the localized area failed in quality control tests were primarily due to the poor weather conditions during construction in September to October 2006 (PSI 2006).

Several potential improvements to the full depth strengthening process were identified from the construction of the C.S. 15-11 test sections (PSI 2006):

- It is recommended that future projects involving the construction of full depth strengthening systems be conducted in the summer months of better climatic conditions during construction. More favourable climatic conditions will allow for less delay in construction and an improved final result of the stabilized system.
- It is recommended that improved compaction equipment be employed to achieve more efficient compaction and reduce the required time for compaction on site.
- The application of asphalt emulsion through a distributor truck was found to be inefficient and resulted in significant delay of compaction and final trimming of the system. Advanced asphalt emulsion application systems involving direct injection during the rotomixing process is required.
- Improved moisture controls for compaction process is recommended to help early densification resulting in an improved final end product.

3.6 Non-Destructive Primary Pavement Deflection Responses Evaluation

Pavement deflection measurements were performed by PSI every 25m along the C.S. 15-11 test sections using a Heavy Weight Deflectometer, as shown in Figure 3-14.

Figure 3-14 Heavy Weight Deflectometer on C.S. 15-11 (Courtesy of Dr. Curtis Berthelot)

Heavy weight deflectometer peak surface deflection measurements were collected across load spectra at primary legal load weight limits (44.6 kN) in both the eastbound and westbound directions on C.S. 15-11, prior to base construction, after base construction, and post paving. The result of deflection under primary legal load weight limits are shown in Table 3-4 and illustrated in Figure 3-15.

The test sections on C.S. 15-11 were found to be structurally sound before the stabilization construction, as shown in Figure 3-15. Figure 3-15 also showed that the base stabilization construction conducted on C.S. 15-11 had reduced the pavement deflection of all test sections. The pavement deflection values were reduced due to the construction of cement stabilization, cement and asphalt stabilization, and remix and recompaction systems are 0.10 mm, 0.06 mm, and 0.09 mm, respectively.

Deflection measurements showed that different base stabilization systems on C.S. 15-11 test section resulted in close primary surface deflection responses after full depth strengthening in October 2006.

Table 3-4 C.S. 15-11 Surface Deflection Summary at Primary Legal Load Weight Limits

Test Section	*A Priori* Unstrengthened			Post Construction Strengthened			Post HMA Paving		
	Mean (mm)	SD (mm)	CV (%)	Mean (mm)	SD (mm)	CV (%)	Mean (mm)	SD (mm)	CV (%)
Cement and Asphalt Emulsion Stabilization	0.65	0.12	18.2	0.59	0.08	13.7	0.56	0.11	19.64
Cement Stabilization	0.67	0.09	12.2	0.57	0.09	16.5	0.57	0.11	19.3
Unstabilized	0.68	0.2	29.2	0.59	0.11	18.6	0.62	0.41	66.13

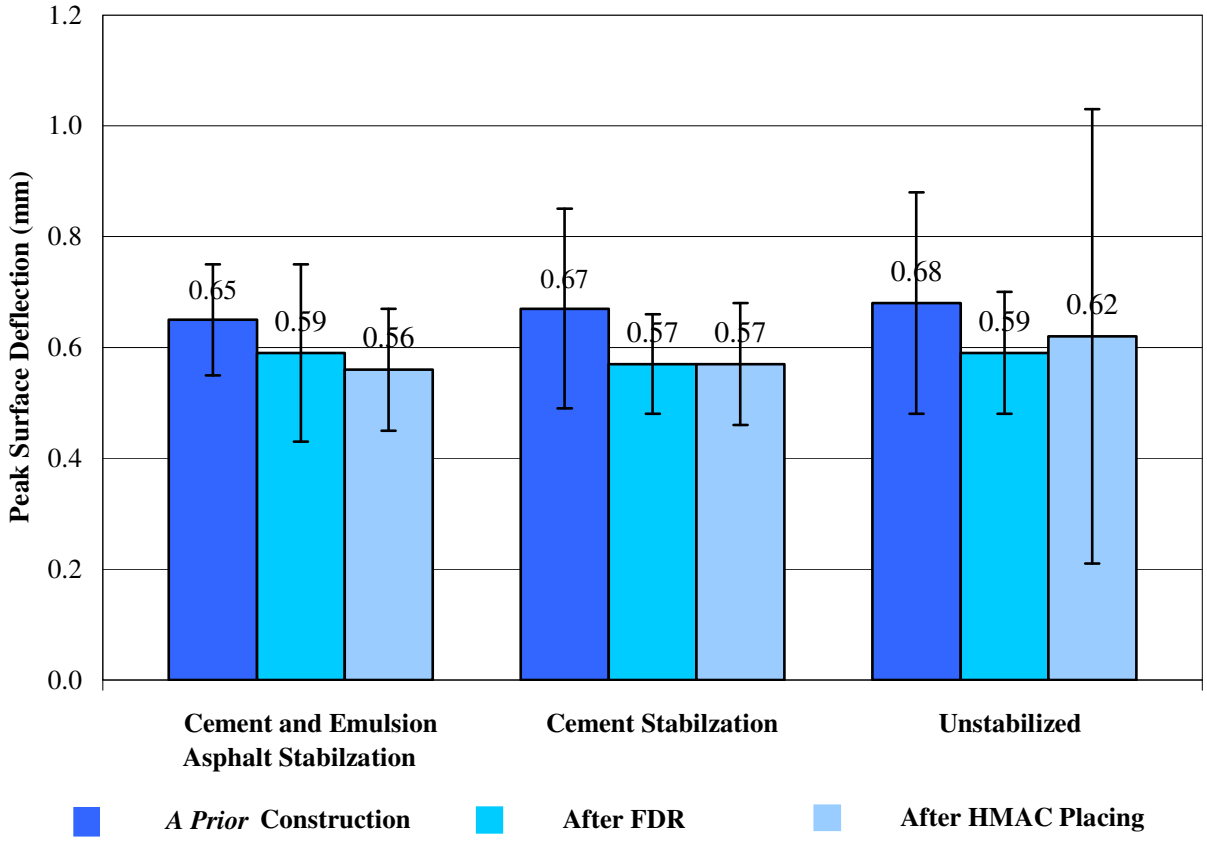

Figure 3-15 Mean Peak Deflection Response at Primary Legal Load Weight Limits (± 2SD)

The test sections constructed on C.S. 15-11 remained unsurfaced throughout the winter of 2006-2007. After spring thaw in 2007, it was found that only minor surface ravelling had occurred across each test section. The sustained quality of the unsurfaced test sections illustrated the ability of stabilized granular base structures to be used as a stop-gap treatment prior to asphalt surfacing.

More deflection reductions were observed on the cement stabilized bases with or without emulsion asphalt post paving in 2007. However, surface deflection of unstabilized test section of C.S. 15-11 after placing asphalt layer increased relative to the deflection measured right after full depth strengthening construction. Furthermore, the variability of deflection measurements of unstabilized test section after placing asphalt layer in 2007 was observed to be significantly higher than the other two test sections on C.S. 15-11. The increase in variability revealed that the freeze-thaw cycles in winter 2006-2007 has significantly affected the performance of unstabilizd test section of C.S. 15-11, which has the lowest climatic durability of all test sections constructed on C.S. 15-11.

The peak surface deflection profiles under primary legal load limits are plotted spatially and compared to the prior structural primary response measurements taken before construction (PSI 2006), as shown in Figure 3-16 and Figure 3-17.

It is found from Figure 3-16 and Figure 3-17 that the full depth strengthening and stabilization systems resulted in improved primary structural response profiles across the spatial limits of all test sections on C.S. 15-11 after base stabilization construction.

It is also found that most of the relatively "weak pavement structure" localized near the centre line of the highway have been eliminated after the base stabilization construction, whereas the weak areas closed to road edges were not significantly improved. It is believed that difficulties in compaction near pavement edges and associated insufficient layer density would be the primary reason of the remaining weak areas observed after construction.

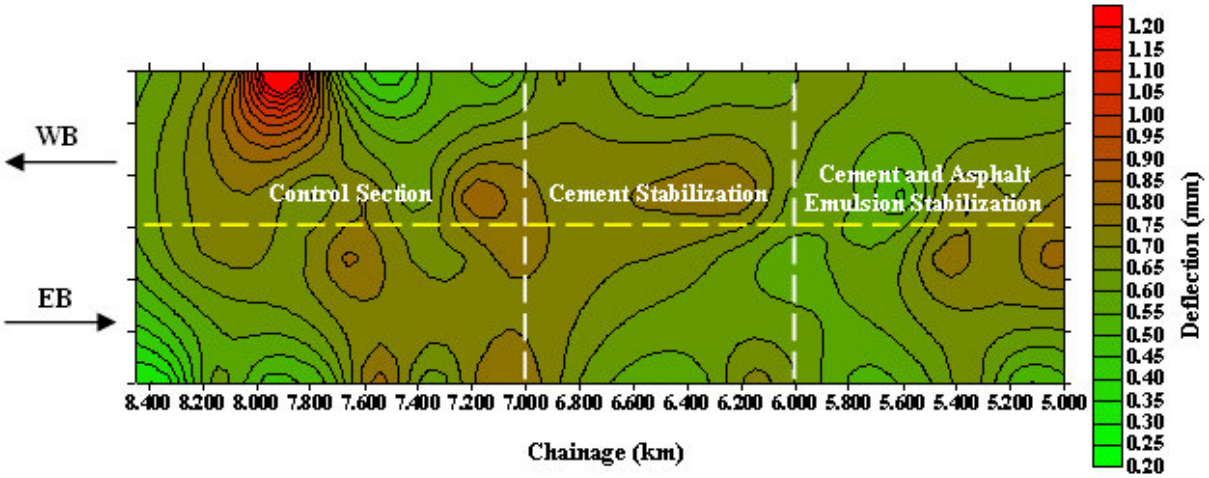

Figure 3-16 *A Priori* Unstrengthened Peak Surface Deflection Contour Profile at Primary Legal Load Weight Limits on C.S. 15-11

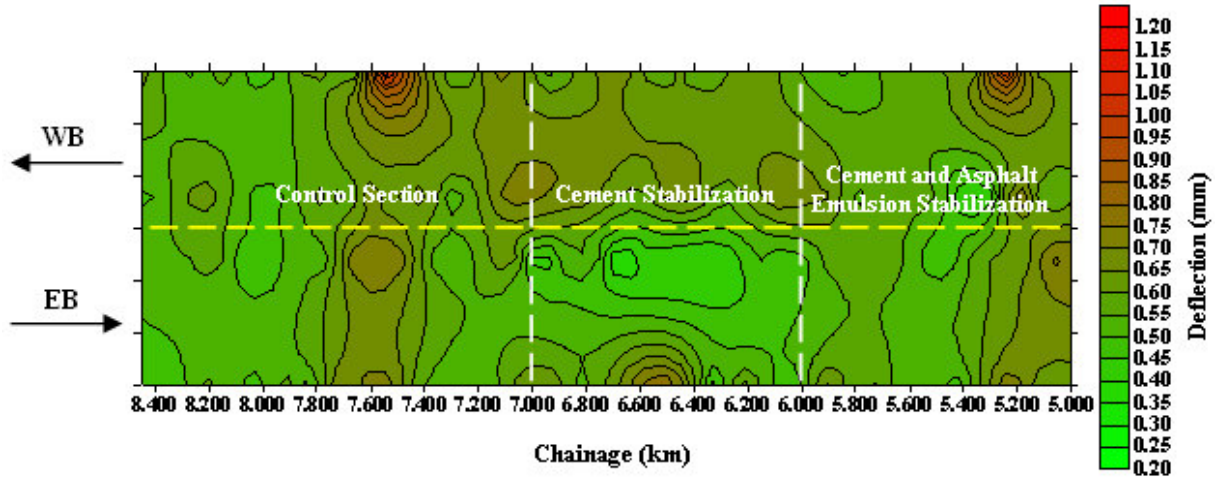

Figure 3-17 Post Construction Strengthened Peak Surface Deflection Contour Profile at Primary Legal Load Weight Limits on C.S. 15-11

3.7 Chapter Summary

Chapter three contains the visual condition survey prior to construction, test section design and layout, and construction process of the control section 15-11 test sections, quality control/quality assurance, and non-destructive deflection test results. This chapter also describes the process of field material sampling.

The visual survey of the pavement condition of C.S. 15-11 prior to construction determined that the pavement is structurally sound with minor potholes, moderate rutting, severe shoving, and seal bleeding. It is suspected that the cause of rutting is a result of poor base course underlying the double seal surface.

Given the results of the visual site condition survey and the non-destructive structural assessment, the limits of the test sections were proposed to be from km 5.0 to km 8.0 on Highway 15-11. The proposed strengthened structure comprise the *in situ* subgrade, 150 mm *in situ* granular subbase, 150 mm strengthened granular base and 40 mm HMAC asphalt surfacing.

The base stabilization and strengthening construction of C.S. 15-11 began on September 25, 2006 and was completed in middle October, 2006. The construction procedures for various stabilization systems on C.S. 15-11 are described in this chapter. Experience from C.S. 15-11 pilot project construction, as well as several potential improvements of the full depth strengthening process were identified and summarized.

The test sections constructed on C.S. 15-11 remained unsurfaced throughout the winter of 2006-2007. After the spring thaw in 2007, it was found that only minor surface ravelling had occurred across each test section. The sustained quality of the unsurfaced test sections shows the ability of stabilized granular base structures to be used as a stop-gap treatment prior to asphalt surfacing. However, surface deflection of the unstabilized test section of C.S. 15-11 after placing the asphalt layer increased relative to the deflection right after full depth strengthening construction. Furthermore, the variability of deflection measurements of unstabilized test section after placing the asphalt layer in 2007 was observed to be significantly higher than any other test sections on C.S. 15-11.

The increased variability revealed that the freeze-thaw cycles in winter 2006-2007 has significantly affected the performance of unstabilizd test section of C.S. 15-11, which has the lowest climatic durability of all test sections constructed on C.S. 15-11.

Improved primary structural response profiles were observed across the spatial limits of the test sections after base stabilization construction. The cement stabilization system was found to have the most significant structure improvement among all test sections.

The peak surface deflection profiles under primary legal load limits are plotted spatially and compared to the prior structural primary response measurements taken before construction. Results showed that the full depth strengthening and stabilization systems resulted in improved primary structural response profiles across the spatial limits of all test sections on C.S. 15-11 after base stabilization construction.

The peak surface deflection profiles under primary legal load limits are plotted spatially and compared to the prior structural primary response measurements taken before construction. The contour plots showed that the full depth strengthening and stabilization systems resulted in improved primary structural response profiles across the spatial limits of all test sections on C.S. 15-11 after base stabilization construction.

CHAPTER 4 CONVENTIONAL LABORATORY CHARACTERIZATION

Design and evaluation of granular base stabilization is often based on several conventional characterization tests. This research employed several conventional laboratory tests to determine the classification, physical properties and mechanical properties of *in situ* and stabilized granular base materials samples applied in C.S. 15-11 construction. Standard Proctor, California bearing ratio, Marshall and gyratory compacted samples were made and cured for conventional laboratory characterization.

The conventional laboratory tests summarized in this chapter include:

- Grain size distribution (ASTM D422)
- Atterberg limits (ASTM D4318)
- Sand equivalent test (ASTM D2419)
- Standard Proctor compaction (ASTM D698)
- California bearing ratio and confined soaked swell test (ASTM D1883)

4.1 On Site Material Sampling

In situ and stabilized base materials were sampled during the construction of the C.S. 15-11 test section. The materials were stored in pails and sealed with lids. The on site sampling process was carried out immediately after the completion of rotomixing process of each stabilization system, as shown in Figure 4-1 and Figure 4-2. All samples were labelled and transported to the University of Saskatchewan Transportation Centre's lab for further laboratory testing.

Figure 4-1 Field Sampling of Stabilized Material on C.S. 15-11

Figure 4-2 Field Sampling of Unstabilized Material on C.S. 15-11

The quantities of sample needed for laboratory characterization in this research were determined prior to field sampling, as listed in Table 4-1. All materials were sampled and transported to the laboratory as summarized in Table 4-2.

Table 4-1 Proposed Quantities of Materials Sampled for Each Test Section on C.S. 15-11

Test Type	Mass of Each Specimen (Kg)	Number of Specimens	Total Mass (Kg)
Grain Size Distribution	15	3	45
Atterberg Limits	4	3	12
Standard Proctor (6 inch)	12	2	24
CBR Swell and Strength	12	3	36
Marshall Specimen (4 inch)	5	10	50
Gyratory Specimen (6 inch)	10	14	140

In this table, the mass of materials denotes mass of *in situ* materials with moisture.

Table 4-2 Materials Sampling Details on C.S. 15-11

Section Name	Sampling Date	Sampling Location	Kilometre Limits
Unstabilized	September 27,2006	Both lanes	5.0 ~8.0
Cement and Asphalt Emulsion	September 29,2006	North Lane	5.0 ~5.5
Cement and Asphalt Emulsion	October 4,2006	South Lane	5.0 ~6.0
Cement	September 27,2006	Both Lanes	5.0 ~8.0

Cement stabilized specimens were made in the laboratory by adding PSICem™ into unstabilized soil.

All materials passing 19 mm sieve were compacted after being transported to the University of Saskatchewan material laboratory as per the specified procedures for CBR, Marshall and gyratory compaction. Samples were then stored in the moist room to cure after the completion of laboratory compaction.

4.2 Grain Size Distribution

The grain size distributions of the *in situ* reclaimed granular base material, cement and asphalt emulsion stabilized base material were determined by washed mechanical sieve analysis prior to and post ignition oven burning. The material grain size distributions are showed in Figure 4-3 and Table 4-3 with comparison to MHI Type 33 granular base gradation envelope. The gradation coefficient of uniformity (Cu) and the coefficient of curvature (Cc) are calculated and listed in Table 4-4.

Table 4-3 Grain Size Distribution of C.S. 15-11 Granular Bases

Sieve size (mm)	Percentage Passing (%) of Granular Base Material				
	In Situ	**Cement & Asphalt Emulsion**	**Cement & Asphalt Emulsion (Ignition Oven)**	**MHI Type 33 Upper Limit**	**MHI Type 33 Lower Limit**
18.0	100.0	100.0	100.0	---	---
16.0	99.4	97.0	98.0	---	---
12.5	95.1	92.1	94.0	75.0	100.0
9.0	86.5	79.9	84.0	63.3	88.3
5.0	71.4	62.2	68.0	50.0	75.0
2.0	52.7	41.3	48.0	32.0	52.0
0.9	40.2	29.2	36.0	20.0	35.0
0.4	25.9	17.6	22.0	15.0	25.0
0.16	12.8	8.4	9.0	8.0	15.0
0.071	9.3	5.3	5.0	6.0	11.0

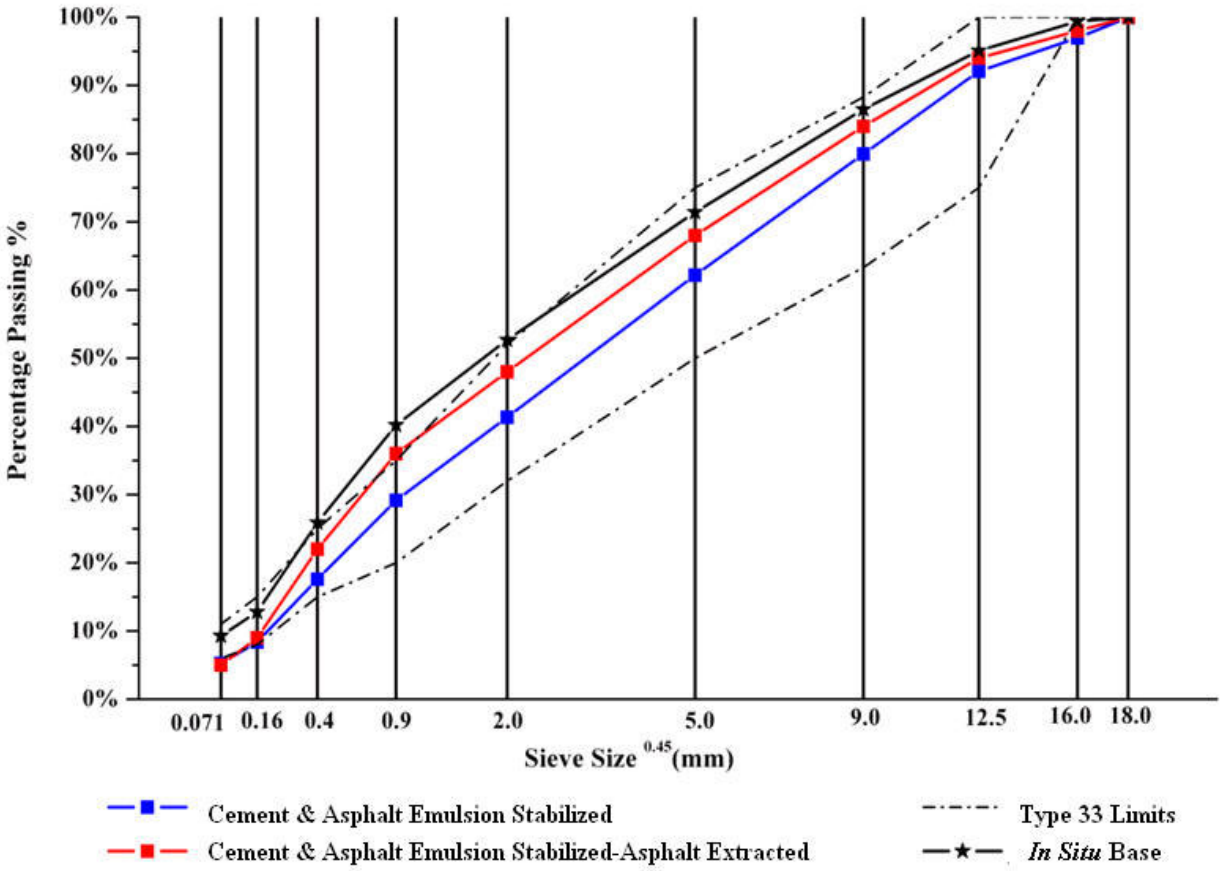

Figure 4-3 Grain Size Distribution of Materials from C.S. 15-11 Granular Bases

Table 4-4 Coefficient of Uniformity (Cu) and Coefficient of Curvature (Cc)

Granular Base System	Cu	Cc
***In Situ* Base**	33	1.11
Cement and Asphalt Emulsion Stabilized Base	23	0.97

As shown in Figure 4-3, the *in situ* granular base sampled from C.S. 15-11 was found to be high at the sand sieve sizes as compared to gradation limits of Saskatchewan MHI Type 33 granular base material, particularly from 0.4 mm to 0.9 mm size range. As a result, the *in situ* granular base is deemed as a marginal sandy granular base material, which may be one of the causes of the pavement shear slippage, shoving and rutting observed on pavement at C.S. 15-11.

As shown in Figure 4-3, the grain size distribution of cement and asphalt emulsion stabilized material falls within the Saskatchewan Type 33 gradation envelope. This showed that cement and asphalt emulsion stabilizer can improve the gradation of granular base by bonding the fines and sandy material together. After burning the asphalt out of the cement and asphalt emulsion stabilized material using an ignition oven, the extracted granular base material exhibits a finer gradation than its gradation prior to burning. This is because the asphalt bonds the fine soil particles together in the mixture. Some particles in the mixture disintegrated during the burning process of the ignition oven.

4.3 Atterberg Limits Characterization

Atterberg limits and plasticity index characterization as specified in ASTM D4318 were performed on the fines (passing No. 200 sieve) of *in situ* unstabilized granular base and stabilized granular base materials. The testing results are summarized in Table 4-5:

Table 4-5 Atterberg Limits and Plastic Index

Granular Base System	Liquid Limit %	Plastic Limit %	Plastic Index %
Unstabilized	20.5	10.0	10.5
Cement and Emulsion Asphalt	N/A	Non-plastic	
Cement	N/A	Non-plastic	

As shown in Table 4-5, the fines of *in situ* granular base have a liquid limit of 20.5, a plastic limit of 10.0 and a plastic index of 10.5. However, both stabilized granular base material are non-plastic materials. Therefore it is concluded that the granular base stabilization of the C.S. 15-11 *in situ* granular base reduced the plasticity of fines content in the granular base material.

4.4 Granular Base USCS and AASHTO Classification

In situ granular base material from C.S. 15-11 is classified by the Unified Soil Classification System (USCS) as specified in ASTM D2487 and AASHTO soil classification system as specified in AASHTO M 145. The *in situ* granular base material

is classified as well-graded sand with clay and gravel (SW-SC) by ASTM or A-2-6 clayey gravel by AASHTO, as shown in Table 4-6.

Figure 4-4 illustrates the USCS soil classification of the fines portions of *in situ* granular base samples retrieved from C.S. 15-11. As shown in Figure 4-4, the fines of *in situ* granular base are classified as CL by ASTM, which is lean clay. The fines can also be classified as an A-6 clay by AASHTO, which is a clayey soil.

Table 4-6 USCS and AASHTO Classification of In Situ Granular Material of C.S. 15-11

Specification System	Soil Classification	Fines Classification
AASHTO Classification	A-2-6	A-6
USCS Classification	SW-SC	CL

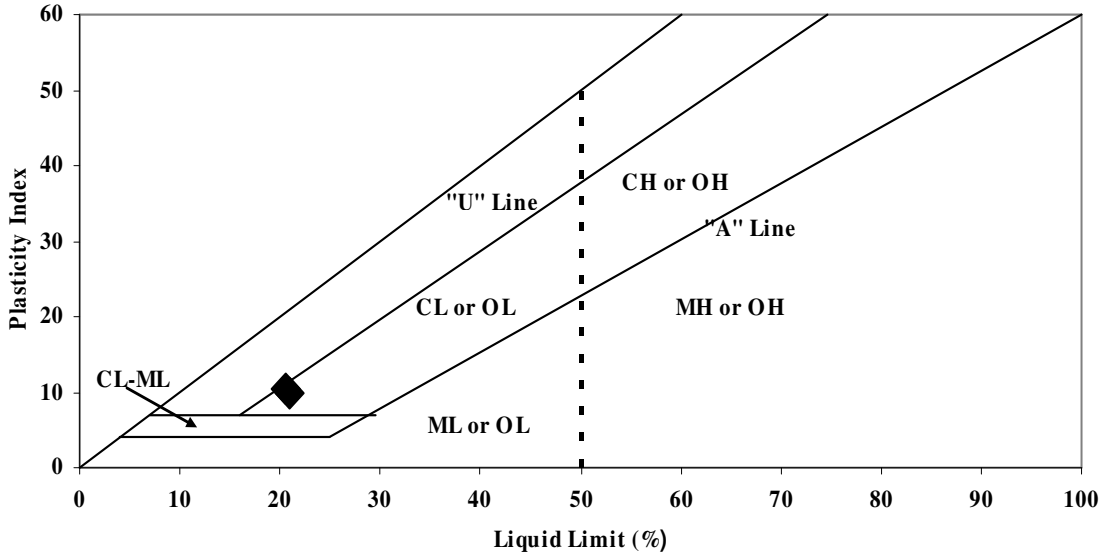

Figure 4-4 USCS Classification of C.S. 15-11 in situ Granular Base Material Fines

4.5 Sand Equivalent Characterization of Granular Bases

The sand equivalency value is defined as the ratio of the sand to clay fractions as determined by settlement in a standing hydrometer. Sand equivalent characterization is performed as specified in ASTM D2419 to determine the relative proportions of clay size particles or plastic fines in granular material that pass the 5.00 mm sieve.

The sand equivalent test was performed on the *in situ* granular base material. Due to the interest in observing the changes in fine contents after incorporating the cement powder into *in situ* granular base, cement stabilized granular base material was also tested using sand equivalent testing. The sand equivalent values of *in situ* granular base and cement stabilized material were found out to be 55.7 and 79.5, respectively, as shown in Table 4-7 and in Figure 4-5.

Table 4-7 Sand Equivalent Characterization of C.S 15-11 Granular Base

Granular Base System	Sand Equivalent Value (%)
Unstabilized	55.7
Cement Stabilized	79.5

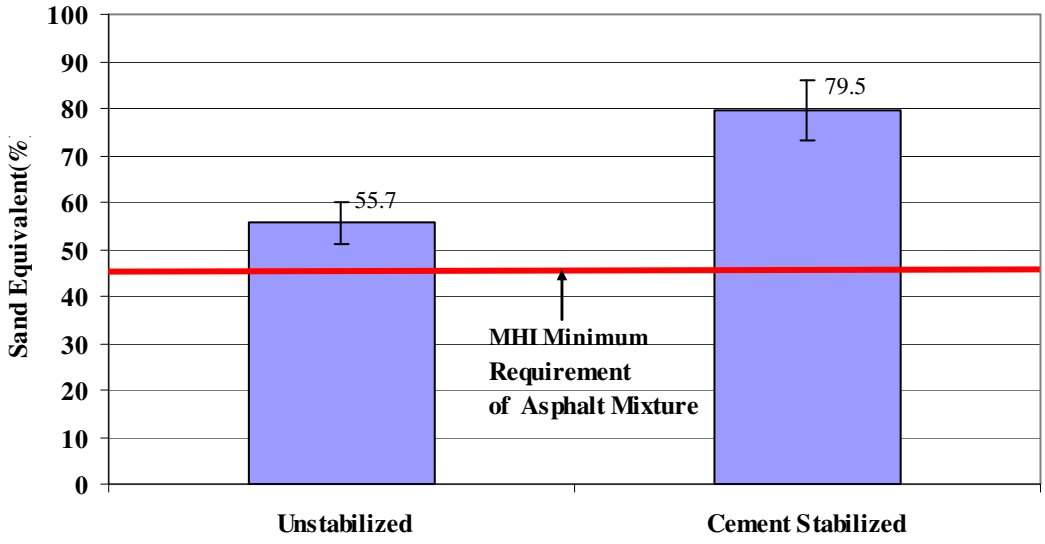

Figure 4-5 Mean Sand Equivalent Values of C.S. 15-11 Granular Base (± 2SD)

Superpave™ requires a minimum sand equivalent of 36 for asphalt mixtures (Asphalt Institute 2001). Saskatchewan MHI specifies a sand equivalent value of 45 for asphalt. However, no sand equivalent value requirement is specified for granular base material (MHI 1999). As shown in Figure 4-5, both *in situ* and cement stabilized granular materials meet the MHI sand equivalent requirement for aggregates of hot mix asphalt. In addition, sand equivalent value of cement stabilized granular base material is

significantly higher than the *in situ* granular base material. This indicates that the cement stabilization cements the fines together and reduces the fines content in the granular material, which may be one of the reasons that the material plasticity was reduced.

4.6 Standard Proctor Moisture Density Relationship Characterization

Standard Proctor moisture density characterization was performed on C.S. 15-11 *in situ* granular base as specified in ASTM D 698. Previous testing performed by PSI Technologies Inc. showed that the maximum density and optimal moisture content of the *in situ* material, cement stabilized material and cement with asphalt emulsion stabilized material on C.S. 15-11 are close to each other (PSI 2006). Therefore only *in situ* granular base material was included in standard Proctor testing in this research. As the grain size distribution of *in situ* granular base material meets the requirements of method C specified in ASTM D 698, the *in situ* granular material was compacted in a 150 diameter mold by 3 layers with standard compaction effort.

The moisture density relationship obtained for C.S. 15-11 *in situ* granular base material was tabulated in Table 4-8 and illustrated in Figure 4-6. The results show that the *in situ* granular base material yielded a maximum standard dry density of 2240 kg/m^3 at an optimal moisture content of 7.8 percent by dry weight of soil. This maximum density obtained from standard Proctor characterization was used as the desired termination density during gyratory sample preparation in this research.

Table 4-8 Standard Proctor Characterization of C.S. 15-11 *in situ* Granular Base Material

Maximum Dry Density (kg/m^3)	Optimal Moisture Content (% by weight of dry soil)
2240	7.8

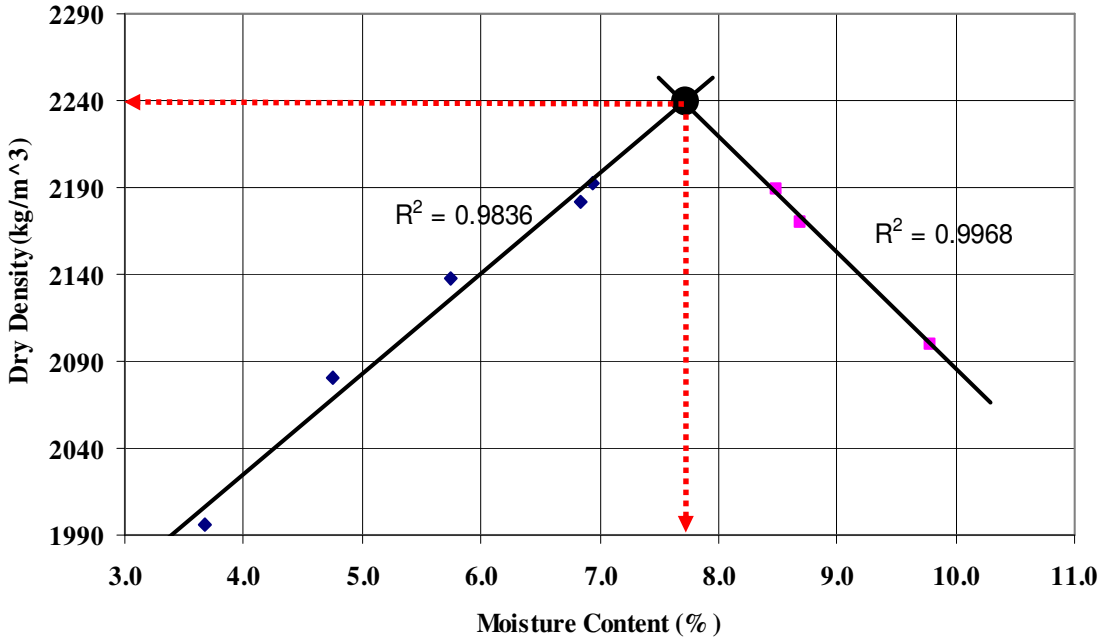

Figure 4-6 Standard Proctor Characterization of C.S. 15-11 *in situ* Granular Base Material

4.7 CBR Soaked Swell and Strength Characterization

The California bearing ratio (CBR) soaked swell and strength characterization were performed as specified in ASTM D1883 on unstabilized, cement stabilized, and cement and asphalt emulsion stabilized granular base samples.

The samples were cured in the moist room prior to testing. The curing durations of various granular materials are listed in Table 4-9.

Table 4-9 Curing Time of Granular Base Material Specimens on C.S. 15-11

Granular Base System	Sample Curing Time (Month)
Unstabilized	4
Cement and Asphalt Emulsion	4
Cement	1

The results of the 96-hour confined soaked swell tests are summarized in Table 4-10 and illustrated in Figure 4.7.

Table 4-10 Peak 96-Hour Confined Soaked Swell of Granular Base Systems on C.S. 15-11

Granular Base System	Peak 96-Hour Soaked Swell (mm)	Coefficient of Variance (%)
Unstabilized	0.13	29.8
Cement and Asphalt Emulsion	0.06	53.7
Cement	0.03	55.6

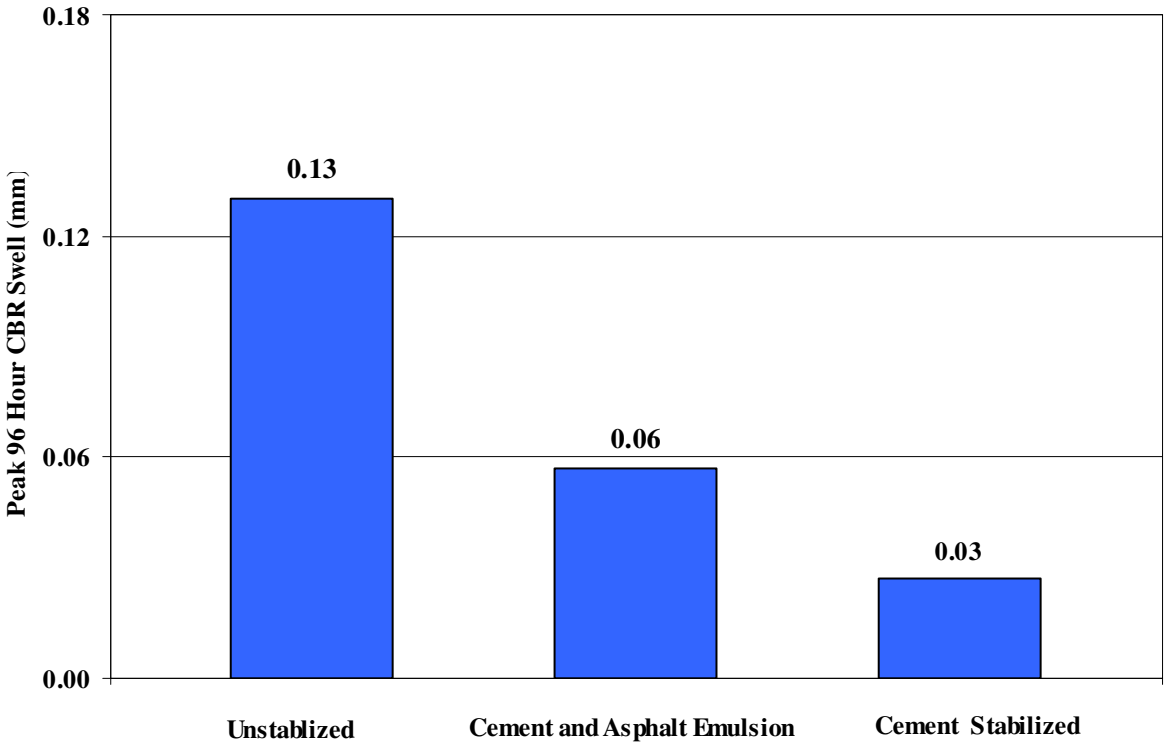

Figure 4-7 Mean Peak 96-Hour Confined Soaked Swell of Granular Base Systems

As shown in Table 4-10, the average peak 96-hour confined soaked swell of samples from unstabilized, cement with asphalt emulsion stabilized, and cement stabilized test sections on C.S. 15-11 are 0.13 mm, 0.06 mm, and 0.03 mm, respectively. The sample swelling was reduced from 0.13 mm to 0.06 mm when cement and asphalt emulsion were incorporated into the *in situ* granular base. Although the samples were cured for less time, the swell was still greatly reduced from 0.13 mm to 0.03 mm as incorporate cement into the *in situ* granular base on C.S. 15-11.

The CBR swelling test results revealed that cement and cement with emulsion asphalt stabilization could reduce swelling potential of *in situ* granular base materials on C.S. 15-11. Cement stabilization was found to have the lowest swelling potential among all three materials on C.S. 15-11. However, it should be noted that, unlike a high swelling potential material such as plastic clay, the *in situ* granular material has relatively low swelling potential even before stabilization.

CBR strength testing was also performed after the 96-hour soaked confined swell testing as specified in ASTM D1883. Results of the soaked CBR test are summarized in Table 4-11 and illustrated in Figure 4.8.

Table 4-11 Soaked CBR Strength of Granular Base Systems on C.S. 15-11

Granular Base System	Mean Soaked CBR Strength	Coefficient of Variance (%)
Unstabilized	22	12.1
Cement and Asphalt Emulsion	68	57.0
Cement	266	16.9

Both cement and cement with asphalt emulsion stabilization were found to effectively increase the CBR strength of the C.S. 15-11 *in situ* granular base material. Cement stabilization was found to provide greater improved strength than the cement and emulsion asphalt stabilization.

Saskatchewan MHI specifies its desired soaked CBR value for Saskatchewan granular bases to be from 40 to 80 in Saskatchewan Surfacing Manual. It should be noted that the stabilized bases of C.S. 15-11 cement stabilized base provided a CBR value greater than 80, which went well beyond the design targeted values in MHI thickness design system. This identifies a need to research into the pavement design methodologies for stabilized pavement structures in Saskatchewan.

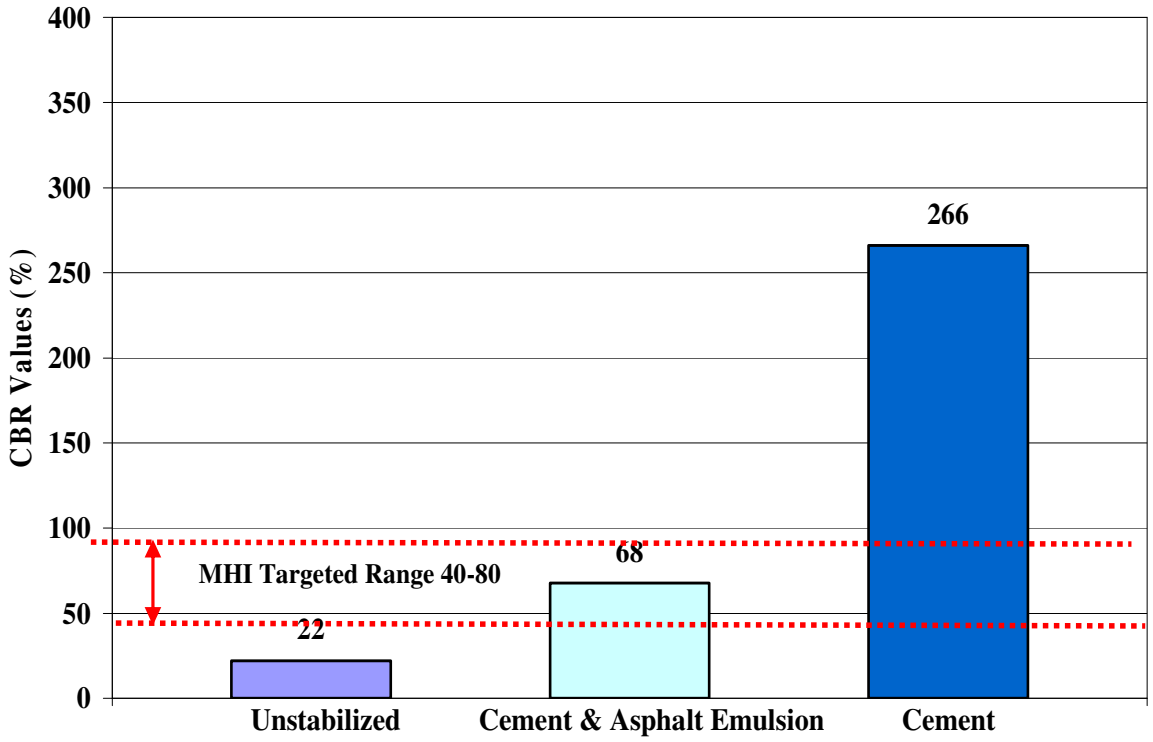

Figure 4-8 Mean Soaked CBR of Granular Base Systems on C.S. 15-11

4.8 Chapter Summary

Chapter four summarises and discusses the results and findings from conventional laboratory testing performed on C.S. 15-11 test section materials.

The *in situ* granular material on C.S. 15-11 was found to be slightly high across the sand sieve sizes as compared to gradation limits for MHI Type 33 granular base specifications, particularly from 0.4 mm to 0.9 mm. The *in situ* granular material was found to be a marginal sandy granular material, which may be one of the causes of the shear slippage, shoving and rutting observed on pavement of C.S. 15-11. The fines content of *in situ* granular material are classified as CL by ASTM, which is a lean clay. The fines can also be classified as A-6 by AASHTO, which is a clayey soil.

The grain size distribution and ignition oven testing revealed that cement and/or asphalt emulsion stabilizer can improve the grain size distribution of C.S. 15-11 granular base by bonding the fines and sandy material together. When the asphalt was burned by

ignition oven, the burned granular base material exhibited a finer gradation than its original gradation prior to burning.

The sand equivalent values of unstabilized and cement stabilized material are 55.7 and 79.5, respectively. Both materials meet the minimum sand equivalent value specified in Saskatchewan MHI specification for aggregates of asphalt concrete. The sand equivalent value of cement stabilized granular base material is significantly higher than the unstabilized material, indicating that the cement stabilization bonds the fines together and reduces the fines content in the granular material. The cementing effect may be one of the reasons that the plasticity was reduced.

The *in situ* material on C.S. 15-11 yielded a standard maximum dry density of 2240 kg/m^3 at an optimal moisture content of 7.8 percent by dry weight of soil. The maximum density obtained from the standard Proctor characterization was used as the desired termination density of gyratory compaction in this research.

The CBR swelling test showed that cement and cement with emulsion asphalt stabilization could reduce swelling potential of unstabilized materials on C.S. 15-11. In addition, cement stabilization was found to have the lowest swelling potential among all three test sections on C.S. 15-11.

Both cement and cement with asphalt emulsion stabilization were found to effectively increase the CBR strength of *in situ* base material. Cement stabilization was found to provide much greater strength than the cement with emulsion asphalt stabilization on C.S. 15-11 granular material.

Saskatchewan MHI specifies its desired soaked CBR value for Saskatchewan granular bases to be from 40 to 80 in Saskatchewan Surfacing Manual. It should be noted that the stabilized bases of C.S. 15-11 test sections provided CBR values greater than 80, which went beyond the design targeted values in MHI thickness design system. The fact found from this research identifies a need to research into the pavement design methodologies for stabilized pavement structures in Saskatchewan.

CHAPTER 5 MOISTURE SENSITIVITY CHARACTERIZATION

A significant factor that influences the field performance of stabilized granular material is sensitivity in the presence of moisture, which is particularly the case in regions with freeze-thaw cycles. Therefore, this research employed three moisture sensitivity laboratory tests to determine the resistance to moisture damage of granular materials applied in C.S. 15-11 test sections.

The moisture sensitivity characterizations presented in this chapter include:

- Indirect tensile strength test (ASTM D698)
- Moisture capillary rise and electric conductivity (Texas Transportation Institute)
- Unconfined compressive strength test (ASTM D5102)

5.1 Indirect Tensile Strength Characterization

Indirect tensile strength testing was performed on C.S. 15-11 test section materials based on a modified ASTM D698 procedure. The testing were performed on both 100 mm samples compacted by Marshall method and 150 mm gyratory compacted samples.

The testing was performed at two conditions: moist cured condition and 24-hour-soaked condition. The curing durations of all samples for indirect tensile strength are listed in Table 5-1.

The mean indirect tensile strength, mean soaked indirect tensile strength, and retained strength ratio of all samples are summarized in Table 5-1 and illustrated in Figure 5-1 and Figure 5.2.

Table 5-1 Indirect Tensile Strength of Samples on C.S. 15-11

Sample Type	Cure Time (Month)	Moist Cured ITS (kPa)	CV (%)	Soaked ITS (kPa)	CV (%)	Retained Tensile Strength (%)
Cement Stabilized (100 mm)	1.5	347	5.9	188	2.6	54
Cement and Asphalt Emulsion Stabilized (100 mm)	4.0	184	13.0	49	10.2	27
Unstabilized (150 mm)	8.0	54	28.5	16	49.6	30
Cement Stabilized (150 mm)	8.0	416	4.8	246	4.2	59
Cement and Asphalt Emulsion Stabilized (150 mm)	8.0	82	10.5	33	33.8	41

Although cured for less time, the 100 mm cement stabilized samples yielded greater indirect tensile strength than the 100 mm cement with asphalt emulsion stabilized samples on C.S. 15-11, as shown in Table 5-1 and Figure 5-1.

As shown in Figure 5-1, indirect tension test on 100 mm samples revealed that the strength of both cement and cement with emulsion stabilization decreased after soaking. However, the cement stabilized samples have higher retained tensile strength values and less loss of strength relative to cement and asphalt emulsion stabilized samples on C.S. 15-11.

As shown in Table 5-1 and Figure 5-2, indirect tension test on 150 mm samples revealed that both cement and cement with emulsion asphalt stabilization systems improved the indirect tensile strength and moisture sensitivity of *in situ* C.S. 15-11 granular base materials. Cement stabilization was found to have greater improvement on the tensile strength and moisture sensitivity relative to the cement and asphalt emulsion stabilization.

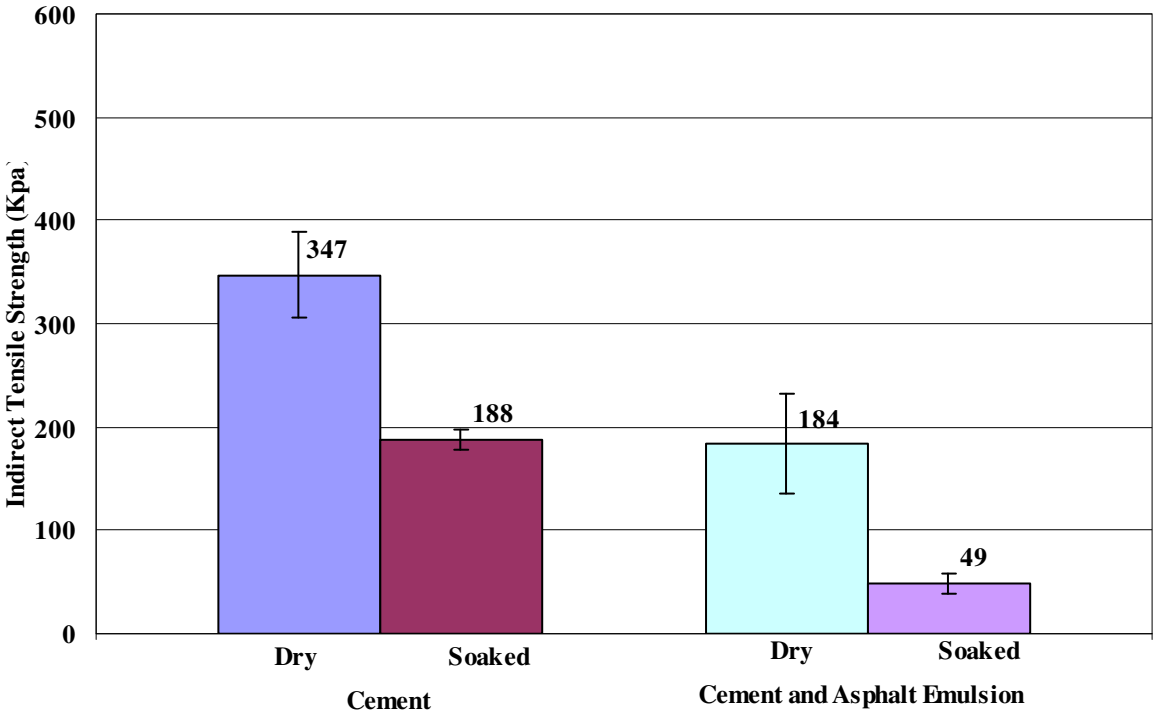

Figure 5-1 Mean Indirect Tensile Strength of 100 mm Samples on C.S. 15-11 (± 2SD)

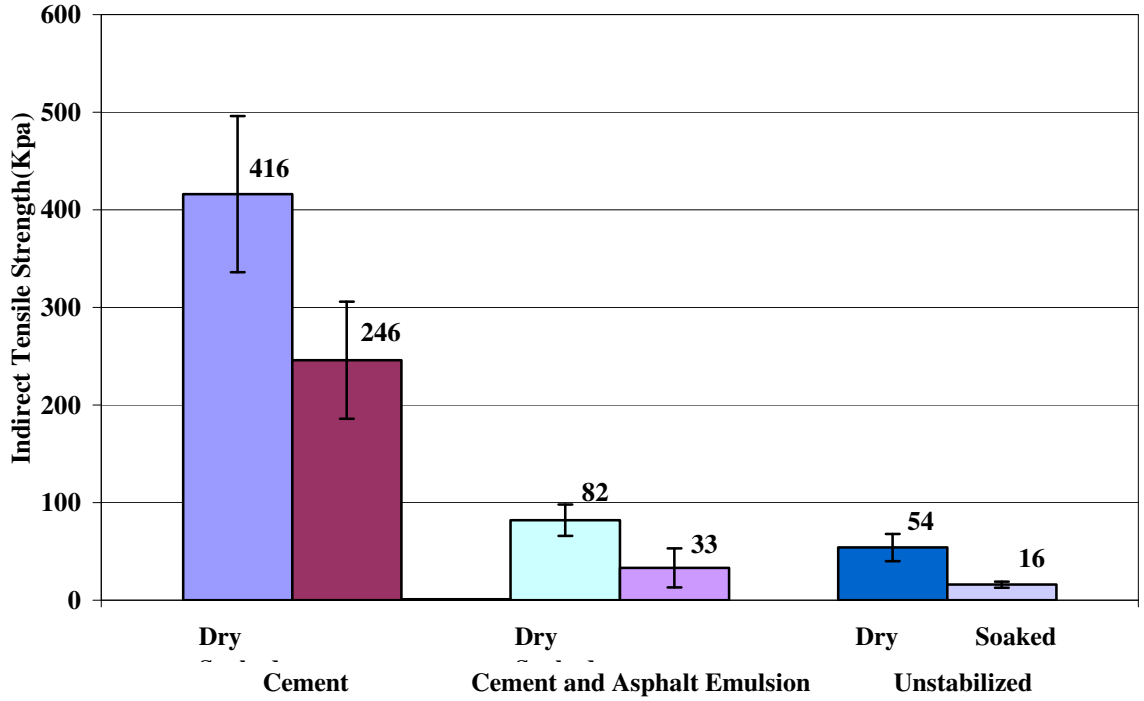

Figure 5-2 Mean Indirect Tensile Strength of 150 mm Samples on C.S. 15-11 (± 2SD)

The testing results showed that indirect tensile strengths from 150 mm samples were not the same as 100 mm samples. For instance, 150 mm cement stabilized samples provided greater strength values than 100 mm cement stabilized samples. In addition, the 150 mm cement with emulsion stabilized samples yielded lower strength as compared to 100 mm cement with emulsion stabilized samples. It is suspected that the curing time, compaction energy, and specimen size may be the sources of the strength disparities. Therefore, future testing may be improved by specifying and standardizing sample curing conditions, curing time, compaction method, and the mould size for QC/QA testing purposes of granular base stabilization in Saskatchewan.

It should be noted that the retained strength ratios of both the 100 mm and 150 mm samples on C.S. 15-11 materials were relatively low, ranging from 25 to 58 percent. It is suspected that the low retained values were a direct result of the length of time taken in sample transportation. Therefore, it is suggested that testing samples shall be compacted at site without delay for construction QA/QC purpose in the future.

5.2 Capillary Moisture Rise and Surface Conductivity Characterization

The capillary moisture rise and surface conductivity test were performed on C.S. 15-11 samples. The testing followed the PSI protocol modelled from the Texas Transportation Institute tube suction specification; however, the sample was not confined during the testing. The sample surface conductivity was recorded at the end of the capillary moisture rise testing.

Testing was conducted on a gyratory compacted cylinder sample 150 mm in height and 150 mm in diameter. Samples were cured for approximately eight months prior to the testing. The testing results across various test sections on C.S. 15-11 are summarized in Table 5-2 and illustrated in Figure 5-3 and Figure 5-4.

Table 5-2 Capillary Moisture Rise and Surface Conductivity Results of C.S. 15-11 Samples

Granular Base System	Water Intake by Sample Mass (%)	Coefficient of Variance (%)	Surface Conductivity (uS/cm)	Coefficient of Variance (%)
Unstabilized	4.2	1.7	77	17.6
Cement	5.2	4.9	7	48.5
Cement and Asphalt Emulsion	6.1	3.3	69	10.3

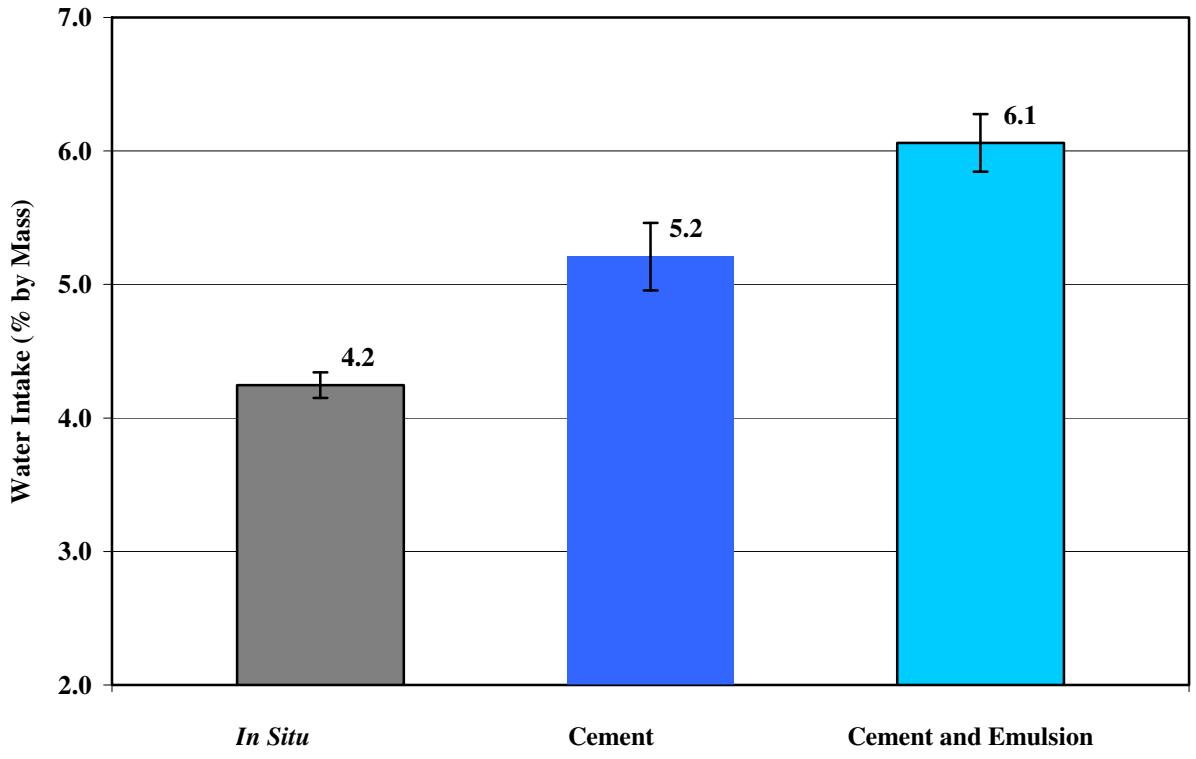

Figure 5-3 Mean Capillary Moisture Intake Results of C.S. 15-11 Materials (± 2SD)

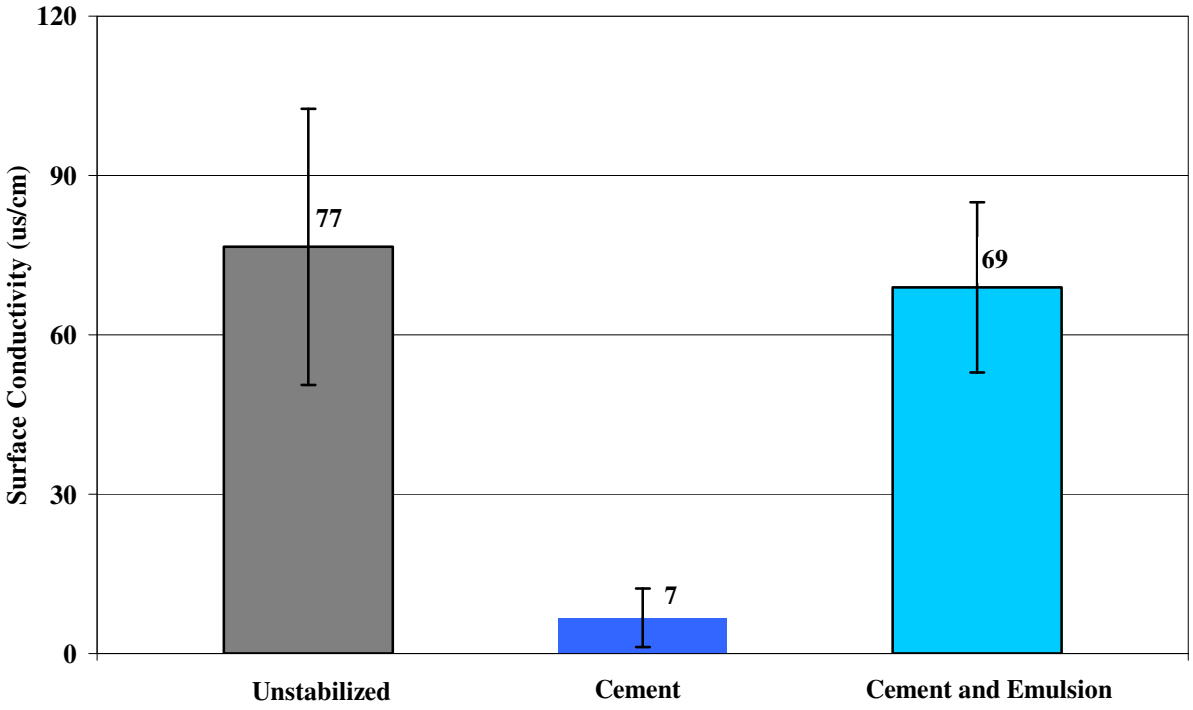

Figure 5-4 Mean Surface Conductivity Results of C.S. 15-11 Materials (± 2SD)

As shown in Table 5-2 and Figure 5-3, the cement stabilization and cement with emulsion asphalt stabilization slightly increased the moisture intake potential of the unstabilized material on C.S. 15-11. The cement with asphalt emulsion stabilization was found to take in more water than the *in situ* granular material, as well as cement stabilized material.

As shown in Figure 5-4, the cement stabilized material yielded the lowest surface conductivity among all three test section materials on C.S. 15-11. This revealed that the cement stabilization provided the best resistance to water damage among all test sections conducted on C.S. 15-11, possibly due to the hydration effects. The cement with emulsion asphalt stabilization on C.S. 15-11 was found to improve the resistance to moisture of *in situ* granular materials. However, the degree of improvement is less than the cement stabilization.

5.3 Unconfined Compressive Strength Characterization

Unconfined compressive strength testing was performed as per ASTM D5102 at dry conditions and 24-hour-soaked conditions on samples of C.S. 15-11 test sections. Samples used in unconfined compressive strength were cured for approximately eight months before testing. The results across various test sections are summarized in Table 5-3 and illustrated in Figure 5-5.

As illustrated in Figure 5-4, both cement stabilization and cement with asphalt emulsion stabilization on C.S. 15-11 increased unconfined compressive strength of unstabilized material. The cement stabilization was found to provide greater strength improvement on C.S. 15-11 *in situ* material than the cement with asphalt emulsion stabilization.

The soaked strength testing results revealed that both cement stabilization and cement with emulsion asphalt increased the soaked unconfined compressive strength, indicating that both stabilization systems reduced the moisture sensitivity of C.S. 15-11 *in situ* granular base material. The cement stabilization on C.S. 15-11 was found to have much greater soaked strength and lower moisture sensitivity than the cement with asphalt emulsion stabilization. These results concur with the findings from the indirect tension testing previously in this research.

Table 5-3 Unconfined Compressive Strength Results of C.S. 15-11 Bases

Granular Base System		Average Unconfined Compressive Strength (kPa)	Coefficient of Variance (%)
Cement Stabilization	**Moist Cured**	3745	1.9
	Soaked	2171	10.6
Cement and Asphalt Emulsion Stabilized	**Moist Cured**	672	5.6
	Soaked	270	29.0
Unstabilized	**Moist Cured**	343	24.7
	Soaked	50	14.1

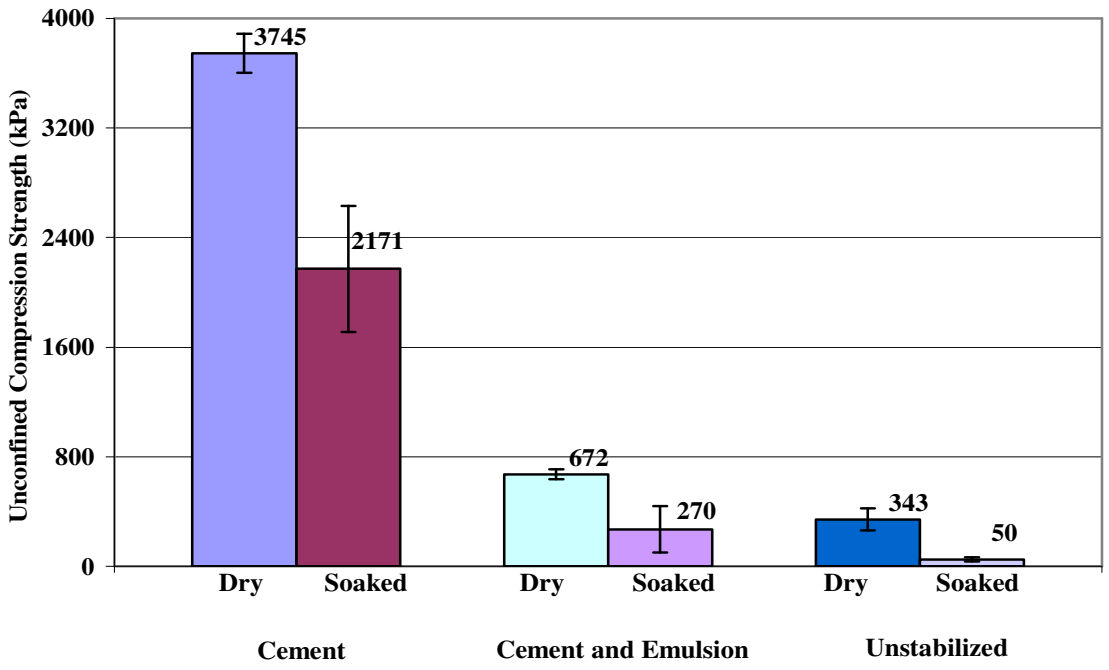

Figure 5-5 Unconfined Compressive Strength Results of C.S. 15-11 Materials

5.4 Chapter Summary

Chapter five provides a summary and discussion of the findings from moisture sensitivity testing performed on various C.S. 15-11 test section materials. The indirect tensile strength test revealed that both cement and cement with emulsion asphalt stabilization systems increased the indirect tensile strength and reduced the moisture susceptibility of *in situ* C.S. 15-11 granular base materials. Cement stabilization was found to have more significant improvement on the tensile strength and moisture resistance than the cement with asphalt emulsion stabilization.

The indirect tensile strength testing results showed that strengths from 150 mm samples were not the same as 100 mm samples. For instance, 150 mm cement stabilized samples provided greater indirect tensile strength values than 100 mm cement stabilized samples. In contrast, the 150 mm cement with emulsion stabilized samples yielded lower indirect tensile strength as compared to 100 mm cement with emulsion stabilized samples. It is suspected that the curing time, compaction energy, and specimen size may be the sources of the strength disparities. Therefore, future testing may be improved by specifying and standardizing sample curing conditions, curing time, compaction method, and the mould size for QC/QA testing purposes of granular base stabilization in Saskatchewan.

It should be noted that the retained indirect tensile strength ratios of both 100 mm and 150 mm sample on C.S. 15-11 materials were relatively low, ranging from 25 to 58 percent. It is suspected that the low retained values were a direct result of the length of time taken in sample transportation from the test section to the laboratory at University of Saskatchewan. Therefore, it is suggested that testing samples shall be compacted at site without delay for construction QA/QC purpose in the future.

Moisture capillary intake testing showed that cement stabilization and cement with emulsion asphalt stabilization slightly increased the moisture intake potential of the *in situ* unstabilized material on C.S. 15-11. The cement with asphalt emulsion stabilization was found to take in more water than the cement stabilization on C.S. 15-11.

The cement stabilized material yielded the lowest surface conductivity values among all three test section materials on C.S. 15-11, indicating that the cement stabilization provided the best resistance to moisture damage among all test sections. The cement with emulsion asphalt conducted on C.S. 15-11 was also found to improve the resistance to moisture of *in situ* granular materials. However, the degree of improvement is less relative to cement stabilization.

Both cement stabilized and cement with asphalt emulsion stabilized samples in C.S. 15-11 increased the unconfined compressive strength of unstabilized material. The cement stabilization was found to provide greater unconfined compressive strength improvement on C.S. 15-11 *in situ* material relative to the cement with asphalt emulsion stabilization.

Both cement stabilization and cement with emulsion asphalt increased the soaked unconfined compressive strength, indicating that both stabilization systems reduced the moisture sensitivity of C.S. 15-11 *in situ* granular base material. Cement stabilization on C.S. 15-11 was found to have greater soaked unconfined compressive strength and lower moisture susceptibility than the cement with asphalt emulsion stabilization. These results concur with the findings from the indirect tension testing performed in this research.

CHAPTER 6 MECHANISTIC RAPID TRIAXIAL CHARACTERIZATION

This chapter presents test results and findings from the rapid triaxial frequency sweep testing. Rapid triaxial frequency sweep testing was performed using the rapid triaxial tester (RaTT) at University of Saskatchewan Transportation Centre, on various materials applied in C.S. 15-11 construction.

The rapid triaxial tester can provide reliable information on the constitutive properties materials in response to dynamic loading, such as dynamic modulus, Poisson's ratio, phase angle, and radial strain behaviour. This chapter presents an evaluation of the constitutive relationships of various materials of C.S. 15-11 test section materials and provides a discussion of the laboratory mechanistic responses to the correlated field performance of pavement.

6.1 Triaxial Frequency Sweep Testing Protocol

The background information of triaxial frequency sweep testing has been presented and discussed in Chapter Two. RaTT has been used successfully for testing various road materials including asphalt and granular materials (Berthelot 1999, Baumgartner 2005, Berthelot et al. 2005, Anthony 2007, Berthelot et al. 2007).

The rapid triaxial testing was performed on samples compacted with *in situ* remixed granular base material, cement stabilized base material, and cement with asphalt emulsion stabilized material applied in C.S. 15-11 construction. Six repeat samples were used for each stabilization type in rapid triaxial testing for this research.

The RaTT apparatus employs samples of a 150 mm diameter and a 150 ± 5 mm height, compacted by the gyratory compactor. The desired termination density of the samples of C.S. 15-11 materials were set to be equal to the maximum dry density of *in situ* granular material under optimum moisture content. All gyratory samples in this research were cured for about 10 months in the moist room prior to rapid triaxial

frequency sweep testing. A picture of one of the samples subjected to RaTT testing is provided in Figure 6-1:

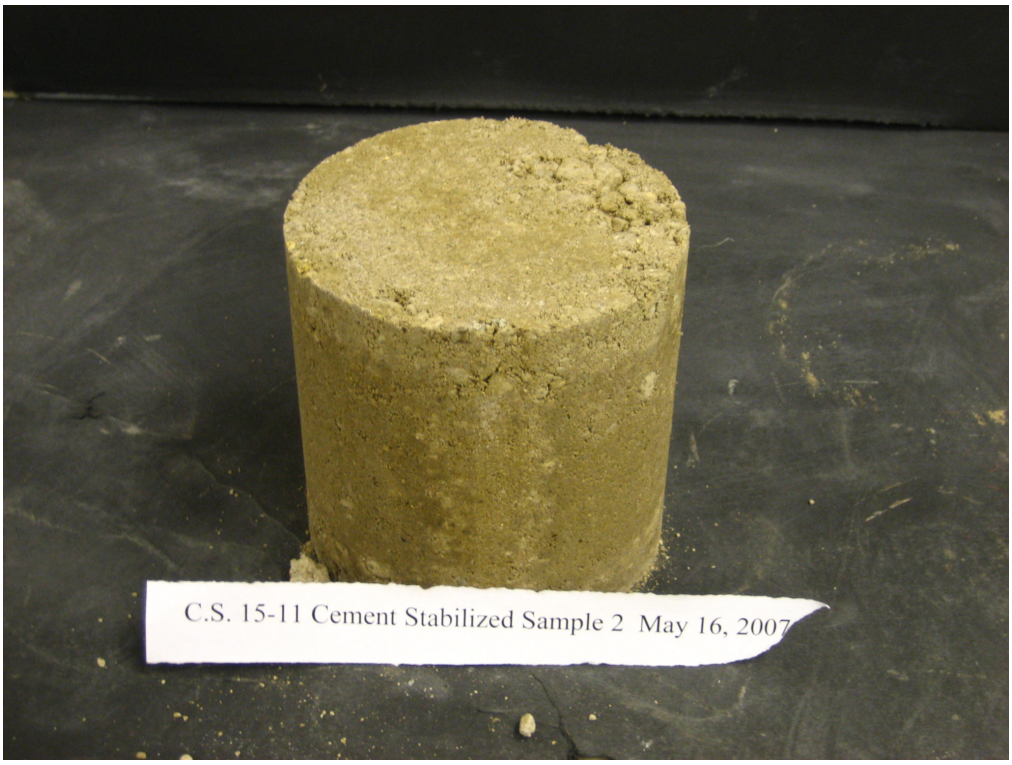

Figure 6-1 Gyratory Compacted Continuum Specimen for RaTT Testing of C.S. 15-11

The testing protocols employed in this research for C.S. 15-11 granular base materials were derived from recent research and experience of various base and subbase materials at University of Saskatchewan (Berthelot et al. 2004; Berthelot et al. 2005; PSI 2006; Berthelot et al. 2007).

The rapid triaxial testing applied in this research consisted of four consecutive stress states at four frequencies at room temperature, as shown in Table 6-1 and Table 6-2. The stress invariant I_1 varied from 850 kPa to 1150 kPa. Accordingly, the deviatoric stress varied from 200 kPa to 550 kPa. The parameters of sample testing shown in Table 6-1 are further explained in Equation 6-1, Equation 6-2, Equation 6-3, and Equation 6-4.

Table 6-1 Laboratory RaTT Testing Protocols for C.S. 15-11 Base Materials

Stress State	Max Axial Traction $\sigma_{a\max}$ (kPa)	Min Axial Traction $\sigma_{a\min}$ (kPa)	Confining Traction σ_c (kPa)	Max Stress Invariant I_1, (kPa)	Max Stress Invariant J_2, (kPa)	Max Deviatoric Stress σ_d (kPa)	Max Shear Stress $\tau_{\max}$ (kPa)
One	450	250	250	950	13333	200	100
Two	650	250	250	1150	53333	400	200
Three	650	100	100	850	100833	550	225
Four (Fully Reversed)	450	150	250	950	13333	200	100

Table 6-2 Triaxial Frequency Sweep Loading Frequency

Testing Sequence	Frequency (Hz)
1	10.0
2	5.0
3	1.0
4	0.5

$$I_1 = 2\sigma_c + \sigma_a \quad \textbf{(6-1)}$$

$$J_2 = \frac{1}{3}(\sigma_a - \sigma_c)^2 \quad \textbf{(6-2)}$$

$$\sigma_d = \sigma_a - \sigma_c \quad \textbf{(6-3)}$$

$$\tau_{\max} = \frac{1}{2}\sigma_d \quad \textbf{(6-4)}$$

Where:

I_1 = first stress invariant of stress tensor

J_2 = second stress invariant of deviatoric stress tensor

σ_d = deviatoric stress

τ_{max} = maximum shear stress

σ_a = axial traction applied on sample during RaTT testing

σ_c = confining traction applied on sample during RaTT testing

The samples were pre-conditioned in the RaTT cell, and then characterized across stress state one through four. Figure 6-2 illustrates the stress state one.

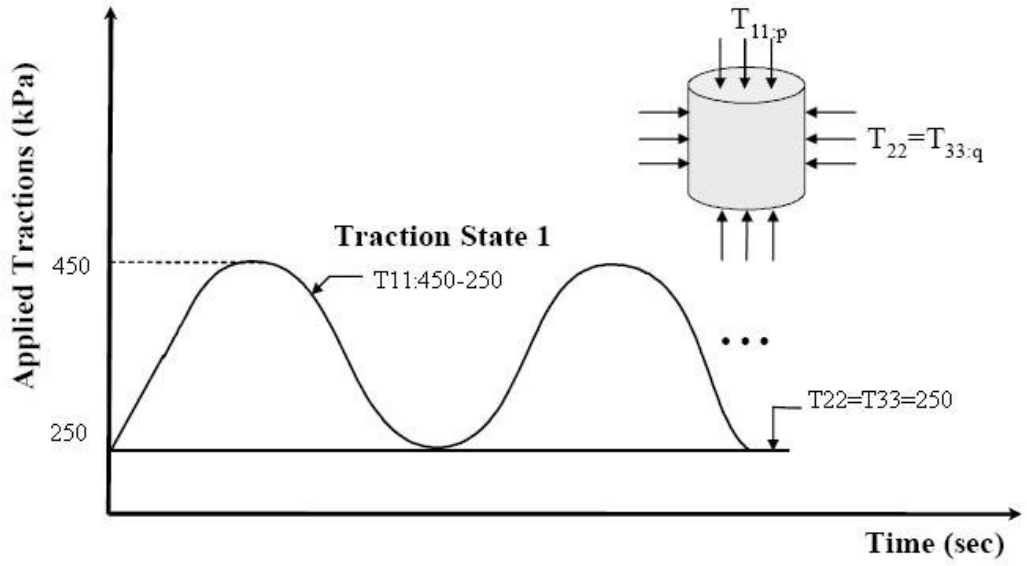

Figure 6-2 Illustration of Applied Tractions Magnitudes of Stress State One

Under stress state one, the rapid triaxial frequency sweep testing started from the least damage-causing high frequency (10 Hz) and progressively increased to higher damage-causing frequency, as shown in Table 6-2. If the sample survived under stress state one, the testing was continued to stress state two, starting again from high frequency to low frequency. The testing included all four stress states unless the sample failed.

The stress state four was found to be the most damage-causing stress state in which the applied axial traction may be less than the confinement stress. As a result, the sample subjected to stress state four can be under extension instead of all compression at first three stress states.

The RaTT characterization calculated four material properties outputs which are thought to be related to C.S. 15-11 performance for the analysis and discussion. The properties calculated include:

- Dynamic Modulus
- Poisson's ratio
- Phase angle
- Recoverable radial microstrain

6.2 Dynamic Modulus Characterization

Dynamic modulus (E_d), is the primary structural design material constitutive property which measures the stiffness. Dynamic modulus can be used to quantify the constitutive relationship of all pavement materials applied in C.S. 15-11 construction under applied dynamic load.

During the rapid triaxial testing, it was observed that the cement stabilized samples can remain intact during the full testing sequence. However, it also showed an abnormal phase angle at the final two frequency sweeps at stress state four. The cement with emulsion stabilized samples showed abnormal phase angle values at the beginning of stress state four without observing any visible cracks on the sample surface after extraction. The unstabilized samples failed at the beginning of stress state two. An evident crack was found on unstabilized sample, as shown in Figure 6-3.

Figure 6-3 Typical Unstabilized Sample Failure in RaTT Testing

Table 6-3 shows the mean dynamic modulus of C.S. 15-11 materials across stress state averaged by frequency. The mean dynamic modulus results are also illustrated in Figure 6-4.

If a specimen failed during the frequency sweep characterization, a value of 0 kPa was assigned for dynamic modulus in Table 6-3. The assigned E_d value represents the range limits measurable by the apparatus at failure.

The rapid triaxial testing results showed that the unstabilized granular base material, the cement with emulsion stabilized material, and the cement stabilized material, averaged by deviatoric stress from 200 kPa to 550 kPa, yielded mean dynamic modulus of 131 kPa, 915 kPa and 1595 kPa, respectively.

As shown in Table 6-3, it was found that both stabilized materials of C.S. 15-11 increased the dynamic modulus of *in situ* unstabilizd granular base material. The cement stabilization showed higher improvement of dynamic modulus relative to the cement with asphalt emulsion stabilization, as expected.

As illustrated in Figure 6-4, although maximum deviatoric stresses were the same (200 kPa), the dynamic modulus of stress state one is significantly higher than the

dynamic modulus of fully reversed stress state four, for all material types used to construct C.S. 15-11.

As shown in Figure 6-4, the dynamic modulus decreases with increasing deviatoric stress for cement with emulsion asphalt stabilized material and unstabilized material of C.S. 15-11. However, the same trend was not evidently shown on cement stabilized materials results, indicating that the cement stabilized material is less sensitive to increasing deviatoric stress.

Table 6-4 shows the mean dynamic modulus of C.S. 15-11 materials across frequency averaged by stress state. If the sample failed in the first three stress states, a value of zero was assigned for calculation. However, fully reversed stress states four are not included in the calculation. The mean dynamic modulus results averaged by stress state are also illustrated in Figure 6-5.

Dynamic modulus results averaged across stress states showed that unstabilized granular base material, the cement with emulsion stabilized material, and the cement stabilized material, averaged by frequency from of 10 Hz to 0.5 Hz, yielded mean dynamic modulus of 175 kPa, 947 kPa and 1708 kPa, respectively.

As shown in Figure 6-5, as the frequency decreases, the dynamic modulus of cement with emulsion asphalt stabilized material and unstabilized material also slightly decrease. However, the cement stabilized materials were found to have minimal sensitivity to frequency of all materials used to construct C.S. 15-11.

Table 6-3 Mean Dynamic Modulus across Stress State averaged by Frequency

Section Name	Deviatoric Stress (kPa)	Mean Dynamic Modulus (kPa)	Coefficient of Variance (%)
Unstabilized	200	524	10.0
	400	0 (Sample Failed)	0
	550	0 (Sample Failed)	0
	200 (Fully Reserved)	0 (Sample Failed)	0
Cement and Emulsion Stabilization	200	1050	13.1
	400	1011	13.0
	550	779	7.9
	200 (Fully Reserved)	821	8.4
Cement Stabilization	200	1658	16.4
	400	1785	16.4
	550	1680	11.6
	200 (Fully Reserved)	1255	39.6

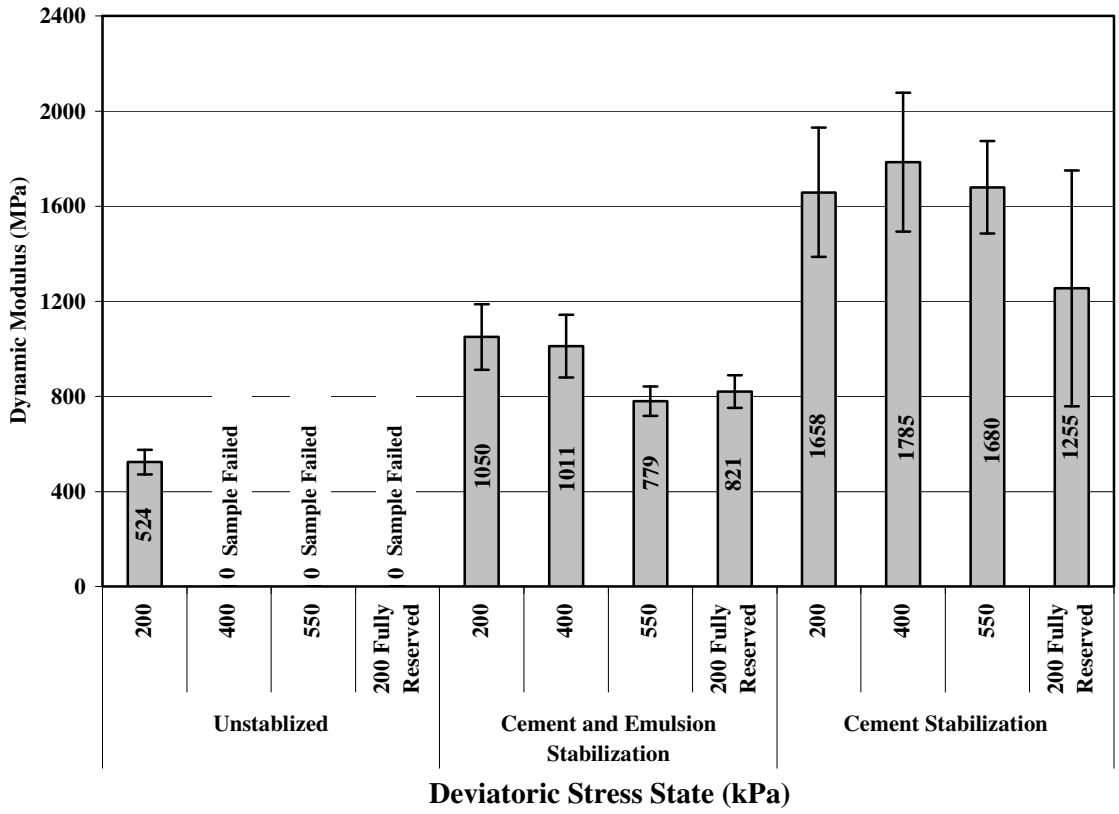

Figure 6-4 Mean Dynamic Modulus across Stress State averaged by Frequency (± 2SD)

Table 6-4 Mean Dynamic Modulus across Frequency averaged by Stress State

Section Name	Frequency (Hz)	Mean Dynamic Modulus (kPa)	Coefficient of Variance (%)
Unstabilized[1]	10	176	73.3
	5	175	73.3
	1	175	73.3
	0.5	174	73.3
Cement and Emulsion Stabilization	10	994	7.7
	5	971	8.3
	1	922	9.2
	0.5	901	9.8
Cement Stabilization	10	1720	8.4
	5	1740	8.7
	1	1689	7.3
	0.5	1683	6.1

1. Failed unstabilized samples were included in the calculation, assuming 0 for dynamic modulus.

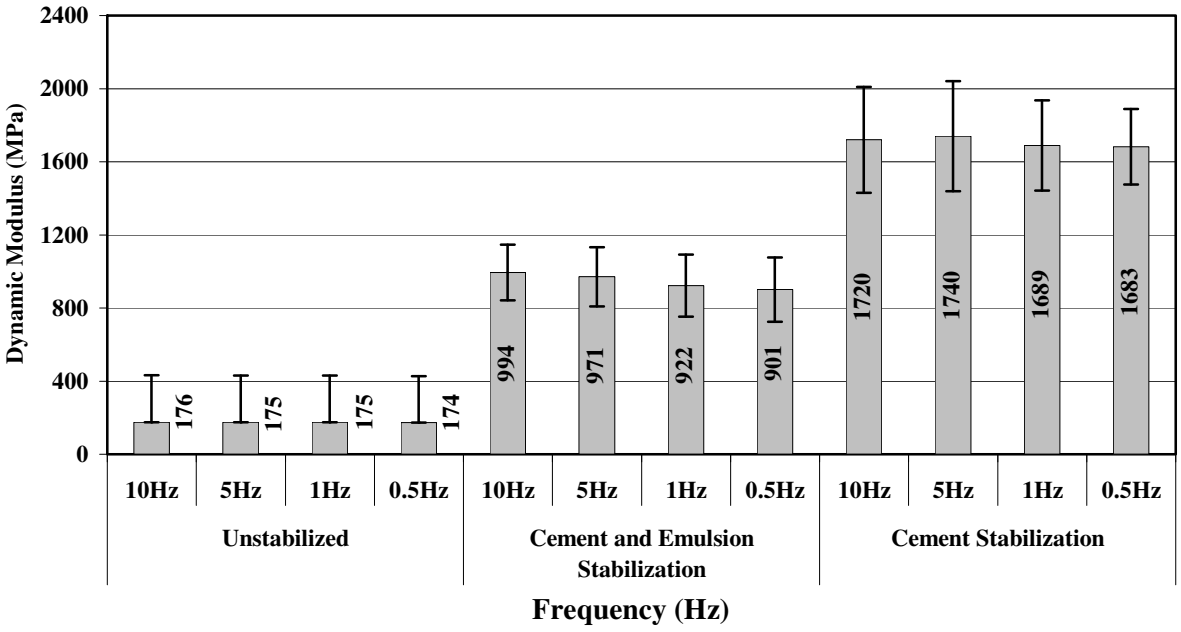

Figure 6-5 Mean Dynamic Modulus across Frequency averaged across Stress State (± 2SD)

Statistical analysis of variance (ANOVA) was performed on dynamic modulus results to evaluate the statistically significance at a 95 percent confidence level across stress states, frequencies and stabilization types. The ANOVA of dynamic modulus results is shown in Table 6-5 .

Table 6-5 ANOVA of Dynamic Modulus of C.S. 15-11 Materials

Effect	Sum of Squares	Degrees of Freedom	Mean Squares	F Statistic	P
Mix	84627693	2	42313847	1434.71	0.00
DS	2402000	2	1201000	40.72	0.00
Frequency	83615	3	27872	0.95	0.42
Mix*DS	3239658	4	809914	27.46	0.00
Mix* Frequency	55066	6	9178	0.31	0.93
DS * Frequency	22681	6	3780	0.13	0.99
Mix* DS *Frequency	58083	12	4840	0.16	1.00
Error	5308736	180	29493		

Mix= Stabilization Type, DS=Deviatoric Stress

As shown in Table 6-5, significant differences of dynamic modulus values exist across the stabilization systems evaluated at the C.S. 15-11. In addition, significant differences of dynamic modulus values were observed to exist across various deviatoric stresses applied in rapid triaxial frequency sweep testing. However, the frequency of rapid triaxial testing was not a factor that resulted in statistical significant differences on dynamic modulus of C.S. 15-11 materials.

In order to further identify which stabilization system and stress state yielded statistically difference of dynamic modulus results, Tukey's homogenous group analysis was performed at a confidence level of 95 percent on the dynamic modulus results. Materials which provide no significantly different dynamic modulus values were grouped in a homogenous group and were labelled with a capital letter for that group. The Tukey's homogeneous group analysis result is shown in Table 6-6 and Table 6-7.

Table 6-6 Tukey's Homogeneous Groups for Dynamic Modulus Grouped by Stabilization System and Deviatoric Stress averaged by Frequency

Stabilization Type	Deviatoric Stress (kPa)	Mean Dynamic Modulus (kPa)	Tukey's Homogeneous Groups				
Unstablized	550	0 (Sample Failed)	A				
	400	0 (Sample Failed)	A				
	200	524		B			
Cement and Asphalt Emulsion	550	779			C		
	400	1011				D	
	200	1050				D	
Cement	550	1680					E
	400	1785					E
	200	1658					E

Table 6-7 Tukey's Homogeneous Groups for Dynamic Modulus Grouped by Stabilization System and Frequency averaged by Stress State

Stabilization Type	Frequency (Hz)	Mean Dynamic Modulus (kPa)	Tukey's Homogeneous Groups			
Unstablized	0.5	174	A			
	1	175	A			
	5	175	A			
	10	176	A			
Cement and Asphalt Emulsion	0.5	901		B		
	1	922		B		
	5	971		B		
	10	994		B		
Cement	0.5	1683				C
	1	1689				C
	5	1740				C
	10	1720				C

Table 6-6 shows the Tukey's homogeneous group result for dynamic modulus averaged by frequency. It is seen that, due to the failure at deviatoric stresses of 550 kPa and 400 Kpa, the unstabilized granular material of C.S. 15-11 yielded lower dynamic modulus at deviatoric stress 400 and 500 kPa, relative to deviatoric stress 200 kPa. Furthermore, unstabilized material at deviatoric stresses of 200 kPa yielded significantly lower dynamic modulus relative to cement with asphalt emulsion stabilized and cement stabilized materials at all stress states.

As shown in Table 6-6, cement with asphalt emulsion stabilized material at deviatoric stresses of 400 and 200 kPa has significantly higher dynamic modulus relative to at deviatoric stress of 550 kPa. The cement stabilized material was found to yield a significantly higher dynamic modulus than other materials on C.S. 15-11 construction.

Table 6-7 shows the Tukey's homogeneous group result for dynamic modulus averaged by stress state. Unstabilized material, cement and emulsion asphalt stabilized material and cement stabilized material yielded no statistically different dynamic modulus across frequency. However, dynamic modulus averaged by stress state is significantly different across stabilization system on C.S. 15-11, as shown in Table 6-7.

6.3 Poisson's Ratio Characterization

Poisson's ratio is a primary material property which is defined as the ratio of the radial strain to the axial strain. Poisson's ratio is one of the most important inputs for pavement modeling and pavement thickness design. The evaluation of Poisson's ratio of C.S. 15-11 materials including *in situ* granular base material, cement stabilized granular base material and cement and emulsion asphalt stabilized granular base material are discussed below.

In analysis of Poisson's ratio of this research, if a specimen failed during the rapid triaxial frequency sweep characterization, a value of 0.9 was assigned for Poisson's ratio. This value represents the range limit measurable by the RaTT apparatus at failure.

Rapid triaxial frequency sweep testing results showed that unstabilized granular base material, the cement with emulsion stabilized material, and the cement stabilized material applied on C.S 15-11, averaged by deviatoric stress from 200 kPa to 550 kPa, yielded Poisson's ratios of 0.78, 0.28 and 0.10, respectively.

As shown in Table 6-8, both stabilization systems applied in C.S. 15-11 construction reduced the Poisson's ratio of *in situ* granular base material. The cement stabilization was observed to produce a greater reduction in Poisson's ratio of *in situ* material relative to cement with emulsion asphalt stabilization.

As shown in Table 6-8 and Figure 6-6, the Poisson's ratio of both stabilized materials applied in C.S. 15-11 construction increase with increasing deviatoric stress under compressive stress states. Poisson's ratio of cement stabilized materials showed less sensitivity to stress states than the Poisson's ratio of cement with emulsion stabilized materials.

Table 6-9 and Figure 6-7 showed the Poisson's ratio of C.S. 15-11 materials across frequency averaged by stress state. If the sample failed in the first three stress states, a value of 0.9 was assigned for calculation. However, fully reversed stress states four are not included in the calculation.

The Poisson's ratio results averaged by stress state showed that unstabilized material, the cement with emulsion stabilized material, and the cement stabilized material of C.S. 15-11, averaged by frequency from of 10 Hz to 0.5 Hz, yielded mean Poisson's ratio of 0.75, 0.27, and 0.11 respectively.

As shown in Figure 6-7, as the frequency decreases, the Poisson's ratios of both C.S. 15-11 stabilized materials increase slightly. However, the cement stabilized material applied on C.S. 15-11 showed less sensitivity to frequency than the cement with asphalt emulsion stabilized material.

Table 6-8 Mean Poisson's Ratio across Stress State averaged by Frequency

Section Name	Deviatoric Stress (kPa)	Mean Poisson's Ratio	Coefficient of Variance (%)
Unstabilized	200	0.44	3.9
	400	0.90 (Sample Failed)	0.0
	550	0.90 (Sample Failed)	0.0
	200 (Fully reversed)	0.90 (Sample Failed)	0.0
Cement and Emulsion Stabilization	200	0.18	36.6
	400	0.26	37.4
	550	0.38	22.1
	200 (Fully reversed)	0.29	25.8
Cement Stabilization	200	0.09	32.0
	400	0.11	26.9
	550	0.12	22.5
	200 (Fully reversed)	0.08	36.7

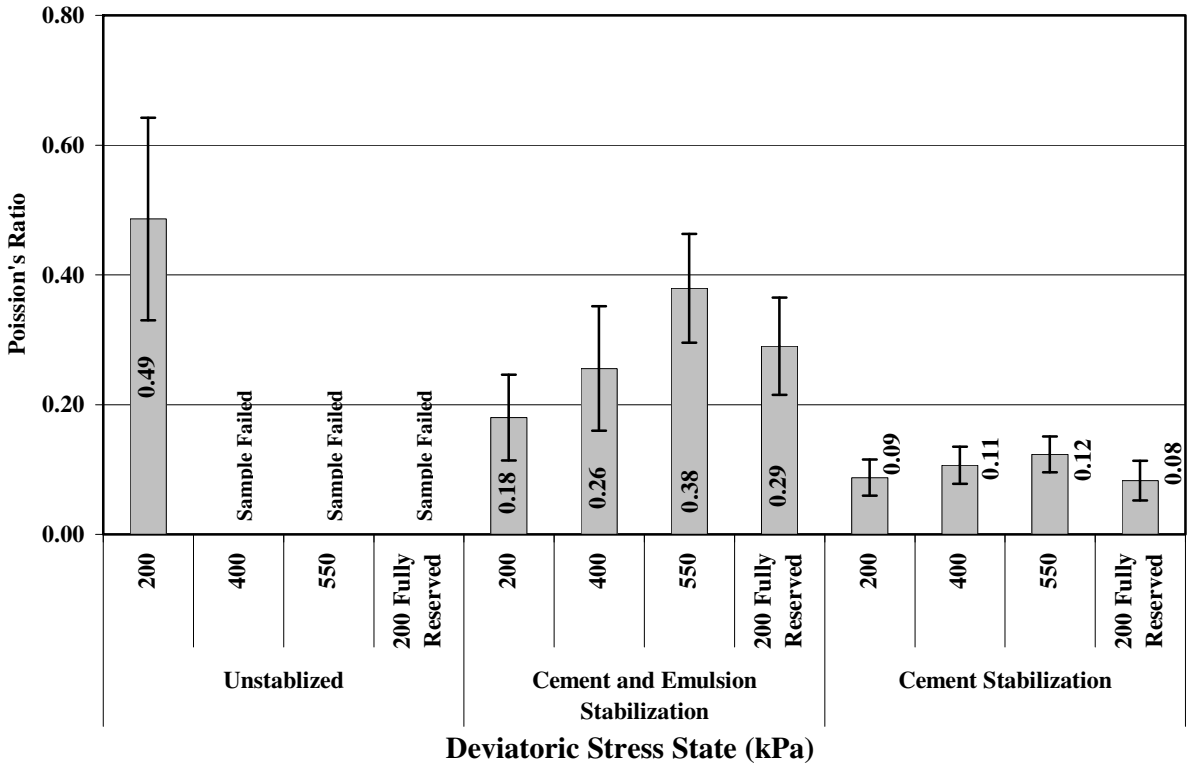

Figure 6-6 Mean Poisson's Ratio across Stress State averaged across Frequency (± 2SD)

Table 6-9 Mean Poisson's Ratio across Frequency averaged by Stress State

Section Name	Frequency (Hz)	Mean Poisson's Ratio	Coefficient of Variance (%)
Unstabilized[1]	10	0.74	30.9
	5	0.75	30.0
	1	0.75	30.0
	0.5	0.75	29.9
Cement and Emulsion Stabilization	10	0.25	38.7
	5	0.26	43.3
	1	0.28	43.6
	0.5	0.30	45.2
Cement Stabilization	10	0.09	42.0
	5	0.10	29.7
	1	0.11	21.5
	0.5	0.12	23.8

1. Failed unstabilized samples were included in the calculation, assuming 0.9 for Poisson's ratio.

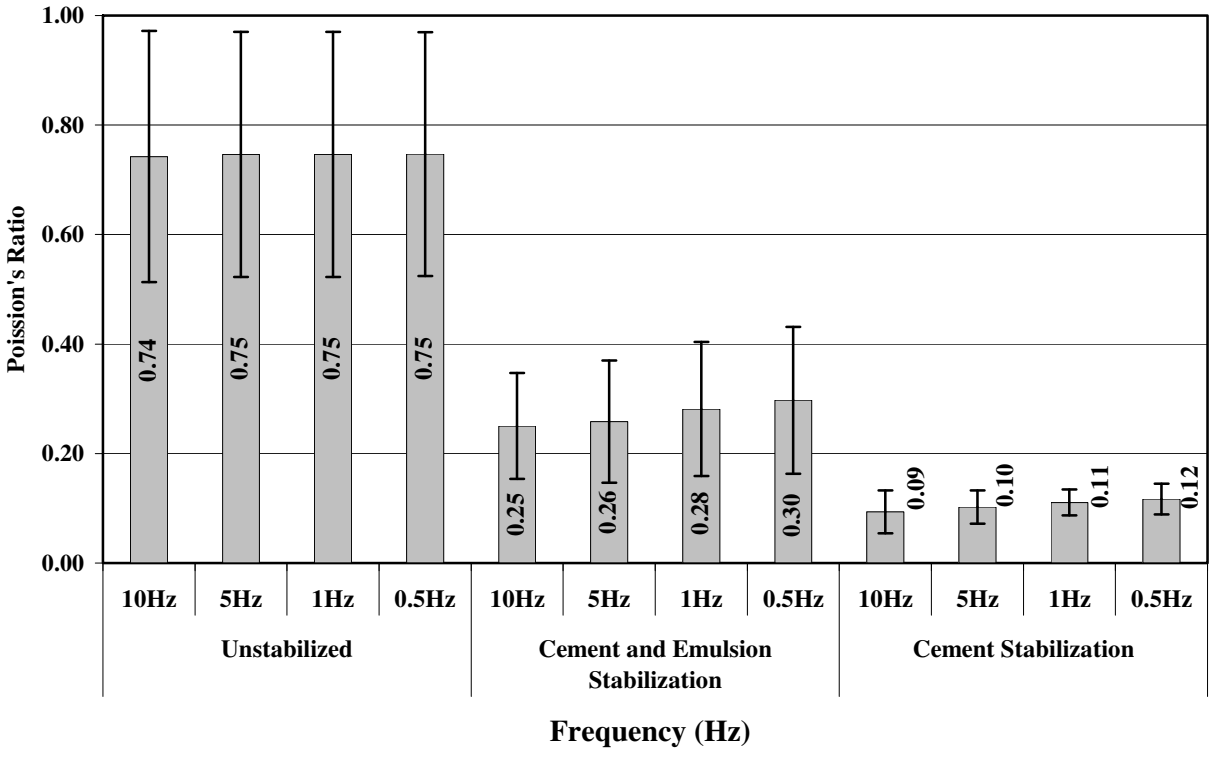

Figure 6-7 Mean Poisson's Ratio across Frequency averaged by Stress State (± 2SD)

The statistical Analysis of Variance (ANOVA) was performed on Poisson's ratio results to evaluate the statistically significant differences across stress states, frequencies and stabilization types at a 95 percent confidence level. The ANOVA results of Poisson's ratio are shown in Table 6-10.

Table 6-10 ANOVA of Poisson's Ratio of C.S. 15-11 Materials

Effect	Sum of Squares	Degrees of Freedom	Mean Squares	F Statistic	P
Mix	15.87	2	7.93	2904.18	0.00
DS	2.18	2	1.09	399.67	0.00
Frequency	0.02	3	0.01	2.42	0.07
Mix*DS	1.75	4	0.44	160.35	0.00
Mix* Frequency	0.01	6	0.00	0.67	0.67
DS * Frequency	0.00	6	0.00	0.18	0.98
Mix* DS *Frequency	0.01	12	0.00	0.26	0.99
Error	0.49	180	0.00		

Mix= Stabilization Type; DS=Deviatoric Stress

As shown in Table 6-10, both stabilization type and deviatoric stress were identified as factors that yielded statistically significant differences on mean Poisson's ratio values of C.S. 15-11 materials. However, testing frequency does not yield significant different Poisson's values.

To further identify which stabilization system and deviatoric stress yielded statistically significant differences of the Poisson's ratio values, Tukey's homogenous group analysis was performed at a confidence level of 95 percent on the Poisson's ratio results. Materials which are not statistically different were grouped in a homogenous group were labelled with a capital letter for that group. The Tukey's homogenous group result is shown in Table 6-11 and Table 6-12.

Table 6-11 Tukey's Homogeneous Groups for Poisson's Ratio Grouped by Stabilization Type and Deviatoric Stresses averaged by Frequency

Stabilization Type	Deviatoric Stress (kPa)	Mean Poisson's Ratio	Tukey's Homogeneous Groups					
Unstabilized	550	Sample Failed (0.9)	A					
	400	Sample Failed (0.9)	A					
	200	0.49		B				
Cement and Asphalt Emulsion	550	0.38			C			
	400	0.26				D		
	200	0.18					E	
Cement	550	0.12						F
	400	0.11						F
	200	0.09						F

Table 6-12 Tukey's Homogeneous Groups for Poisson's Ratio Grouped by Stabilization System and Frequency averaged by Stress State

Stabilization Type	Frequency (Hz)	Mean Poisson's Ratio	Tukey's Homogeneous Groups		
Unstablized	0.5	0.75	A		
	1	0.75	A		
	5	0.75	A		
	10	0.74	A		
Cement and Asphalt Emulsion	0.5	0.30		B	
	1	0.28		B	
	5	0.26		B	
	10	0.25		B	
Cement	0.5	0.12			C
	1	0.11			C
	5	0.10			C
	10	0.09			C

Table 6-11 showed the Tukey's homogeneous groups for Poisson's ratio grouped by stabilization type and deviatoric stresses averaged by frequency. Due to the failure occuring during testing, unstabilized granular materials of C.S. 15-11 test section at

higher deviatoric stresses (400 kPa and 550 kPa) yielded significant lower Poisson's ratios relative to deviatoric stress of 200 kPa. Furthermore, unstabilized materials generally yield significantly higher Poisson's ratio values relative to the cement stabilized and cement with emulsion stabilized materials.

As also seen in Table 6-11, the cement with asphalt emulsion stabilized materials at three deviatoric stresses are significant different from each other, showing that the Poisson's ratio value of cement and emulsion material had relatively large sensitivity to stress state. The result concurs with the conclusions in Figure 6-7. The cement stabilized materials on C.S. 15-11 showed no statistically significant difference across stress states. In addition, the cement stabilized materials yielded significantly lowest Poisson's ratio among all materials applied in C.S. 15-11 construction.

Table 6-12 shows the Tukey's homogeneous group result for Poisson's ratio averaged by stress state. Unstabilized material, cement and emulsion asphalt stabilized material, and cement stabilized material yielded no statistically different Poisson's ratio across frequency. However, Poisson's ratio averaged by stress state is significantly different across stabilization system on C.S. 15-11.

6.4 Radial Strain Characterization

Radial strain is believed to be a primary indicator of materials tendency of edge shear failure under typical truck loading and field state conditions (Berthelot 2007).

If a sample failed during the frequency sweep characterization, a value of 400 $\times 10^{-6}$ was assigned for recoverable radial strain in Table 6-13. The assigned radial strain value represents the range limits measurable by the apparatus at failure.

As shown in Table 6-13, the unstabilized granular material, the cement with emulsion stabilized material, and the cement stabilized material applied in C.S. 15-11 construction, averaged by deviatoric stress from 200 kPa to 550 kPa, yielded mean radial strains of 341 $\times 10^{-6}$, 135 $\times 10^{-6}$ and 24 $\times 10^{-6}$, respectively.

The unstabilized material had the greatest radial strain among all stabilized materials applied on C.S. 15-11. These relatively large radial strains were believed to be one of the causes of shear failures observed in C.S. 15-11 granular base. However, cement and cement with emulsion asphalt stabilization materials applied in C.S. 15-11 significantly reduced the radial strains of *in situ* unstabilized granular material, indicating that these stabilization systems may be appropriate solutions for solving the pavement failure on C.S. 15-11. Furthermore, the cement stabilization was found to produce a greater reduction in radial strain relative to the cement with emulsion asphalt stabilization.

As shown in Figure 6-8, the radial strains of both stabilized materials increased with increasing deviatoric stress. The cement stabilized material was found to be less sensitive to the deviatoric stress, as compared to the cement with asphalt emulsion stabilized material. Samples at fully reversed stress state four yielded larger radial strain relative to stress state one.

Table 6-14 shows the mean radial strain of C.S. 15-11 materials across frequency averaged by stress state, which are also illustrated in Figure 6-9. If the sample failed in the first three stress states, a value of 400 was assigned for calculation. However, fully reversed stress states four are not included in the calculation.

Table 6-13 Mean Radial Strain across Stress State averaged by Frequency

Section Name	Deviatoric Stress (kPa)	Mean Radial Strain (10^{-6})	Coefficient of Variance (%)
Unstabilized	200	163	8.0
	400	400 (Sample failed)	0.0
	550	400 (Sample failed)	0.0
	200(Fully Reversed)	400 (Sample failed)	0.0
Cement and Emulsion Stabilization	200	36	54.3
	400	107	58.9
	550	255	29.4
	200(Fully Reversed)	143	56.0
Cement Stabilization	200	10	27.7
	400	24	30.9
	550	40	24.8
	200(Fully Reversed)	23	58.0

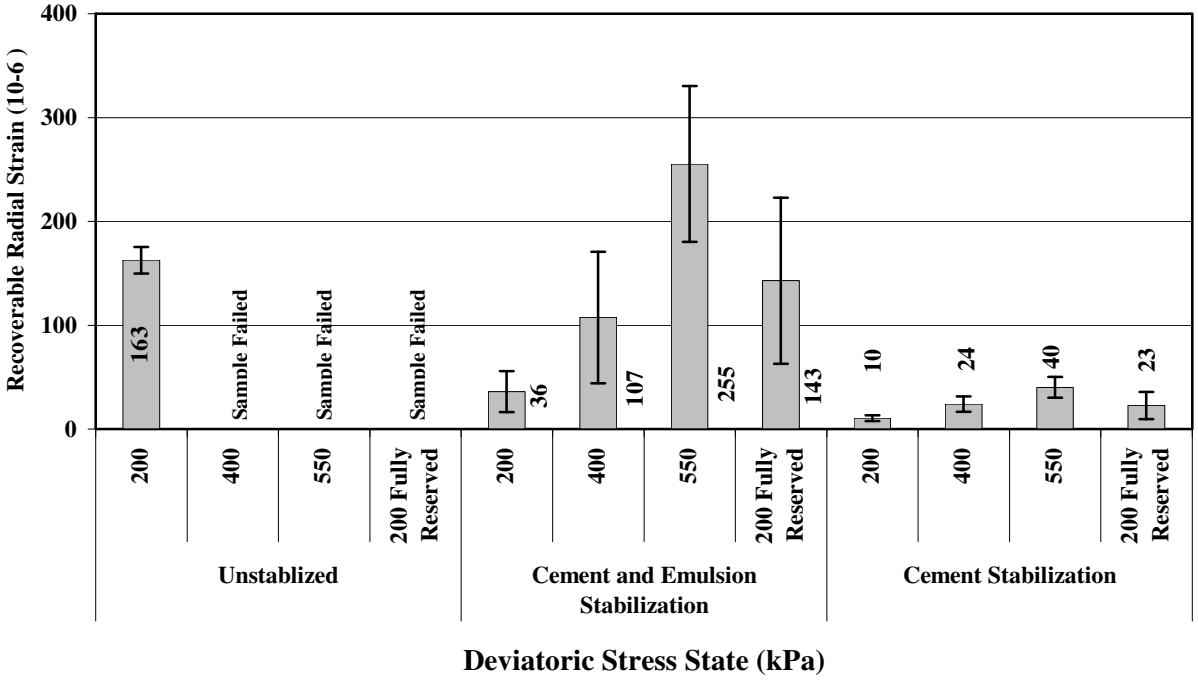

Figure 6-8 Mean Radial Strain across Stress State averaged by Frequency (± 2SD)

Table 6-14 Mean Radial Strain across Frequency averaged by Stress State

Section Name	Frequency (Hz)	Mean Radial Strain (10^{-6})	Coefficient of Variance (%)
Unstabilized[1]	10	319	36.8
	5	321	35.7
	1	321	35.7
	0.5	322	35.6
Cement and Emulsion Stabilization	10	110	79.4
	5	122	80.9
	1	143	81.8
	0.5	157	82.9
Cement Stabilization	10	22	66.9
	5	24	57.2
	1	26	53.3
	0.5	28	54.6

1. Failed unstabilized samples were included in the calculation, assuming 400× 10^{-6} for radial strain.

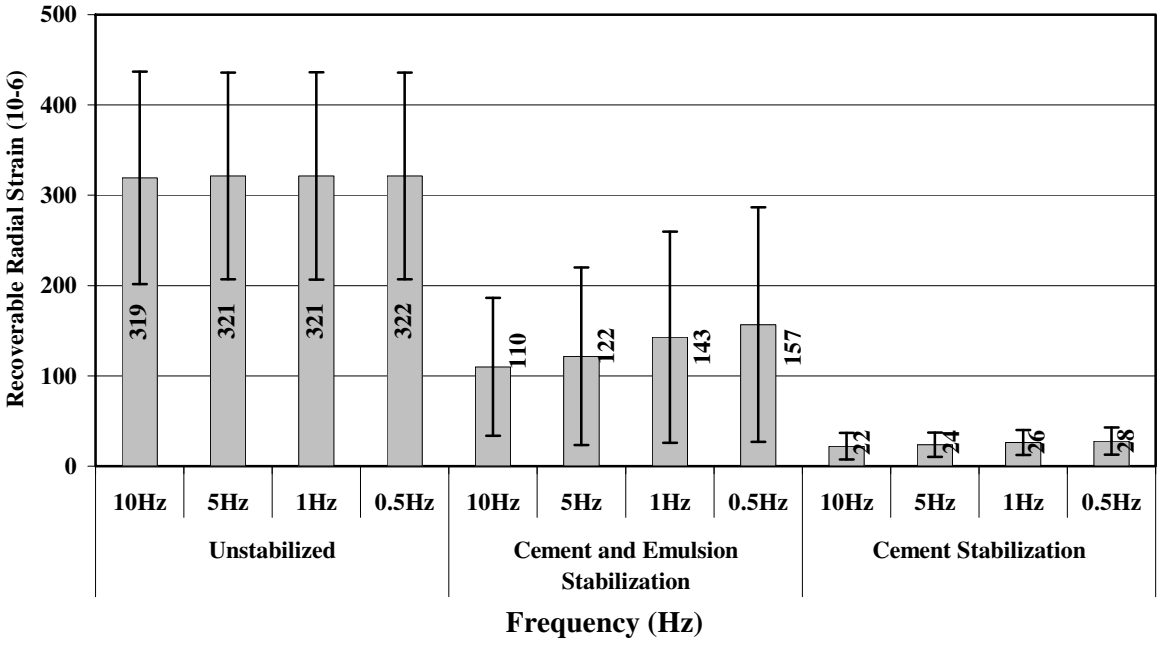

Figure 6-9 Mean Radial Strain across Frequency averaged by Stress State (± 2SD)

As shown in Table 6-14 and Figure 6-9, for both stabilized materials constructed on C.S. 15-11, the radial strain values increase with decreasing frequency. However, the cement stabilization was found to have less sensitivity to the frequency than the cement with emulsion stabilization, as expected.

The statistical Analysis of Variance (ANOVA) was performed on the radial strain results to evaluate the statistically significant differences at a 95 percent confidence level across stress states, frequencies and stabilization types. The ANOVA of radial strain results are shown in Table 6-15.

Table 6-15 ANOVA of Radial Strain of C.S. 15-11 Materials

Effect	Sum of Squares	Degrees of Freedom	Mean Squares	F Statistic	P
Mix	3230320	2	1615160	1462.58	0.00
DS	979178	2	489589	443.34	0.00
Frequency	10483	3	3494	3.16	0.03
Mix*DS	532662	4	133165	120.59	0.00
Mix* Frequency	13268	6	2211	2.00	0.07
DS * Frequency	5158	6	860	0.78	0.59
Mix* DS *Frequency	10537	12	878	0.80	0.66
Error	198779	180	1104		

Mix= Stabilization Type; DS=Deviatoric Stress

As shown in Table 6-15, factors of stabilization type, deviatoric stress and frequency all resulted in significant differences of radial strain values in rapid triaxial testing.

To further identify which stabilization type, deviatoric stress or frequency yielded statistically significant radial strain results, Tukey's homogenous group analysis was performed at a confidence level of 95 percent on the compression dynamic modulus test results. The combinations which have no significantly different radial strain values were grouped in a homogenous group and labelled with a capital letter for that group. The Tukey's homogeneous group analysis result is shown in Table 6-16 and Table 6-17.

Table 6-16 Tukey's Homogeneous Groups for Radial Strain Grouped by Stabilization System and Deviatoric Stress averaged by Frequency

Stabilization Type	Deviatoric Stress (kPa)	Mean Radial Strain (10^{-6})	Tukey's Homogeneous Groups				
Unstablized	200	163	A				
	400	400 (Sample Failed)		B			
	550	400 (Sample Failed)		B			
Cement and Asphalt Emulsion Stabilization	200	36			C		
	400	107				D	
	550	255					E
Cement Stabilization	200	10			C		
	400	24			C		
	550	40			C		

Table 6-17 Tukey's Homogeneous Groups for Radial Strain Grouped by Stabilization System and Frequency averaged by Stress State

Stabilization Type	Frequency (Hz)	Mean Radial Strain (10^{-6})	Tukey's Homogeneous Groups			
Unstablized	10	319	A			
	5	321	A			
	1	321	A			
	0.5	322	A			
Cement and Asphalt Emulsion	10	110		B		
	5	122		B	C	
	1	143		B	C	
	0.5	157			C	
Cement	10	22				D
	5	24				D
	1	26				D
	0.5	28				D

Table 6-16 shows the Tukey's homogeneous groups for radial strain grouped by stabilization system and deviatoric stress averaged by frequency. The unstabilized material has significant higher radial strain values relative to cement with emulsion asphalt stabilized material and cement stabilized material applied in C.S. 15-11 construction.

As also seen in Table 6-16, the cement with asphalt emulsion stabilized materials yielded significantly different radial strains under each deviatoric stress. The cement with asphalt emulsion stabilized materials yielded significantly different radial strains relative to cement stabilized materials, with an exception at deviatoric stress of 200 kPa which yielded similar radial strains as cement stabilized materials. The cement stabilized materials yielded no significantly different radial strain at all three deviatoric stresses, showing that cement stabilized material has minimal sensitivity to deviatoric stress of all materials applied in C.S. 15-11 construction.

Table 6-17 shows the Tukey's homogeneous group result for radial strain averaged by stress state. Radial strain averaged by stress state is significantly different across stabilization system on C.S. 15-11. However, cement and emulsion stabilized materials yielded statistically the same radial strain at 1 Hz, 5 Hz and 10 Hz. In addition, cement and emulsion stabilized materials yielded statistically the same radial strain at 0.5 Hz, 1 Hz and 5 Hz. This revealed that cement and emulsion stabilized materials are more sensitive to frequency than other materials on C.S. 15-11 with regards to radial strain.

6.5 Phase Angle Characterization

Phase angle is a measurement of the delay in observed strain response resulting from an applied traction state. Phase angle is considered to be an indication of the visco-elastic properties of the material.

It is known that if the phase angle is zero, the material is fully elastic and if the phase angle is 90 degrees, the material is purely viscous. In the case of this research, phase angle identifies the effect that the addition of asphalt emulsion has on stabilized granular bases. However, the phase angle is not yet fully understood with regard to how it relates to field performance. It is hypothesized that increasing phase angle may be an indication of increasing fracture toughness of stabilization systems (Berthelot et al. 2007). However, this hypothesis needs to be validated through observed long term field performance of test sections.

In this research, if the sample failed, a value of 25° was assigned, which represents the range limit measurable by the RaTT apparatus at failure.

The average phase angle across stress states showed that the unstabilized granular base material, the cement with emulsion stabilized material, and the cement stabilized material, averaged by deviatoric stress from 200 kPa to 550 kPa, yielded a mean phase angle of 21.1 degrees, 10.9 degrees, and 7.1 degrees, respectively.

As shown in Table 6-18 and Figure 6-10, the cement stabilization has significantly reduced the phase angle of *in situ* granular materials. The cement with emulsion asphalt stabilization did not show significant reduction of phase angle as compared to unstabilized *in situ* granular materials.

The phase angles of both stabilized materials at fully reversed stress state four are higher than the phase angles for the first three stress states in compression. In addition, in compressive stress states, the phase angles of both stabilized materials were found to increase with increasing deviatoric stress. However, as expected, the cement stabilized materials showed less sensitivity to deviatoric stress than the cement with emulsion stabilized materials.

Table 6-18 Mean Phase Angle across Stress State averaged by Frequency

Section Name	Deviatoric Stress (kPa)	Mean Phase Angle (Degrees)	Coefficient of Variance (%)
Unstabilized	200	9.2	16.3
	400	25.0 (Sample Failed)	0.0
	550	25.0 (Sample Failed)	0.0
	200(Fully reversed)	25.0 (Sample Failed)	0.0
Cement and Emulsion	200	9.0	12.7
	400	10.3	10.1
	550	11.9	8.2
	200(Fully reversed)	12.5	4.1
Cement	200	5.7	30.9
	400	6.6	24.1
	550	7.9	40.9
	200(Fully reversed)	8.3	18.5

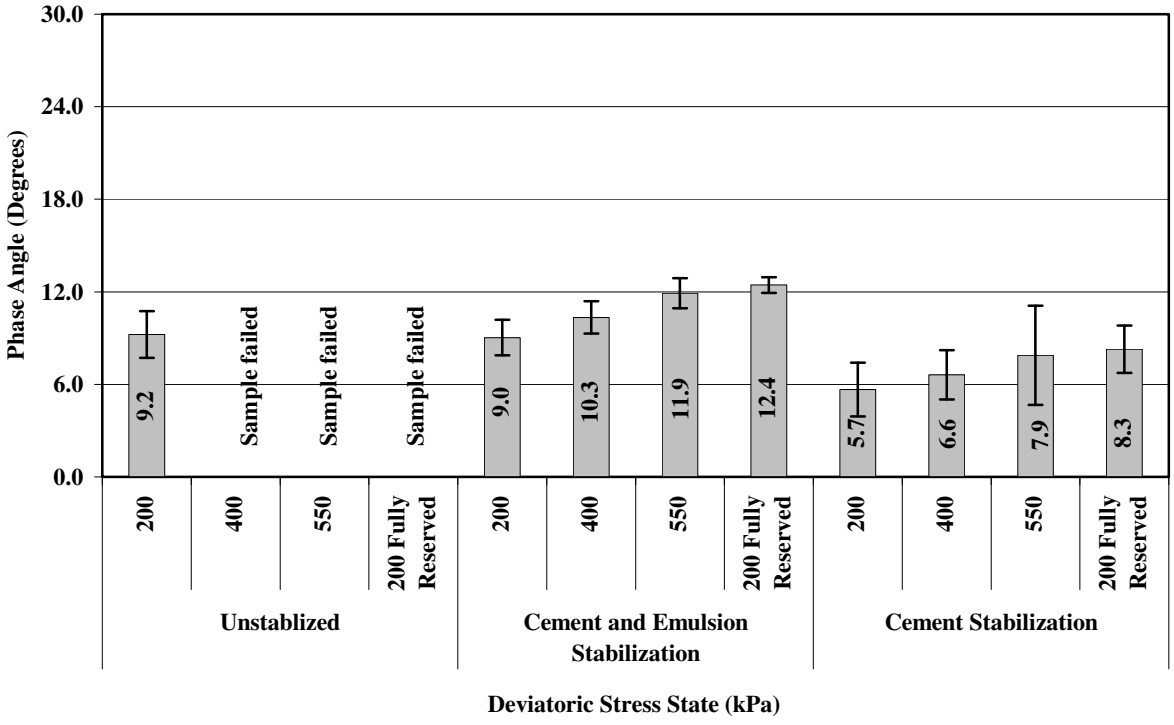

Figure 6-10 Mean Phase Angle across Stress State averaged by Frequency (± 2SD)

Table 6-19 Mean Phase Angle across Frequency averaged by Stress State

Section Name	Frequency (Hz)	Mean Phase Angle (degrees)	Coefficient of Variance (%)
Unstabilized[1]	10	20.31	33.7
	5	19.81	38.2
	1	19.52	41.1
	0.5	19.35	42.7
Cement and Emulsion Stabilization	10	11.87	10.5
	5	10.54	11.9
	1	9.71	13.8
	0.5	9.57	14.5
Cement	10	9.51	33.8
	5	6.38	17.2
	1	5.53	17.4
	0.5	5.45	19.2

1. Failed unstabilized samples were included in the calculation, assuming 25 degrees for phase angle.

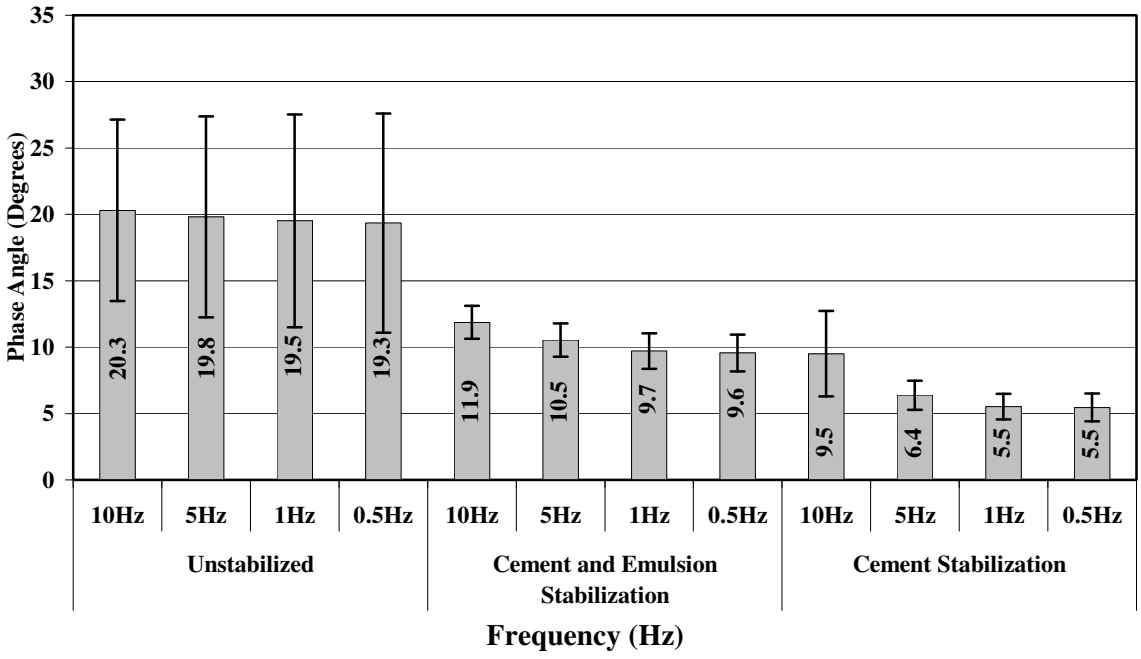

Figure 6-11 Mean Phase Angle across Frequency averaged by Stress State (± 2SD)

Table 6-19 shows the mean phase angle of materials on C.S. 15-11 across frequency averaged by stress state. The mean phase angle results are also illustrated in Figure 6-11. If the sample failed in the first three stress states, a value of 25° was assigned for calculation. However, fully reversed stress states four are not included in the calculation.

As shown in Table 6-19 and Figure 6-11, phase angles of both stabilized materials decreased with decreasing testing frequency for all materials on C.S. 15-11. As expected, the cement stabilized materials showed less sensitivity to frequency than the cement with emulsion materials applied on C.S. 15-11.

The analysis of variance (ANOVA) of the phase angle results across stress states, frequencies and stabilization types were performed to evaluate the statistically significant differences at a 95 percent confidence level. The ANOVA of phase angle results are listed in Table 6-20.

Table 6-20 ANOVA of Phase Angle of C.S. 15-11 Materials

Effect	Sum of Squares	Degrees of Freedom	Mean Squares	F Statistic	P
Mix	6488.41	2	3244.20	2948.43	0.00
DS	2049.72	2	1024.86	931.42	0.00
Frequency	203.69	3	67.90	61.71	0.00
Mix*DS	2088.35	4	522.09	474.49	0.00
Mix* Frequency	62.67	6	10.45	9.49	0.00
DS * Frequency	7.27	6	1.21	1.10	0.36
Mix* DS *Frequency	24.81	12	2.07	1.88	0.04
Error	198.06	180	1.10		

Mix= Stabilization Type; DS=Deviatoric Stress

As shown in Table 6-20, factors of stabilization type, deviatoric stress and frequency all yielded statistically significant differences on the phase angle values of materials applied on C.S. 15-11. In addition, Tukey's homogenous group analysis was performed at a confidence level of 95 percent on the phase angle test results. The result is shown in Table 6-21 and Table 6-22.

Table 6-21 Tukey's Homogeneous Groups for Phase Angle Grouped by Stabilization Type and Deviatoric Stresses averaged by Frequency

Stabilization Type	Deviatoric Stress (kPa)	Mean Phase Angle (Degrees)	Tukey's Homogeneous Groups						
Unstabilized	200	9.2	A						
	400	Sample Failed (25.0)		B					
	550	Sample Failed (25.0)		B					
Cement and Asphalt Emulsion	200	9.0	A						
	400	10.3			C				
	550	11.9				D			
Cement	200	5.7					E		
	400	6.6						F	
	550	7.9							G

Table 6-22 Tukey's Homogeneous Groups for Phase Angle Grouped by Stabilization System and Frequency averaged by Stress State

Stabilization Type	Frequency (Hz)	Mean Phase Angle (Degrees)	Tukey's Homogeneous Groups			
Unstablized	0.5	19.3	A			
	1	19.5	A			
	5	19.8	A			
	10	20.3	A			
Cement and Asphalt Emulsion	0.5	9.6		B		
	1	9.7		B		
	5	10.5		B		
	10	11.9			C	
Cement	0.5	5.5				D
	1	5.5				D
	5	6.4				D
	10	9.5		B		

Table 6-21 shows the Tukey's homogeneous groups for phase angle grouped by stabilization type and deviatoric stresses averaged by frequency. Due to failure occurred in testing, the unstabilized materials yielded significantly higher phase angles at deviatoric stresses of 400 kPa and 550 kPa relative to a deviatoric stress of 200 kPa. However, the phase angle of unstabilized material at the deviatoric stress of 200 kPa was statistically the same as the phase angle of cement with emulsion asphalt stabilized material at deviatoric stress of 200 kPa.

As shown in Table 6-21, the cement with emulsion asphalt stabilization and cement stabilization materials yielded significant different phase angles across deviatoric stress, showing that the phase angle values of both stabilized material on C.S. 15-11 are sensitive to deviatoric stress. The cement stabilization was found to provide the lowest overall phase angle among all materials applied in C.S. 15-11 construction.

Table 6-22 shows the Tukey's homogeneous group result for phase angle averaged by stress state. Phase angles of unstabilized material are statistically the same across frequency. In addition, the averaged phase angle of unstabilized material is significantly different than other materials on C.S. 15-11.

Cement and emulsion stabilized materials at 0.5 Hz, 1 Hz, and 5 Hz yielded statistically different phase angles relative to 10 Hz, showing that cement and emulsion stabilized material is sensitive to frequency with regard to phase angle. However, cement and emulsion stabilized materials at 0.5 Hz, 1 Hz, and 5 Hz yielded statistically the same phase angle as cement stabilized material at 10 Hz. This revealed that the cement stabilization is able to more significantly reduce phase angle relative to cement and emulsion stabilization.

Cement stabilized materials at 0.5 Hz, 1 Hz, and 5 Hz yielded statistically different phase angle relative to 10 Hz, showing that cement stabilized material is sensitive to frequency with regard to phase angle.

6.6 Experimental Errors and Limitations

One of the benefits of the rapid triaxial testing is that it is fully computer controlled, human interaction is almost eliminated. As a result, the effect of the experience of the laboratory personnel is minimized. However, some experimental and systematic errors that may have affected the specimen responses to loading and frequency still exist. These errors maybe from:

- Different moisture contents among samples due to the moisture variability within moist room.
- Permanent deformation occurred during testing, which may affect the measurement in consequent stress states and frequencies.

The limitations of the rapid triaxial testing characterizations of the C.S. 15-11 materials may include:

- The effect of climatic durability can not be characterized by RaTT because of weak samples after moisture soaking or freeze-thaw testing.
- Calculations are based on an assumption that no shear stress existing on the edges of specimen.

6.7 Chapter Summary

The rapid triaxial testing was performed on samples compacted using *in situ* remixed granular base material, cement stabilized base material, and cement with asphalt emulsion stabilized material applied in C.S. 15-11 construction.

The *in situ* unstabilized material applied on C.S. 15-11 test sections was found to provide the lowest mean dynamic modulus, highest mean Poisson's ratio, highest mean radial strain, and highest mean phase angle, if averaged by stress state or frequency, among all three types of material tested in this research. The cement stabilized material yielded the highest mean dynamic modulus, lowest mean Poisson's ratio, lowest mean radial strain, and lowest mean phase angle. This reveals that performance of *in situ* granular material was significantly improved by cement stabilization. The mean dynamic

modulus, mean Poisson's ratio, mean radial strain, and mean phase angle of cement with emulsion asphalt stabilized materials were found to be between the values of cement stabilized and unstabilized material. This shows that cement and emulsion asphalt provided considerable improvement on the mechanistic behaviour of *in situ* material. However, the degree of improvement is not as much as with cement stabilization.

Due to the failure of many unstabilized materials samples during rapid triaxial testing, the trends on mechanistic parameters of unstabilized materials were not evident in this research. However, the rapid triaxial testing results revealed that, under compressive stress states, as deviatoric stress increases, the Poisson's ratio, the radial strains and the phase angle also increase for both stabilized materials applied in C.S. 15-11 construction. As the deviatoric stress increases, a decreasing trend of dynamic modulus was observed for cement and emulsion asphalt stabilized material but not for cement stabilized material. In addition, the cement stabilized materials were found to have less sensitivity to the increasing deviatoric stress relative to cement with emulsion stabilized materials and unstabilized granular material, with regard to Poisson's ratio, radial strains and the phase angle.

It was observed that, as the frequency increases, the phase angle also increases for both stabilized materials applied in C.S. 15-11 construction. However, as frequency increases, the Poisson's ratio and radial strain decrease for both stabilized materials applied in C.S. 15-11 construction. In addition, as the deviatoric stress increases, an increasing trend of dynamic modulus was observed for cement and emulsion asphalt stabilized materials but not for cement stabilized materials. The cement stabilized materials were found to have less sensitivity to the testing frequency than cement with emulsion stabilized materials, as expected.

Stress state one and fully reversed stress state four have the same maximum deviatoric stress. However, different sample responses were observed between these two stress states due to the application of the fully reversed stress state in RaTT testing. The observations include:

- Dynamic modulus at fully reversed stress state four is lower relative to compressive stress state one, for both cement and cement and emulsion asphalt stabilized materials.
- Poisson's ratio of cement and emulsion stabilized material at fully reversed stress state four is higher relative to stress state one. However, Poisson's ratio of cement stabilized material at fully reversed stress state four is lower relative to stress state one.
- Radial strain at fully reversed stress state four is higher relative to compressive stress state one, for both cement and cement and emulsion asphalt stabilized materials.
- Phase angle at fully reversed stress state four is higher relative to compressive stress state one, for both cement and cement and emulsion asphalt stabilized materials.

The ANOVA performed on dynamic modulus, Poisson's ratio, radial strain, and phase angle showed that, for materials applied on C.S. 15-11:

- Stabilization type resulted in statistically significant difference of values of dynamic modulus, Poisson's ratio, radial strain, and phase angle.
- Deviatoric stress resulted in statistically significant difference of values of dynamic modulus, Poisson's ratio, radial strain, and phase angle.
- Frequency applied in RaTT testing resulted in statistically significantly different values of radial strain, and phase angle. However, the differences in frequency did not result in significant difference values of dynamic modulus and Poisson's ratio.

To further identify which combination of stabilization type and deviatoric stress yielded statistically significant differences in mechanical behaviour of materials applied in C.S. 15-11, Tukey's homogenous group analysis was performed at a confidence level of 95 percent on the testing results. The homogenous group analysis results showed that the cement stabilization applied in C.S. 15-11 significantly improved the mechanistic behaviour of *in situ* unstabilized material. In addition, the cement stabilization showed the least sensitivity to deviatoric stress and frequency.

CHAPTER 7 PAVEMENT DESIGN AND ANALYSIS

7.1 Pavement Thickness Design and Analysis of C.S. 15-11

Traffic information for C.S. 15-11 was collected from Saskatchewan MHI traffic engineers (Anderson 2007):

- Design life: 15 years
- 2006 Annual Average Daily Traffic (AADT): 650
- Truck percentage: 20%
- Growth factor: 1.05
- Direction split: 50/50
- Traffic load equivalency factor: 2.5 Equivalent Single Axial Load per Truck

The traffic analysis of C.S. 15-11 was performed according to Saskatchewan surfacing manual SM 502-1 (MHI 1981). The calculation showed that the total number of Equivalent Single Axial Loads (ESAL) over 15-year design life (N15) of C.S. 15-11 test section is 0.91 million. N15 is used as the input of pavement structure thickness design with Saskatchewan thickness design nomographs.

Table 7-1 shows and Figure 7-1 illustrates two possible thickness design solutions for C.S. 15-11 test sections. As shown in Table 7-1, Alternative 1 consists of a 40 mm asphalt surface, a 190 mm subbase course of CBR 20 material, a 100 mm base course of CBR 40 material, and a 125 mm base course of CBR 80 material for a total granular thickness of 415 mm. This design example meets the rutting criterion but failed to meet the fatigue criterion.

Alternative 2 consists of a 190 mm subbase course of CBR 20 material, a 100 mm base course of CBR 40 material, and a 10 mm base course of CBR 80 material for a total

granular thickness of 300 mm. The asphalt layer for Alternative 2 is 120 mm. This design example meets both the fatigue and rutting criteria.

Table 7-1 Pavement Design Alternatives of C.S. 15-11

	CBR 20 Thickness (mm)	CBR 40 Thickness (mm)	CBR 80 Thickness (mm)	Total Granular Thickness (mm)	Asphalt Thickness (mm)
Alternative 1	190	100	125	415	40
Alternative 2	190	100	10	300	120

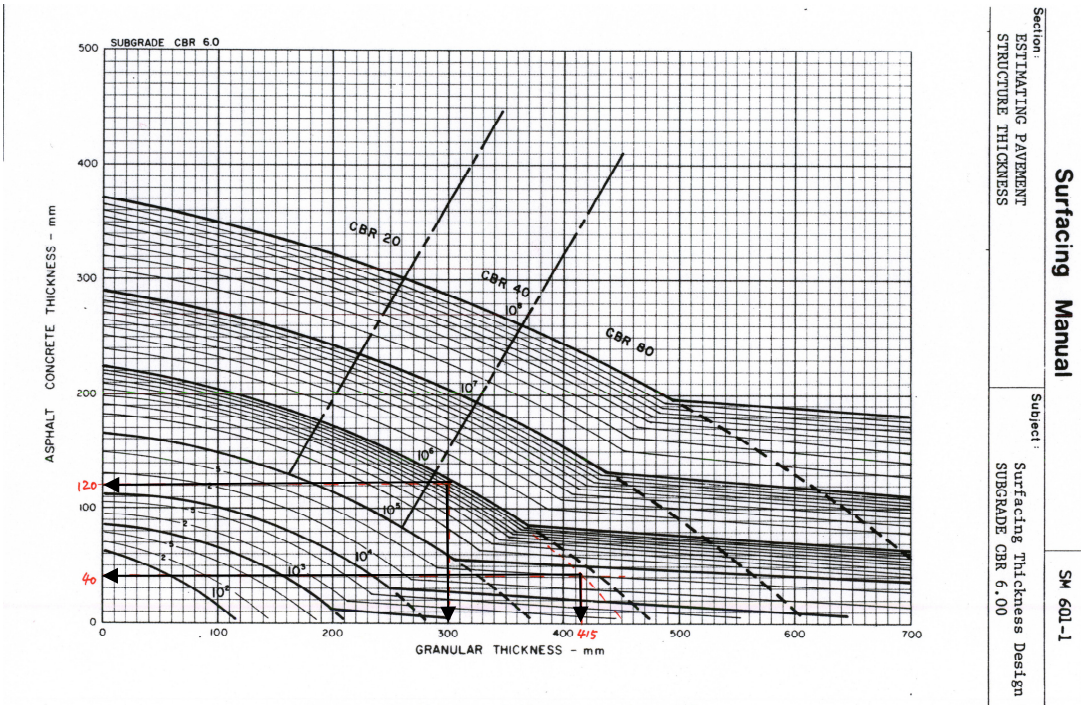

Figure 7-1 Illustration of Thickness Design by Saskatchewan CBR Nomograph

It should be noted from the above thickness design examples that Saskatchewan MHI design chart has only three base course material alternatives which are limited to CBR 20, 40, and 80 materials. As a result, the design charts are not applicable for designing stabilized granular pavement systems. For instance, the cement stabilized base course of the C.S. 15-11 test section has a 150 mm subbase and 150 mm cement

stabilized base course with CBR value of 266. It would be difficult to convert 150 mm CBR 266 material to an equivalent thickness of CBR 80 material, as well as to determine the required asphalt layer thickness using MHI design charts.

7.2 Evaluation of Pavement Design of C.S. 15-11

The C.S. 15-11 test sections were surfaced with a 40 mm hot mix asphalt layer on top of a 150 mm stabilized or remixed base courses in 2007. However, the asphalt surface thickness applied was chosen primarily based on local construction practices and engineering judgement. There is a need to validate the design using mechanistic pavement analysis methods.

BISAR (Bitumen Stress Analysis in Roads) software was chosen to calculate pavement strains and stress of the C.S. 15-11 test sections. BISAR was introduced in Chapter two. A four layer elastic system was modeled in BISAR according to actual pavement structures applied on C.S. 15-11 test sections. Full inter-layer bonding was assumed between pavement layers.

Traffic loading applied to pavement is assumed to be a typical 2-tire 80 kN single axle load with a 2.4 m tire spacing. Tires contact the pavement surface in a pattern of circular area (0.15 m radius) and apply 566 kPa pressure to the pavement.

Pavement layer thicknesses and elastic material properties are listed in Table 7-2. Loading inputs of BISAR are listed in Table 7-3, and pavement scheme is illustrated in Figure 7-2. Elastic modulus and Poisson's ratio inputs for BISAR are based on laboratory rapid triaxial testing in this research as well as engineering judgement.

Table 7-2 Layer Thickness and Material Properties for BISAR (from RaTT Testing)

Material Properties	Asphalt Surface	Base Courses			Subbase	Subgrade
		Cement Stablized	Cement Emulsion Stabilized	Unstablized		
Young's Modulus (MPa)	2000	1500	950	500	300	60
Poisson's Ratio	0.30	0.10	0.20	0.40	0.40	0.40
Layer Thickness (mm)	40	150	150	150	150	N/A

Table 7-3 Loading Inputs for BISAR

Wheel Spacing (m)	Axle Weight (kN)	Tire Radius (m)
2.4	80	0.15

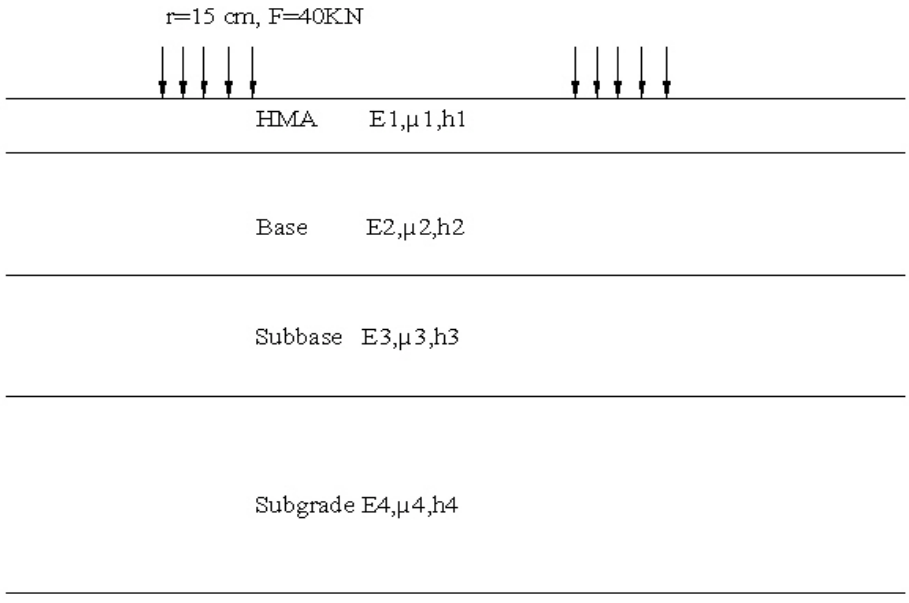

Figure 7-2 Scheme of Pavement Structure Analyzed in BISAR

Two critical strains specified within the MHI design method are the horizontal tensile strain at the bottom of the asphalt concrete layer and the vertical compressive strain at the top of the subgrade layer (MHI 1981). The MHI allowable critical strains under a 0.91 million ESAL number were determined from MHI curves specified in the pavement surfacing manual, as illustrated in Figure 7-3 and Figure 7-4. The MHI allowable maximum strains are listed in Table 7-4.

In order to evaluate the pavement responses of the C.S. 15-11 test sections, critical horizontal tensile strains at the bottom of asphalt layer and the vertical compressive strains on top of subgrade of each C.S. 15-11 test section were calculated at the point under the centre of circular tire loading, as shown in Table 7-4. In this research, a compressive strain was assigned a negative value and the tensile strain was positive value.

Table 7-4 Critical Strains of C.S. 15-11 Pavement Structures under a 80kN Load

Test Section	Horizontal Strain at Bottom of HMA ($\times 10^{-6}$)	Vertical Strain on top of Subgrade ($\times 10^{-6}$)
Unstabilized	37	-911 (Failed)
Cement and Asphalt Emulsion Stabilization	-91	-750 (Failed)
Cement Stabilization	-129	-669
MHI Max Allowable Strains	170	-680

As shown in Table 7-4, the pavement structure of unstabilized base course, cement with asphalt emulsion stabilized base course, and cement stabilized base course yielded horizontal strains at the bottom of asphalt layer of 37×10^{-6}, -91×10^{-6}, and -129×10^{-6}, respectively. The compressive strains on top of subgrade of three types of bases are -911×10^{-6}, -750×10^{-6}, and -669×10^{-6}, respectively.

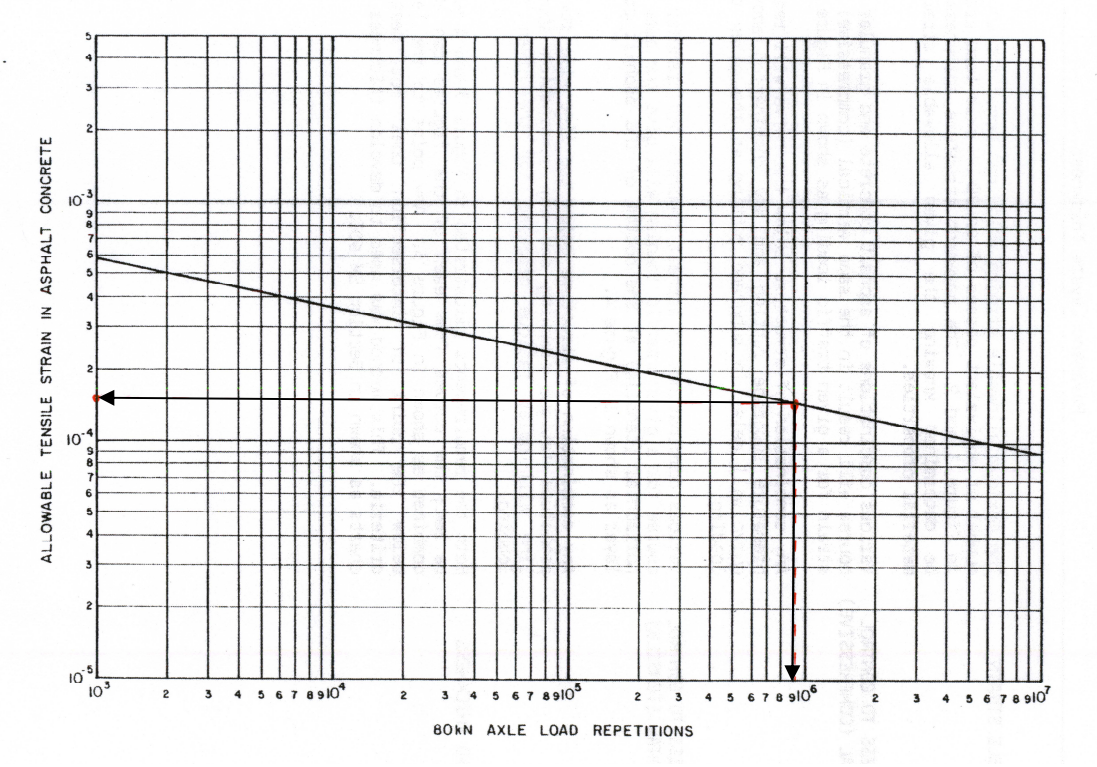

Figure 7-3 Determination of Allowable Horizontal Tensile Strain (MHI 1981)

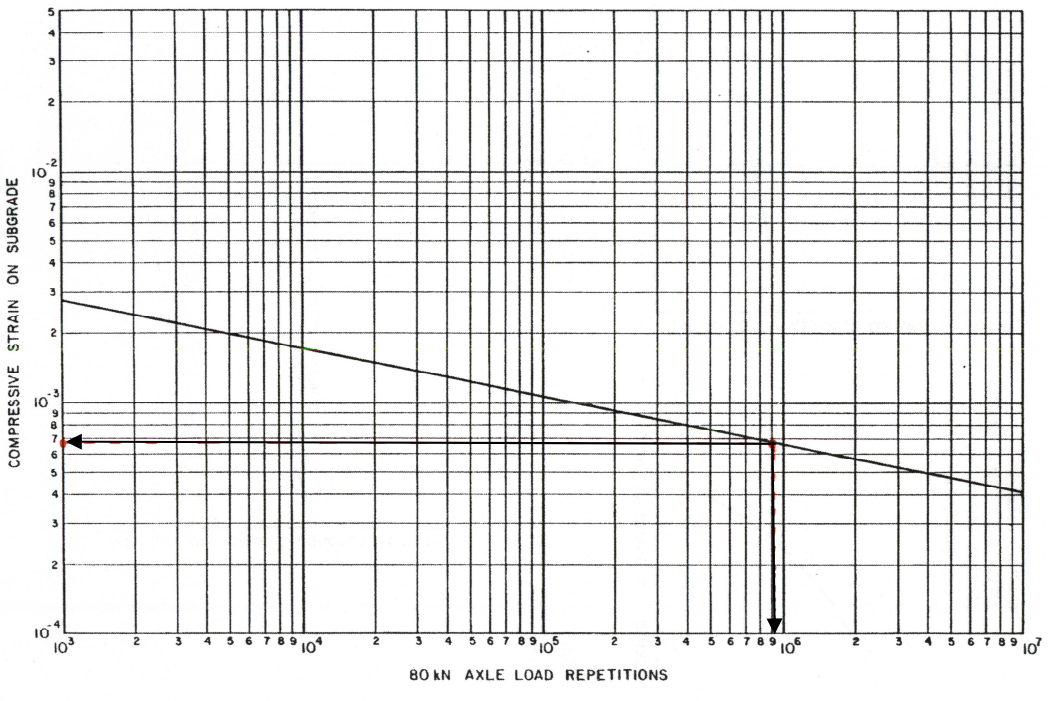

Figure 7-4 Determination of Allowable Vertical Compressive Strain (MHI 1981)

As shown in Table 7-4, the horizontal strain at the bottom of HMA layer of pavement with an unstabilized base course or a cement with asphalt emulsion stabilized base course on C.S. 15-11 met the MHI maximum allowable strain requirement. However, the compressive strain on top of the subgrade for pavement with the unstabilized base course or the cement with asphalt emulsion stabilized base course exceeded the maximum allowable value specified by the MHI structural design system. The pavement structures on C.S. 15-11 stabilized by cement yielded satisfactory strains that are lower than the maximum allowable values specified by MHI, at both the bottom of HMA and the top of subgrade.

In summary, the evaluation of C.S. 15-11 test sections thickness design showed that pavement design with cement stabilized granular base course satisfied the Saskatchewan MHI design criteria. However, pavement with an unstabilized granular base course or cement with asphalt emulsion stabilized base course only met the criterion of fatigue cracking but failed to meet the criterion of structural rutting, as specified in MHI design manual. The calculated results of unstabilized material concur with the observed performance of C.S. 15-11 prior to strengthening.

This design example revealed that, to optimize the thickness design and the long term performance, mechanistic pavement response analysis and validation are necessary steps in the thickness design of stabilized granular systems such as C.S. 15-11, where a traditional MHI design system is not applicable.

Errors and limitations of the evaluation may result from:

- Calculations assumed a linear elastic model and fully bonded layers. The asphalt and granular materials under field conditions are more complex and usually non-linear in their mechanistic behaviour.
- MHI design criteria are derived from Shell methods which are based on the AASHO road test. The pavement structure, climatic and traffic conditions of the AASHO road test may be significantly different than Saskatchewan conditions. As a result, the design criteria may be not appropriate to use in Saskatchewan.

- The inputs of pavement analysis are from limited sources, such as rapid triaxial testing results under limited stress states in this research, or from engineering judgements. It is not certain how sensitive the pavement responses results are based on the mechanistic parameters input.

7.3 Evaluation and Comparison of Pavement Structure Responses of C.S. 15-11

A two dimensional finite element model was created using ANSYS® program to compute significant C.S. 15-11 test section pavement responses such as shear stresses under a single axle 80 kN load. The model applied in this research assumed a linear elastic constitutive relationship and was subjected to a static distributed loading.

Due to vertical axle symmetry, only half of the pavement structure was modelled. The axis of symmetry is located in the middle of two wheels. The model was meshed with the plane 82 elements under the plane strain option. The edge constraints applied for the model are:

- At the left boundary, the model degrees of freedom are fully constrained.
- At the axis of symmetry, the horizontal displacements are constrained.
- At the bottom boundary, the model degrees of freedom are fully constrained.

Initial results showed that vertical strain and horizontal strain of the C.S. 15-11 pavement structure from ANSYS® are very dependent on the width and subgrade depth of the model. The model was finally chosen to consist of a 5 m deep subgrade and a 3 m wide pavement structure by balancing both computation accuracy and maximum meshing capability of ANSYS® software at University of Saskatchewan computer lab. A BISAR calculation of the same pavement structure was performed to compare with ANSYS® results.

It was found that strains from ANSYS® were different from BISAR results by a range of 30% to 70%. The disparities in results may come from:

- 3D problem was simplified and modelled by 2D elements.

- Semi-infinite pavement structure was modeled by a limited size model with limited depth of subgrade.
- Constraints on ANSYS® model may not represent realistic conditions in the field.

ANSYS® can easily generate stress distribution contours across a pavement structure with acceptable accuracy. Therefore, ANSYS® was used to determine locations with maximum or minimum pavement responses in the first step of pavement analysis. BISAR software was applied afterwards to quantify the stresses at locations identified by ANSYS®. A contour plot of shear stress distribution across pavement structure with a cement stabilized granular base course is illustrated in Figure 7-5.

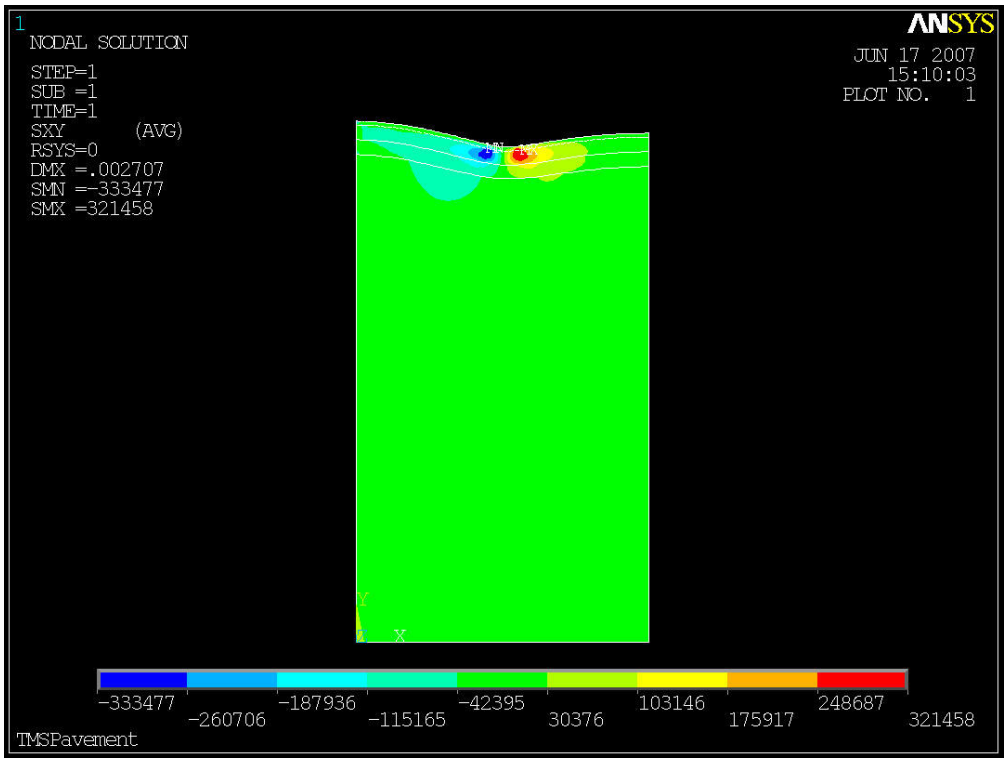

Figure 7-5 Distribution of Shear Stress in Pavement Structure (Cement Stabilized Base, from ANSYS® Software)

As shown in Figure 7-5, for C.S. 15-11 pavement structure with a cement stabilized base course, the locations of maximum shear stress are under the edges of circular wheel loadings.

Contour plots of C.S. 15-11 test sections with an unstabilized base course and cement with emulsion asphalt stabilized base course were also generated from ANSYS®. Plots showed that maximum shear stress locations are also under the edges of the circular wheel loadings. However, the magnitude of the maximum stress varies across different test sections.

Given the findings from finite element modeling and illustration, it was decided that pavement responses under the edge and the centre of circular loadings to be investigated with the aid of BISAR software, as shown in Figure 7-6 and Table 7-5. Only half of the loading and pavement structure were modelled due to central symmetry.

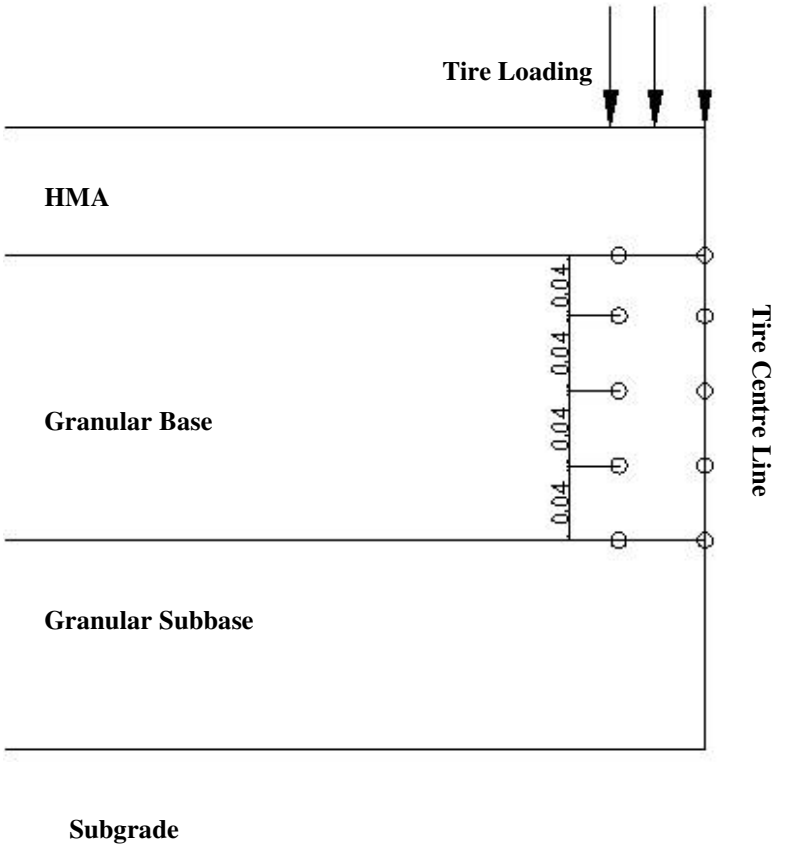

Figure 7-6 Locations for Pavement Responses Calculation

Table 7-5 Locations for Pavement Response (Calculation from ANSYS® Software)

Horizontal Locations	Centre of Tire			Tire Edge	
Vertical Locations (m)	0.04	0.08	0.12	0.16	0.19

Pavement responses for C.S. 15-11 pavement structures of various granular bases under a single axle 80kN loading were calculated using BISAR. Given that base course shear failure was one of the major distresses observed on C.S. 15-11 prior to construction, the maximum shear stresses in cement stabilized base course of C.S. 15-11 were listed in Table 7-6 and illustrated in Figure 7-7.

As shown in Table 7-6, the maximum shear stresses in cement stabilized base course on C.S. 15-11 under the tire edge and centre are 254 kPa and 249 kPa, respectively, which is also illustrated in Figure 7-7.

Table 7-6 Maximum Shear Stress in Cement Stabilized Base course on C.S. 15-11 (from BISAR Software)

Depth from Surface (m)	Absolute Values of Maximum Shear Stress (kPa)	
	Tire Edge	Tire Centre
0.04	254	132
0.08	222	173
0.12	193	183
0.16	168	203
0.19	189	249
Maximum Value (kPa)	254	249

Maximum shear stress at a given point equals to half of the differences of principal stresses at the same point.

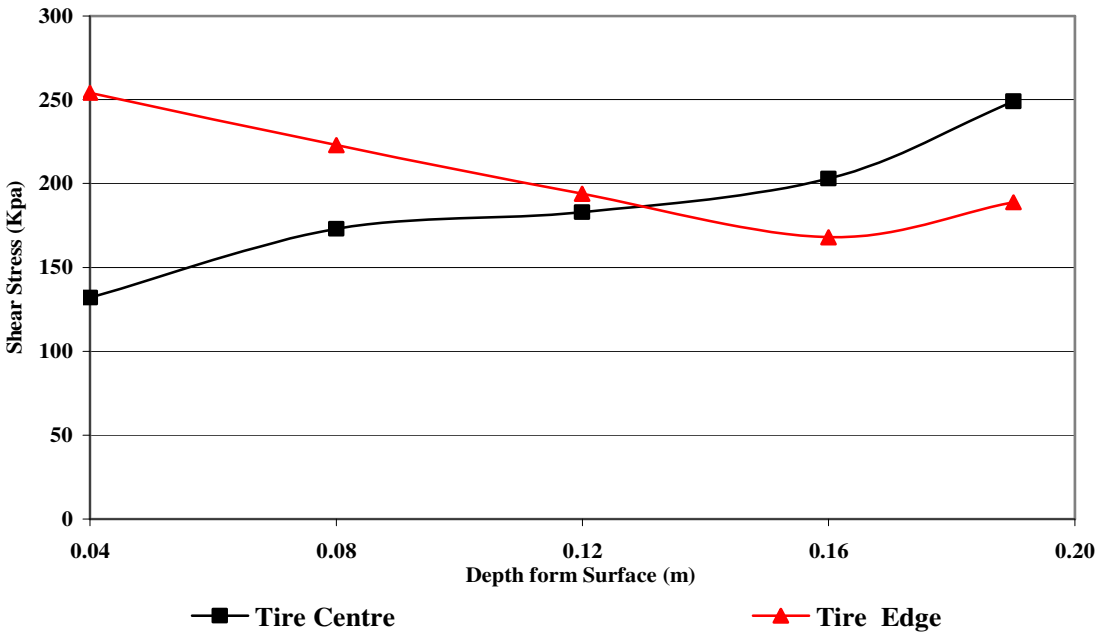

Figure 7-7 Maximum Shear Stress in Cement Stabilized Base course on C.S. 15-11 (from BISAR)

Pavement responses in the cement with asphalt emulsion stabilized base course and the unstabilized base course of C.S. 15-11 were also calculated by BISAR, as presented in Appendix C. Maximum shear stresses and deviatoric stresses of all granular base courses on C.S. 15-11 are summarized in Table 7-7.

Table 7-7 Maximum Shear Stress of Various Bases on C.S. 15-11 Test Section under Typical 80 kN load (Calculate by BISAR)

Base Type	Depth to Pavement Surface (m)	Maximum Shear Stress (kPa)	Maximum Deviatoric Stress (kPa)
Unstabilized Base	0.04	177	354
Cement and Asphalt Emulsion Stabilized Base	0.04	240	480
Cement Stabilized Base	0.04	254	508

Maximum shear stress at a point equals to half of the differences of principal stresses.

Given the laboratory rapid triaxial testing discussed in Chapter Six of this research, it is known that C.S. 15-11 unstabilized granular base course material sample failed in rapid triaxial testing under a maximum shear stress of 200 kPa in stress state two. Cement with asphalt emulsion stabilized samples failed under a maximum shear stress of 225 kPa in stress state three, and the cement stabilized sample remained intact until subjected to fully reversed condition at stress state four. The stress states at which samples failed in the laboratory rapid triaxial testing are summarized in Table 7-8, with a comparison to field stresses in C.S. 15-11 pavement structures calculated in this chapter by numerical modeling.

As shown in Table 7-7, the maximum shear stresses occurred in samples during laboratory rapid triaxial testing in this research were close to shear stresses within granular base courses structure computed from elastic modeling and calculation, for all test sections of C.S. 15-11. These agreements confirmed that rapid triaxial testing protocols applied in this research were representative of the realistic field stress states of granular base materials on C.S. 15-11 test sections.

Table 7-8 Comparison of Shear Stress in the Field and Laboratory

Granular Base System	Maximum Shear Stress within Base Course in the Field Computed by Modeling (kPa)	Maximum Shear Stress of Sample at Failure in RaTT Testing (kPa)
Unstabilized	177	200
Cement and Asphalt Emulsion Stabilized	240	225
Cement Stabilized	254	> 225

Maximum shear stress at a point equals to half of the differences of principal stresses.

7.4 Chapter Summary

Two alternatives were analyzed with Saskatchewan MHI design charts of subgrade CBR 6.0. The thickness design examples illustrated that Saskatchewan MHI design chart has three base course material alternatives which are limited to CBR 20, 40, and 80 materials. As a result, the design charts are not applicable for designing stabilized granular pavement systems, such as C.S. 15-11 pavements.

The evaluation of C.S. 15-11 test sections thickness designs showed that C.S. 15-11 with a cement stabilized base course satisfied Saskatchewan MHI design criteria. However, a pavement structure with an unstabilized base course and a cement with asphalt emulsion stabilized base course only met the criterion of fatigue cracking but failed to meet the criterion of structural rutting, as specified in MHI design manual. This conclusion concurs with the observed performance of C.S. 15-11 prior to strengthening. In addition, the analysis in this chapter revealed that analyses of pavement response and validation are necessary for thickness design of stabilized granular systems such as C.S. 15-11, where the traditional MHI design system is not applicable.

Locations of maximum shear stress within various base courses of C.S. 15-11 test sections were identified by ANSYS®. Stresses were calculated by BISAR based on a linear elastic pavement model. Analysis showed that maximum shear stress within various base courses of C.S. 15-11 test sections occur under loading centres and edges. The value of maximum shear stresses in various granular bases of C.S. 15-11 ranged from 177 kPa to 254 kPa.

Maximum shear stresses in samples during laboratory rapid triaxial testing in this research were compared with realistic shear stresses within granular bases structure under field conditions computed by modeling. Agreement within laboratory and field pavement responses was observed, which indicates that rapid triaxial testing protocols applied in this research were well representative of the realistic field stress states of granular base materials on C.S. 15-11 test sections.

CHAPTER 8 SUMMARY AND CONCLUSIONS

The goal of this research is to improve the engineering design and performance of recycled and stabilized granular base systems under Saskatchewan field state conditions. The specific objectives are to characterize the conventional, mechanistic, and moisture sensitivity behaviour of various granular base strengthening systems in the laboratory, to mechanistically characterize the structural responses of various granular base strengthening systems in the field, and to validate the pavement thickness design and responses of various granular base strengthening systems.

8.1 Objective 1: Characterize the Laboratory Behaviour of Various Granular Base Strengthening Systems

8.1.1 Conventional Characterization of Granular Material

Conventional laboratory characterizations of granular material were performed in this research to characterize various granular materials from C.S. 15-11. The laboratory test methods performed included: grain size distribution, Atterberg limits and soil classification, sand equivalent value testing, standard Proctor compaction, California bearing ratio strength and swell test.

Grain size distribution analysis found that *in situ* granular base material from C.S. 15-11 was high across the sand sieve sizes as compared to gradation limits of Saskatchewan MHI Type 33 granular base material, particularly from the 0.4 mm to 0.9 mm size range. As a result, *in situ* granular base is considered as a marginal sandy granular base material, which may be one of the causes of pavement shear slippage, shoving and rutting observed on C.S. 15-11 pavement structure prior to strengthening construction. Grain size distribution analysis also showed that cement and asphalt emulsion stabilizer improved the gradation of granular base material by bonding the fines and sandy material together.

The Atterberg limits showed that fines of *in situ* granular base has a liquid limit of 20.5, plastic limit of 10.0 and a plastic index of 10.5, while both stabilized granular base material were non-plastic materials. Therefore, *in situ* granular base material was classified as well graded sand with clay and gravel (SW-SC) by ASTM or A-2-6 clayey gravel by AASHTO.

Sand equivalent values of *in situ* granular material and cement stabilized material were found to be 55.7 and 79.5, respectively. Both *in situ* and cement stabilized granular material met the minimum sand equivalent requirement of MHI specification for hot mix asphalt concrete. However, the sand equivalent value of cement stabilized granular base material was significantly higher than the *in situ* granular base material. This suggests that the cement stabilization cements the fines together and reduces the fines content in the granular material, which may be one of the reasons that the material plasticity was reduced.

Moisture density relationship obtained for C.S. 15-11 *in situ* granular base material showed that *in situ* granular base material yielded a standard maximum Proctor dry density of 2240 kg/m^3 at optimal moisture content of 7.8 percent by dry mass of soil. The maximum density obtained from standard Proctor characterization was used as the termination density during gyratory compaction in this research.

CBR tests showed that cement stabilization and cement with emulsion asphalt stabilization reduced swelling potential and increased the strength of *in situ* granular base materials on C.S. 15-11. Cement stabilization was found to have the most significant improvement among all three test sections materials on C.S. 15-11.

8.1.2 Moisture Sensitivity Characterizations of Granular Materials

This research employed three laboratory tests to determine moisture sensitivity of granular materials applied in C.S. 15-11 construction. The laboratory tests included: indirect tensile strength test, moisture rise and conductivity test, and unconfined compressive strength test.

The indirect tensile strength test showed that both cement and cement with emulsion asphalt stabilization systems increased the indirect tensile strength and reduced the moisture susceptibility of *in situ* C.S. 15-11 granular base materials. Cement stabilization was found to have more significant improvement on the tensile strength and moisture susceptibility than the cement with asphalt emulsion stabilization.

The moisture capillary rise test showed that cement stabilization and cement with emulsion asphalt stabilization slightly increased the moisture intake potential of *in situ* unstabilized material on C.S. 15-11. Furthermore, the cement with asphalt emulsion stabilization was found to take in more water than the cement stabilization system on C.S. 15-11.

The cement stabilized material yielded the lowest surface conductivity values among all three test section materials of C.S. 15-11, indicating that the cement stabilization provided the best resistance to moisture damage among all test sections, possibly due to the hydration effects. Cement with emulsion asphalt of C.S. 15-11 showed lower surface conductivity values relative to unstabilized material, which means that cement with emulsion asphalt stabilization, also improved the resistance to moisture damage of *in situ* granular materials. However, the degree of improvement is less than the cement stabilization.

Both cement stabilization and cement with asphalt emulsion stabilization on C.S. 15-11 increased the unconfined compressive strength and resistance to moisture damage of unstabilized material. The cement stabilization was found to provide greater improvement on C.S. 15-11 *in situ* material than the cement with asphalt emulsion stabilization. These results concur with the findings from the indirect tension testing performed in this research.

8.1.3 Mechanistic Characterizations

The rapid triaxial testing was performed on samples compacted with *in situ* remixed granular material, cement stabilized base material, and cement with asphalt emulsion stabilized material applied in C.S. 15-11 construction.

The *in situ* unstabilized material applied on C.S. 15-11 test sections was found to provide the lowest mean dynamic modulus, highest mean Poisson's ratio, highest mean radial strain, and highest mean phase angle, if averaged by stress state or frequency, among all three types of material tested in this research. The cement stabilized material yielded the highest mean dynamic modulus, lowest mean Poisson's ratio, lowest mean radial strain, and lowest mean phase angle. This reveals that performance of *in situ* granular material was significantly improved by cement stabilization. The mean dynamic modulus, mean Poisson's ratio, mean radial strain, and mean phase angle of cement with emulsion asphalt stabilized materials were found to be between the values of cement stabilized and unstabilized material. This shows that cement and emulsion asphalt showed considerable improvement on the mechanistic behaviour of *in situ* material. However, the degree of improvement was not as extensive as cement stabilization.

As deviatoric stress increases, Poisson's ratio, radial strains and phase angle also increase for both stabilized materials applied in C.S. 15-11 construction. However, as deviatoric stress increases, a decreasing trend of dynamic modulus was observed for cement and emulsion asphalt stabilized material but not for cement stabilized material. In addition, with respect to Poisson's ratio, radial strains and phase angle, the cement stabilized materials were found to have less sensitivity to the increasing deviatoric stress relative to cement with emulsion stabilized materials and unstabilized granular material.

As frequency increases, the phase angle also increases for both stabilized materials applied in C.S. 15-11 construction. However, as frequency increases, Poisson's ratio and radial strain decrease for both stabilized materials applied in C.S. 15-11 construction. In addition, as deviatoric stress increases, an increasing trend of dynamic modulus was observed for cement and emulsion asphalt stabilized material but not for cement stabilized material. The cement stabilized materials were found to have less sensitivity to the testing frequency than cement with emulsion stabilized materials, as expected.

Stress state one and fully reversed stress state four have the same maximum deviatoric stress. However, different sample responses were observed between these

two stress states due to the application of the fully reversed stress state in RaTT testing, such as:

- Dynamic modulus at fully reversed stress state four is lower relative to compressive stress state one, for both cement and cement and emulsion asphalt stabilized materials.
- Poisson's ratio of cement and emulsion stabilized material at fully reversed stress state four is higher relative to stress state one. However, Poisson's ratio of cement stabilized material at fully reversed stress state four is lower relative to stress state one.
- Radial strain at fully reversed stress state four is higher relative to compressive stress state one, for both cement and cement and emulsion asphalt stabilized materials.
- Phase angle at fully reversed stress state four is higher relative to compressive stress state one, for both cement and cement and emulsion asphalt stabilized materials.

The ANOVA performed on dynamic modulus, Poisson's ratio, radial strain, and phase angle showed that, for materials applied on C.S. 15-11:

- Stabilization type resulted in statistically significant difference of values of dynamic modulus, Poisson's ratio, radial strain, and phase angle.
- Deviatoric stress resulted in statistically significantly different values of dynamic modulus, Poisson's ratio, radial strain, and phase angle.
- Frequency applied in RaTT testing resulted in statistically significantly different values of radial strain, and phase angle. However, the frequency did not result in significantly different values of dynamic modulus and Poisson's ratio.

8.2 Objective 2: Mechanistically Characterize the Structural Responses of Various Granular Base Strengthening Systems in the Field

The heavy weight deflectometer peak surface deflection measurements were collected across load spectra at primary legal load weight limits (44.6 kN) in both the eastbound and westbound directions on C.S. 15-11, prior to base construction, after base construction, and post hot mix asphalt paving.

Improved primary structural response profiles were observed across the spatial limits of the test sections after base stabilization construction. The cement stabilization system was found to have the most significant structural improvement among all test sections.

However, surface deflection of the unstabilized test section of C.S. 15-11 after HMAC placing increased relative to the deflection right after full depth strengthening construction. Furthermore, the variability of deflection measurements of unstabilized test section after placing HMAC in 2007 was observed to be significantly higher than any other test sections on C.S. 15-11. It is believed that the freeze-thaw cycles in winter 2006-2007 have significantly affected the performance of the unstabilizd test section of C.S. 15-11, which is associated with the lowest climatic durability of all test sections constructed on C.S. 15-11.

The test sections constructed on C.S. 15-11 remained unsurfaced throughout the winter of 2006-2007. After spring thaw in 2007, it was found that only minor surface ravelling had occurred on test sections, showing that stabilized granular base structures can be used as a stop-gap treatment prior to asphalt surfacing.

8.3 Objective 3: Validate the Pavement Thickness Design and Responses of Various Granular Base Strengthening Systems

This research demonstrated that the MHI structural design system is not applicable to stabilized granular base systems. The evaluation of the thickness design for C.S. 15-11 showed that the unstabilized and cement with asphalt emulsion stabilized test sections met the criterion of fatigue cracking, but failed to meet the criterion of

structural rutting. However, the cement stabilized section met both criterions of MHI design system. The structural evaluation also showed that mechanistic pavement response analysis and validation are necessary in the thickness design of stabilized granular systems such as C.S. 15-11, where the traditional MHI design system is not applicable.

This research employed finite element modeling and linear elastic pavement modeling software to determine the maximum shear stresses within granular base under typical Saskatchewan stress state conditions. The maximum shear stress values calculated by numerical modeling were found to range from 177 kPa to 254 kPa. These maximum shear stresses were compared to maximum shear stresses occurring within samples measured by rapid triaxial testing performed in this research. The comparison showed that the ranges of shear stresses applied in the laboratory RaTT testing were close to the calculated shear stresses of granular bases in the field computed from modeling.

8.4 Future Research

This research characterized several granular base materials applied in C.S. 15-11 test section construction. The cement and/or asphalt emulsion content are limited at only the design content for C.S. 15-11 materials. It is recommended that future research be performed on materials at a wider range of cement content and/or asphalt emulsion content. Therefore, the sensitivity of various testing results on cement content and/or asphalt emulsion content can be evaluated.

This research used field sampled materials from C.S. 15-11 construction. The materials were transported to the laboratory instead of being compacted on site. As a result, the time spent transporting the samples affected the testing results to some extent. It is recommended that future research involve both materials fabricated in the laboratory and compacted on site to evaluate and quantify the differences between testing results.

Another future research area is the evaluation of the effect of curing time on the results. In this research, most samples were cured for more than 6 months to evaluate the long term performance of research materials. In future research, it may be worthwhile to investigate the materials performance changes with time and thus to understand the performance of materials at their early stages of curing.

This research evaluated the moisture sensitivity of granular base materials. Future research could also be performed to determine the unstabilized and stabilized material resistance to freeze thaw cycles, which was not included in this research.

This research characterized the materials by rapid triaxial testing at deviatoric stresses from 200 kPa to 500 kPa. In addition, the testing protocol applied in this research was proven to be representative of the true field conditions by numerical modeling. However, the deviatoric stress is relatively high for weak unstabilized samples and thus the sample failed at stress states two. In future research, lower deviatoric stress states could be added to the testing sequence. Therefore, more data, such as the relationship of mechanistic behaviour vary with stress state, may be quantified.

Finally, future research may include the evaluation of pavement responses by viscoelastic modeling. Advanced viscoelastic modeling techniques would provide responses closer in accuracy to true field state conditions and allow the comparison to existing results with current research results based on the linear elastic model.

LIST OF REFERENCES

Australian Asphalt Pavement Association (AAPA), 1998, Guide to Stabilization in Roadworks, Austroads Incorporated, Sydney, Australia.

AASHTO-AGC-ARTBA Joint Committee, 1998, Report on Cold Recycling of Asphalt Pavement, American Association of State Highway and Transportation Officials, Washington D.C.

AASHTO, 1986, AASHTO Guide for Design of Pavement Structures, American Association of State Highway and Transportation Officials, Washington D.C.

AASHTO, 1993, AASHTO Guide for Design of Pavement Structures, American Association of State Highway and Transportation Officials, Washington D.C.

AASHTO M 147, 1986, Materials for Aggregate and Soil-Aggregate Subbase, Base and Surface Courses, American Association of State Highway and Transportation Officials Standards, Washington D.C.

AASHTO T 283, 1986, Standard Method of Test for Resistance of Compacted Hot Mix Asphalt (HMA) to Moisture-Induced Damage, American Association of State Highway and Transportation Officials Standards, Washington D.C.

Ahlborn, G., 1972, ELSYM5 Computer Program for Determining Stresses and Deformation in Five Layer Elastic Systems. University of California, Berkeley, Berkeley, California.

Alberta Infrastructure and Transportation (AIT), 2003, Standard Specifications for Highway Construction, Alberta Infrastructure and Transportation, Edmonton, Alberta

Anderson, T. , 2007, Senior Traffic Engineer, Saskatchewan Ministry of Highways and Infrastructure, Personal Communication.

Anthony, A., 2007, Mechanistic Fine Contents, Master's Thesis University of Saskatchewan, Saskatoon, Saskatchewan.

Asphalt Institute, 1983, Asphalt Cold Mix Recycling, MS-21, Asphalt Institute, Lexington, KY.

Asphalt Institute, 1987, Asphalt Overlays for Highway and Street Rehabilitation, Asphalt Institute, Lexington, KY.

Asphalt Institute, 1987, a Basic Asphalt Emulsion Manual, MS 19, Asphalt Institute, Lexington, KY.

Asphalt Institute, 1991, Thickness Design, MS1, Asphalt Institute, Lexington KY.
Asphalt Institute, 2001, Superpave Mix Design, Asphalt Institute, Lexington, KY.

Portland Cement Association, 1992, Soil-cement Laboratory Handbook, Portland Cement Association, Skokie, Ill.

ASTM D 422, 2003, Standard Test Method for Particle-Size Analysis of Soils, Annual Book of ASTM Standards, American Society for Testing and Materials.

ASTM D 698, 2003, Laboratory Compaction Characteristics of Soil using Standard Effort, Annual Book of ASTM Standards, American Society for Testing and Materials.

ASTM D 1883, 2003, Standard Test Method for CBR (California Bearing Ratio) of Laboratory Compacted Soils, Annual Book of ASTM Standards, American Society for Testing and Materials.

ASTM D 2419, 2003, Standard Test Method for Sand Equivalent Value for Soils and Fine Aggregate, Annual Book of ASTM Standards, American Society for Testing and Materials.

ASTM D 4123, 2003, Standard Test Method for Indirect Tension Test for Resilient Modulus of Bituminous Mixtures, Annual Book of ASTM Standards, American Society for Testing and Materials.

ASTM D 4318, 2003, Standard Test Method Liquid Limit, Plastic Limit, and Plasticity Index of Soils, Annual Book of ASTM Standards, American Society for Testing and Materials.

ASTM D 4718, 2003, Correction of Unit Weight and Water Content for Soils Containing Oversize, Annual Book of ASTM Standards, American Society for Testing and Materials.

ASTM D 5102, 2003, Standard Test Method for Unconfined Compressive Strength of Compacted Soil-Lime Mixtures, Annual Book of ASTM Standards, American Society for Testing and Materials.

Atkins, H. N, 1997, Highway Materials, Soils, and Concretes, Prentice Hall, Upper Saddle River, N.J.

Atterberg, A., 1911, On the Investigation of The Physical Properties of Soils and on the Plasticity of Clays, Int. Mitt. Fur Bodenkunde, I, pp. 10-43.

Aucm, W. E. A., and Fox, L., 1951, Computation of Load Stresses in a Three Layered System, Highway Research Record.

Baker, D., Wourms, O., Berthelot, C., and Gerbrandt, R., 2000, Cold In Place Recycling Using Asphalt Emulsion for Strengthening For Saskatchewan Low Volume Roads, Canadian Technical Asphalt Association Proceedings 45th Annual Conference XLVII, 145-166.

Bandara, N., and Briggs, R. C. , 2004, Non-destructive Testing of Pavement Structures, American Society for Non-destructive Testing.

Barbu, B., McManis, K., and Nataraj, M., 2003, Study of Silts Moisture Susceptibility Using the Tube Suction Test, Transportation Research Board Annual Conference, Washington D.C.

Barksdale, R. D., 1973, Material Characterization and Layered Theory for Use in Fatigue Analysis, Special Report#140, Highway Research Board, Washington D.C.

Baumgarther, E. D., 2005, Triaxial frequency Sweep Characterization for Dense Graded Hot Mix Asphalt Concrete Mix Design, University of Saskatchewan, Saskatoon, Saskatchewan.

Berthelot, C., Courand A., Ritchile H., and Palm B., 2007, City of Regina Field Demonstration of Engineered In-Place Recycling and Structural Rehabilitation of Roads to Develop Sustainable "Green Urban Structural Asset Management", Annual Conference of the Transportation Association of Canada, Saskatoon, Saskatchewan.

Berthelot, C., Crocford B., White S., Gordon S., 1997, Mechanistic Quality Control/Quality Assurance Evaluation of Saskatchewan Specific Pavement Studies-9A Asphalt Mixes, Canadian Technical Asphalt Association Proceedings 42nd Annual Conference XLII. pp 201-227.

Berthelot, C., Gerbrandt, R., and Baker, D., 2000,Full Depth Cold In-Place Recycling Stabilization For Low Volume Road Strengthening: A Case Study On HWY 19-06, 2000 Annual Conference of the Transportation Association of Canada, Edmonton, Alberta.

Berthelot, C., Marjerison, B., and McCaig, J., 2007, Mechanistic Comparison of Cement and Bituminous Stabilized Granular Base Systems. Transportation Research Board CD-ROM, Washington D.C.

Berthelot, C., Raducanu, C., Scullion, T., and Luhr, D., 2005, Investigation of Cement Modification of Granular Base and Subbase Materials using Triaxial Frequency Sweep Characterization, Transportation Research Board, Washington D.C.

Berthelot, C., Tom, S., Ron, G., and Larry, S., 2001,Ground-Penetrating Radar for Cold In-Place Recycled Road Systems, Journal of Transportation Engineering, 127(4), 269-274.

Berthelot, C., Widger, A., and Gehlen, T., 2004, Mechanistic Investigation of Granular Base and Subbase Materials A Saskatchewan Case Study, Annual Conference of the Transportation Association of Canada, Quebec City, Quebec.

Berthelot, C.,1999, Mechanistic Modeling of Saskatchewan Specific Pavement Studies-9A Asphalt Concrete Pavements, Texas A&M, College Station, Texas, USA.

Berthelot, C., 2005, Pavement Structural Design Class Notes, Saskatoon, Saskatchewan.
Berthelot, C., 2006, Mechanistic Pavement Material Design, CE417 Class Notes, Saskatoon, Saskatchewan.

Berthelot, C., David, H. A., and Chad, R. S., 2003, Method for Performing Accelerated Characterization of Viscoelastic Constitutive Behavior of Asphaltic Concrete. Journal of Materials in Civil Engineering, 15(5), 496-505.

Berthelot, C., Podborochynski D., Fair J., Anthony A., and Marjerison B., 2007, Mechanistic-Climatic Characterization of Foamed Asphalt Stabilized Granular Pavements in Saskatchewan, Annual Conference of the Transportation Association of Canada, Saskatoon, Saskatchewan.

British Standard 1377, 1990, Methods of Test of Soils for Civil Engineering Purposes, British Standard Institution, London, UK

Brown, D., 2006, the Future of Asphalt Materials, Magazine of Asphalt Institute, pp. 22-25.

Burmister, D. M., 1943, The Theory of Stresses and Displacements in Layered Systems and Applications to the Design of Airport Runways, Proceedings Highway Research Board, Vol 23, pp. 126-144.

Burmister, D. M., 1945, The Genera Theory of Stresses and Displacements in Layered Systems, Jour.Appl. Phys, Vol 16(No.2, No5.), pp. 89-96, pp.296-302.

C-SHRP, 2002, Pavement Structural Practices across Canada, C-SHRP Technical Brief 23#.

Casagrande, A., 1932, Research on The Atterberg Limits of Soils, Public Roads, Vol. 13, No. 8, pp 121-136.

Chehab, G.R., O.Quinn, E., Kim, Y.R., 2000, Specimen Geometry Study for Direct Tension Test Based on Mechanical Tests and Air Void Variation in Asphalt Concrete Specimens Compacted by Superpave Gyratory Compactor., Transportation Research Record, No. 1723, pp. 125-132

Clyne, T. R., Xinjun Li, Marasteanu, M. O., and Skok, E. L., 2003, Dynamic and Resilient Modulus of Mn/DOT Asphalt Mixtures, MN/RC – 2003-09, Department of Civil Engineering, University of Minnesota, Minneapolis, Minnesota.

Collings, D. C., 2001, Experiences Gained From Ten Years of Pavement Rehabilitation By In Situ Recycling With Cement and Combinations of Cement/Bituminous Stabilizing Agents, 1st International Symposium on Subgrade Stabilization and In situ pavement Recycling, Salamanca, Spain.

Consedine, R. L., 2002, Foamed asphalt base recycling gains momentum in Quebec, Accessed at June 7, 2007, http://rocktoroad.com/index.html.

Craig, R.F., 2004, Craig's Soil Mechanics, 7th ed., Spon Press, London.

Cragg, R., Pell, P.S. ,1971, Dynamic Stiffness of Bituminous Road Materials., Asphalt Paving Technology: Association of Asphalt Paving Technologists-Proceedings of the Technical Sessions, 1971, pp. 126-147

Crockford, W. W., 1997, Rapid Triaxial Testing Approach to Flexible Pavement QC/QA, Accessed at Aug. 2006,http://ourworld.compuserve.com/homepages/tslco/whtznew1.htm

Crockford, W. W., Berthelot, C., Tritt, B., and Sinadinos, C., 2002, Rapid Triaxial Test, Journal of the Association of Asphalt Paving Technologists, Colorado Springs, Colorado, pp 71.

Codutto, Donald P. , 2001, Foundation Design, 2nd ed., Prentice-Hall Inc., New Jersey,US.

MHI, 1981, Design manual, Saskatchewan Ministry of Highways and Infrastructure, Regina, Saskatchewan.

MHI,1981,Surfacing Manual, Saskatchewan Highways and Transportation, Regina, Saskatchewan.

MHI, 1982, Pavement Technology Manual, Saskatchewan Ministry of Highways and Infrastructure, Regina, Saskatchewan.

MHI, 1999, SK 4100 Specification for Asphalt Concrete, Saskatchewan Ministry of Highways and Infrastructure, Regina, Saskatchewan.

MHI, 2000, 3505-Specification for Granular Base Course, Saskatchewan Ministry of Highways and Infrastructure, Regina, Saskatchewan.

Epps, J. A. ,1990, Cold Recycled Bituminous Concrete Using Bituminous Materials. NCHRP Synthesis 160, Transportation Research Board, Washington D. C.

FHWA-LTPP, 2000, LTPP Manual for Falling Weight Deflectometer Measurements Operational Field Guidelines, Federal Highway Administration, Beltsville, Maryland.

FHWA, 1997, User Guidelines for Waste and Byproduct Materials in Pavement Construction, Accessed in June 2007,http://www.fhwa.dot.gov/pavement/pub_details.cfm?id=384.

FHWA, 2006, Bituminous Mixtures Laboratory (BML) Equipment SuperPave Indirect Tensile Test, Accessed at August 5, 2006.
http://www.fhwa.dot.gov/pavement/asphalt/labs/mixtures/idt.cfm

FWHA, Cold-Mix Asphalt Recycling (Material and Mix Design), Accessed at November 19, 2007, http://www.fhwa.dot.gov/pavement/recycling/98042/chpt_14.pdf

G.Vorobieff, and Wilmot, T., 2001, Australian Experience on Subgrade Stabilization and Pavement Recycling, 1st International Symposium on Subgrade Stabilization and Insitu pavement Recycling, Salamanca, Spain.

Guthrie, S., Ellis, P. M., and Tom, S., 2001, Repeatability and Reliability of the Tube Suction Test, Transportation Research Record (1772), pp. 151-157.

Head K.H., 1980, Manual of Soil Laboratory Testing, Volume 1: Soil Classification and Compaction Tests, John Wiley and Sons, Toronto.

Hoffman, M. S., and Thompson, M. R., 1981, Non-destructive testing of pavements field testing program summary, University of Illinois Urbana-Champaign, Urbana-Champaign, Illinois.

Hudson, W. R., G.E., E., W., U., and T., R. K., 1987, Evaluation of Pavement Deflection Measuring Equipment FH 67.1, Austin Res. Engineers, Austin, Texas.

Kenis, W. J. ,1978, Predictive Design Procedures, VESYS User's Manual: An Interim Design Method for Flexible Pavements Using the VESYS Structural Subsystem, FHWA-RD-164, Federal Highways Administration, U.S. Department of Transportation, Washington D.C.

Kowalski, T.E., Starry D.W., 2007, Cold Recycling Using Foamed Bitumen. Annual Conference of the Transportation Association of Canada, Saskatoon, Saskatchewan

Lane, B., and Kazmierowski, T., 2005, Implementation of Cold In-Place Recycling with Expanded Asphalt Technology in Canada, Transportation Research Record (1905), pp. 17-24.

Lay, M. G., 1998, Handbook of Road Technology, Gordon and Breach, Amsterdam, Netherlands.

Little, D. N., 1999, Evaluation of Structural Properties of Lime Stabilized Soils and Aggregates, Texas A&M University, Texas.

Little, D. N., 2000, Evaluation of Structural Properties of Lime Stabilized Soils and Aggregates, Texas A&M University, Texas.

Marjerison, B., 2004, A Study of Aggregate Supply and Usage in Saskatchewan. CE 867 Class Report, University of Saskatchewan, Saskatoon, Saskatchewan.

Marjerision, B., 2005, Conventional Flexible pavement Structural Design Introduction. CE 417 Class Notes, Saskatchewan Ministry of Highways and Infrastructure, Saskatoon, Saskatchewan.

Monismith, C. L., 2004, Evolution of Long-Lasting Asphalt Pavement Design Mythology: A Perspective. International Symposium on Design and Construction of Long Lasting Asphalt Pavements, Alabama, USA.

Muench, S., 2004, Washington DOT Pavement Online Guide, Accessed on July 2006, http://training.ce.washington.edu/WSDOT/Modules/05_mix_design/05-6_body.htm#tmd

NCHRP, 2004, Laboratory Determination of Resilient Modulus for Flexible Pavement Design. Research Result Digest (Number 285).

Newman, K., and Tingle, J. S., 2004, Stabilization of Silty Sand Using Polymer Emulsions, Transportation Research Board Annual Conference CD ROM, Washington, DC.

Nilsson, R. N., Oost, I., and Hopman., P. C. ,1996, Viscoelastic Analysis of Full-Scale Pavements: Validation of VEROAD, Transportation Research Record 1539, pp. 145-168.

O'Flaherty, C. A., 1986, Highways, E. Arnold, London, UK.

Oglesby, C. H., and Hicks, R. G. ,1982, Highway Engineering, Wiley, New York.

Peattie, K. R.,1963, A Fundamental Approach to the Design of Flexible Pavements, International Conference on the Structural Design of Asphalt Pavements, University of Michigan, Ann Arbor, Michigan, pp. 412-440.

Proctor,R.R.,1933, Fundamental Principles of Soil Compaction, Engineering News Record, Vol.111, No.9.

PSI, 2006, MHI Control Section 15-11 Granular Structure Strengthening Pilot Test Section Construction Report, Saskatoon, Saskatchewan.

PSI, 2006, MHI Control Section 15-11 Preliminary Site Investigation and Cement Strengthening Design Report, Saskatoon, Saskatchewan.

Roberts, F. L., Kandhal P.S., Brown E.R., Lee D., Kennedy T. W., 1996, Hot Mix Asphalt Materials, Mixture Design, and Construction, NAPA Educational Foundation, Lanham, Maryland.

Rohde, G. T., and R.E.Smith., 1991, Determining Depth to Apparent Stiff Layer from FWD Data, Texas Transportation Institute, College Station, Texas.

Romanoschi, S. A., Heitzman, M., and Gisi, A. J., 2003, Foamed Asphalt Stabilized Reclaimed Asphalt Pavement, A Promising technology for Mid-western Roads, Proceedings of the 2003 Mid-Continent Transportation Research Symposium, Ames, Iowa.

Saarenketo, T., 2000, Tube Suction Test-Result of Round Robin Test On Unbound Aggregate. Report No. 19/2000, Finnish National Road Administration, Finland.

Saarenketo, T., 2006, Accessed at August 8, 2006, http://www.roadscanners.com/index.html

Safronetz, J. D., 2003, Project Level Highway Management Framework, M.Sc Thesis, Civil and Geological Engineering Department, University of Saskatchewan, Saskatoon, Saskatchewan.

Scullion, T., and Saarenketo, T., 1997, Using Suction and Dielectirc Measurements as Performance Indicators for Aggregate Base Materials, Transportation Research Record (1577), pp. 37-42.

Shell, 1978, Shell Pavement Design Manual : Asphalt Pavements and Overlays for Road Traffic, Shell International Petroleum Company, London, UK.

Shell, 1998, Bisar 3.0 Help Manual.

Shiffman, R. L., 1962, General Analysis of Stresses and Displacements in Layered Elastic Systems,International Conference on The Structural Design of Asphalt Pavements, Ann Arbor, Michigan.pp. 710-721.

Shook, J.F., 1984, Structural Analysis of Asphalt Pavements Using Computers, Transportation Forum, Transportation Association of Canada, Vol. 1 No. 2, pp. 5-13

Skok, E. L., and Finn, F. N., 1963, Theoretical Concept Applied to Asphalt Concrete Pavement Design, International Conference on the Structural Design of Asphalt Pavements, University of Michigan, Ann Arbor, Michigan. pp. 412-440.

Syed, I., Tom, S., and Randolph, R. B., 2000, Tube Suction Test for Evaluating Aggregate Base Materials in Frost- and Moisture-Susceptible Environments. Transportation Research Record (1709), pp. 78-90.

TFHRC, 2002, Granular Base. Accessed in November 2007. http://www.tfhrc.gov/hnr20/recycle/waste/app3.htm

Thomas L., Berthelot, C. F., and Taylor B., 2007, Mechanistic-based ESALS for Urban Pavements, Annual Conference of the Transportation Association of Canada, Saskatoon, Saskatchewan

TRB, 1954, WASHO Road Test-Part 1: Design, Construction, and Testing Procedures, Accessed in December 2007, http://www.trb.org/news/blurb_detail.asp?id=2908

TRB, 2007, Strategic Highway Research Program, Accessed in June 2007, http://www.trb.org/shrp2/

Ullidtz, P., 1987, Pavement Analysis, Elsevier, Amsterdam, Netherlands.

Vaswani, N. K., 1971, Method for Separately Evaluating Structural Performance of Subgrades and Overlying Flexible Pavements. Highway Research Record 362, pp. 48-62.

VicRoads, 1993, Foamed Bitumen Stabilized Pavements, Technology Department Australian, Technical Note No. 8.

Vuong, B. T., Sharp, K. G., Baran, E., and Hohnson, J., 1995, The Influence of Pavement Thickness, Material Quality and Bitumen/Cement Stabilization on The Performance of Recycled Sandstone Bases under Accelerated Loading, ARRB Report WD RI95/001, Victoria, Australia.

Wardle, L. J., 1977, CIRCLY Program, A Computer Program for the Analysis of Multiple Complex Circular Loads on Layered Anisotropic Media, Division of Applied Geomechanics, Commonwealth Scientific and Industrial Research Organization, Victoria, Australia.

Warren, H., and Dieckmann, W.,1963,Numerical Computation of Stresses and Strain in a Multiple-Layer Asphalt Pavement System, Chevron Research Corporation, Richmond, California

Whiffin, A. C., and Lister, N. W.,1963, The Application of Elastic Theory to Flexible Pavements, International Conference on the Structural Design of Asphalt Pavements, University of Michigan, Ann Arbor, Michigan, pp. 499-552.

Whiteoak, D., and Read, J., 2003, The Shell Bitumen Handbook, Thomas Telford, London, UK.

Wilson, E. L., Jones, R. M., and Organization. A. F. S. A. M.,1967, Finite Element Stress Analysis of Axisymmetric Solids with Orthotropic, Temperature Dependent Material Properties, Aerospace Corporation, San Bernardino, California.

Wirtgen, 2004, Cold Recycling Manual, Wirtgen GmbH., Windhagen, Germany.

Witczak, M. W., Kaloush, K., Pellinen, T., and Basyouny, M. E. ,2002, Simple Performance Test for Superpave Mix Design, NCHRP Project 465 Report, Transportation Research Board,Washington D.C.

Witczak, M. W., Kaloush, K. E., and Quintus, H. V., 2002, Pursuit of the Simple Perfromance Test for Asphalt Mixture Rutting, Proceedings of the Association of Asphalt Paving Technologists, Ann Arbor, Michigan, Vol. 71.

Witczak, M. W., Pellinen, T. K., and Basyouny, M. M. E., 2002, Pursuit of the Simple Perfromance Test for Asphalt Concrete Fracture/Cracking. Proceedings of the Association of Asphalt Paving Technologists, Ann Arbor, Michigan.Vol. 71. pp.39-54.

Witczak, M. W., 2005, Simple Performance Test : Summary of Recommended Methods and Database, NCHRP Project Report 547, Transportation Research Board, Washington D.C.

Wright, P. H. ,1996, Highway Engineering, Wiley, New York.

Zienkiewicz, O. C., and Taylor, R. L.,2000, The Finite Element Method, Butterworth-Heinemann, Oxford, Boston.

APPENDIX A. CONVENTIONAL LARORATORY TESTING DATA

Table A.1 Sand Equivalent Characterization of C.S 15-11 Unstabilizd Material

	Sample 1	Sample 2	Sample 3
Sand Height	5.3	5.3	5.4
Clay Height	12.9	13.0	13.0
Sand Equivalent	54.7	56.6	55.8
Mean Sand Equivalent		55.7	

Table A.2 Sand Equivalent Characterization of C.S 15-11 Cement Stabilized Material

	Sample 1	Sample 2	Sample 3
Sand Height	5.1	5.0	5.0
Clay Height	14.0	14.0	14.0
Sand Equivalent	78.4	80.0	80.0
Mean Sand Equivalent		79.5	

Table A.3 Standard Proctor Characterization of C.S. 15-11 *in situ* Granular Material

Sample No.	**1**	**2**	**3**	**4**	**5**	**6**	**7**	**8**
Unit Weight Determination								
Wt. Sample Wet + Mold (g)	6241.9	6344.1	6420.3	6487.1	6499.8	6527.6	6512.8	6462.6
Wt. Mold (g)	4302.0	4302.0	4302.0	4302.0	4302.0	4302.0	4302.0	4302.0
Wt. Sample Wet (g)	1939.9	2042.1	2118.3	2185.1	2197.8	2225.6	2210.8	2160.6
Volume Mold (m^{-3})	0.9373	0.9373	0.9373	0.9373	0.9373	0.9373	0.9373	0.9373
Wet Density (kg/ m^{-3})	2070	2179	2260	2331	2345	2374	2359	2305
Dry Density (kg/ m^{-3})	1996	2080	2137	2182	2193	2189	2170	2099
Moisture Content Determination								
Wt. Sample Wet + Tare (g)	946.5	1995.0	1561.5	2187.4	2200.7	2230.3	2170.3	2040.5
Wt. Sample Dry + Tare (g)	913.5	1905.3	1477.6	2048.4	2058.9	2057.1	1998.2	1860.0
Wt. Water (g)	33.0	89.7	83.9	139.0	141.8	173.2	172.1	180.5
Tare Container (g)	17.0	16.7	16.8	16.8	17.1	16.8	17.2	17.3
Wt. Dry Soil (g)	896.5	1888.6	1460.8	2031.6	2041.8	2040.3	1981.0	1842.7
Moisture Content (%)	3.7	4.7	5.7	6.8	6.9	8.5	8.7	9.8

Table A.4 Peak 96-Hour Confined Soaked Swell of C.S 15-11 Unstabilizd Material

Sample No.	1	2	3
Swell (mm)	0.18	0.10	0.10
Mean Swell (mm)		0.13	
Std Dev (mm)		0.04	
CV (%)		29.8	

Table A.5 Peak 96-Hour Confined Soaked Swell of C.S 15-11 Cement with Asphalt Emulsion Stabilized Material

Sample No.	1	2	3	4	5	6	7	8	9
Swell (mm)	0.00	0.07	0.08	0.04	0.06	0.02	0.06	0.05	0.10
Mean Swell (mm)					0.06				
Std Dev (mm)					0.03				
CV (%)					53.7				

Table A.6 Peak 96-Hour Confined Soaked Swell of C.S 15-11 Cement Stabilized Material

Sample No.	1	2	3
Swell (mm)	0.01	0.04	0.03
Mean Swell (mm)		0.03	
Std Dev (mm)		0.02	
CV (%)		55.6	

Table A.7 CBR Strength Values of C.S 15-11 Unstabilizd Material

Sample No.	1	2	3
CBR Strength	23	23	18
Mean CBR Strength		22	
Std Dev		2.6	
CV (%)		12.1	

Table A.8 CBR Strength Values of C.S 15-11 Cement with Asphalt Emulsion Stabilized Material

Sample No.	1	2	3	4	5	6	7	8	9
CBR Strength	40	135	130	51	53	76	49	38	38
Mean CBR Strength					68				
Std Dev					38.6				
CV (%)					57.0				

Table A.9 CBR Strength Values of C.S 15-11 Cement Stabilized Material

Sample No.	1	2	3
CBR Strength	218	274	306
Mean CBR Strength		266	
Std Dev		44.9	
CV (%)		16.9	

Table A.10 Indirect Tensile Strength of Cement Stabilized Samples on C.S. 15-11 (100 mm Sample, Moisture Cured Condition)

Sample No.	Peak Load (kN)	Sample Thickness (mm)	Tensile Strength (kPa)
1	3.23	62.33	325
2	3.52	62.77	351
3	3.66	62.78	365
Mean Value	3.47	62.63	347
Std Dev	0.22	0.26	21
CV %	6.3	0.4	5.9

Table A.11 Indirect Tensile Strength of Cement Stabilized Samples on C.S. 15-11 (100 mm Sample, Soaked Condition)

Sample No.	Peak Load (kN)	Sample Thickness (mm)	Soaked Tensile Strength (kPa)	Retained Strength Ratio (%)
1	1.92	62.96	191	59
2	1.83	62.81	183	52
3	1.92	63.05	191	52
Mean Value	1.89	62.94	188	54
Std Dev	0.1	0.12	5	4
CV %	2.8	0.2	2.6	7.2

Table A.12 Indirect Tensile Strength of Cement with Asphalt Emulsion Stabilized Samples on C.S. 15-11 (100 mm Sample, Moisture Cured Condition)

Sample No.	Peak Load (kN)	Sample Thickness (mm)	Tensile Strength (kPa)
1	2.32	64.67	225
2	2.03	64.59	197
3	1.70	64.68	165
4	1.85	65.40	177
5	1.67	64.74	162
6	1.62	64.86	157
7	2.13	64.93	206
8	1.73	64.89	167
9	2.08	64.46	202
Mean Value	1.90	64.80	184
Std Dev	0.25	0.27	24
CV %	12.9	0.4	13.0

Table A.13 Indirect Tensile Strength of Cement with Asphalt Emulsion Stabilized Samples on C.S. 15-11 (100 mm Sample, Soaked Condition)

Sample No.	Peak Load (kN)	Sample Thickness (mm)	Soaked Tensile Strength (kPa)	Retained Strength Ratio (%)
1	0.55	65.50	53	23
2	0.55	66.08	52	27
3	0.55	64.72	53	32
4	0.46	64.73	45	25
5	0.53	64.58	51	32
6	0.47	64.77	46	29
7	0.40	65.39	38	19
8	0.52	65.20	50	30
9	0.53	64.68	51	25
Mean Value	0.51	65.07	49	27
Std Dev	0.05	0.51	5	4
CV %	10.3	0.8	10.2	14.8

Table A.14 Indirect Tensile Strength of Unstabilized Samples on C.S. 15-11 (150 mm Sample, Moisture Cured Condition)

Sample No.	Peak Load (kN)	Sample Thickness (mm)	Tensile Strength (kPa)
1	1.50	149.0	43
2	2.26	148.9	64
Mean Value	1.88	148.9	54
Std Dev	0.53	0.1	15
CV %	28.4	0.1	28.5

Table A.15 Indirect Tensile Strength of Unstabilized Samples on C.S. 15-11 (150 mm Sample, Soaked Condition)

Sample No.	Peak Load (kN)	Sample Thickness (mm)	Tensile Strength (kPa)	Retained Strength Ratio (%)
1	0.38	150.0	11	26
2	0.78	150.0	22	34
Mean Value	0.58	150.0	16	30
Std Dev	0.29	0.0	8	6
CV %	49.6	0.0	49.6	21

Table A.16 Indirect Tensile Strength of Cement Stabilized Samples on C.S. 15-11 (150 mm Sample, Moisture Cured Condition)

Sample No.	Peak Load (kN)	Sample Thickness (mm)	Tensile Strength (kPa)
1	14.09	148.9	402
2	15.10	149.0	430
Mean Value	14.60	148.9	416
Std Dev	0.71	0.1	20
CV %	4.9	0.1	4.8

Table A.17 Indirect Tensile Strength of Cement Stabilized Samples on C.S. 15-11 (150 mm Sample, Soaked Condition)

Sample No.	Peak Load (kN)	Sample Thickness (mm)	Tensile Strength (kPa)	Retained Strength Ratio (%)
1	8.48	150.6	239	59
2	8.97	150.1	254	59
Mean Value	8.72	150.3	246	59
Std Dev	0.35	0.3	10	0
CV %	4.0	0.2	4.2	0

Table A.18 Indirect Tensile Strength of Cement and Asphalt Emulsion Stabilized Samples on C.S. 15-11 (150 mm Sample, Moisture Cured Condition)

Sample No.	Peak Load (kN)	Sample Thickness (mm)	Tensile Strength (kPa)
1	2.84	150.0	80
2	3.25	151.6	91
3	2.63	151.2	74
Mean Value	2.91	150.9	82
Std Dev	0.31	0.8	9
CV %	10.8	0.5	10.5

Table A.19 Indirect Tensile Strength of Cement and Asphalt Emulsion Stabilized Samples on C.S. 15-11 (150 mm Sample, Soaked Condition)

Sample No.	Peak Load (kN)	Sample Thickness (mm)	Tensile Strength (kPa)	Retained Strength Ratio (%)
1	1.64	150.0	46	58
2	0.99	151.6	28	31
3	0.79	151.1	26	35
Mean Value	1.14	150.9	33	41
Std Dev	0.45	0.8	11	14
CV %	39.2	0.5	33.8	35

Table A.20 Capillary Moisture Rise and Surface Conductivity Results of Unstabilized Samples on C.S. 15-11

Sample No.	Dry Weight (g)	Sutured Weight (g)	Water Intake by Sample Weight (%)	Average Surface Conductivity (uS/cm)
1	5616.2	5858.5	4.3	86
2	5589.5	5823.0	4.2	67
Mean Value	5602.9	5840.8	4.3	77
Std Dev	18.9	25.1	0.1	13
CV %	0.3	0.4	1.7	17.6

Table A.21 Capillary Moisture Rise and Surface Conductivity Results of Cement and Emulsion Asphalt Stabilized Samples on C.S. 15-11

Sample No.	Dry Weight (g)	Sutured Weight (g)	Water Intake by Sample Weight (%)	Average Surface Conductivity (uS/cm)
1	5655.6	6001.0	6.1	55
2	5663.1	6002.4	6.0	72
3	5643.9	5973.9	5.8	76
4	5639.9	5971.5	5.9	70
5	5622.4	5984.7	6.4	74
6	5619.4	5961.6	6.1	66
Mean Value	5640.7	5982.5	6.1	69
Std Dev	15.9	15.1	0.2	7
CV %	0.3	0.3	3.3	10.3

Table A.22 Capillary Moisture Rise and Surface Conductivity Results of Cement Stabilized Samples on C.S. 15-11

Sample No.	Dry Weight (g)	Sutured Weight (g)	Water Intake by Sample Weight (%)	Average Surface Conductivity (uS/cm)
1	5700.5	6007.6	5.4	9
2	5710.3	5997.5	5.0	4
Mean Value	5705.4	6002.6	5.2	7
Std Dev	6.9	7.1	0.3	3
CV %	0.1	0.1	4.9	48.5

Table A.23 Unconfined Compressive Strength of Unstabilized Samples on C.S. 15-11 (Moisture Cured, 150 mm Gyratory Compacted Sample)

Sample No.	Peak Load (kN)	Compressive Strength (kPa)
1	5	283
2	7	403
Mean Value	4	343
Std Dev	4	85
CV %	106.1	24.7

Table A.24 Unconfined Compressive Strength of Cement and Asphalt Emulsion Stabilized Samples on C.S. 15-11 (Moisture Cured, 150 mm Gyratory Compacted Sample)

Sample No.	Peak Load (kN)	Compressive Strength (kPa)
1	11	638
2	13	732
3	12	675
4	12	667
5	11	629
6	12	692
Mean Value	12	672
Std Dev	1	38
CV %	5.6	5.6

Table A.25 Unconfined Compressive Strength of Cement Stabilized Samples on C.S. 15-11 (Moisture Cured, 150 mm Gyratory Compacted Sample)

Sample No.	Peak Load (kN)	Compressive Strength (kPa)
1	65	3693
2	67	3796
Mean Value	66	3745
Std Dev	1	73
CV %	2.1	1.9

Table A.26 Unconfined Compressive Strength of Unstabilized Samples on C.S. 15-11 (Soaked Condition, 150 mm Gyratory Compacted Sample)

Sample No.	Peak Load (kN)	Compressive Strength (kPa)
1	0.8	45
2	1.0	55
Mean Value	0.9	50
Std Dev	0.1	7
CV %	14.1	14.1

Table A.27 Unconfined Compressive Strength of Cement and Asphalt Emulsion Stabilized Samples on C.S. 15-11 (Soaked Condition, 150 mm Gyratory Compacted Sample)

Sample No.	Peak Load (kN)	Compressive Strength (kPa)
1	3	196
2	4	214
3	4	254
4	4	219
5	7	375
6	6	360
Mean Value	5	270
Std Dev	1	78
CV %	29.0	29.0

Table A.28 Unconfined Compressive Strength of Cement Stabilized Samples on C.S. 15-11 (Soaked Condition, 150 mm Gyratory Compacted Sample)

Sample No.	Peak Load (kN)	Compressive Strength (kPa)
1	35	2009
2	41	2334
Mean Value	38	2171
Std Dev	4	230
CV %	10.6	10.6

APPENDIX B. MECHANISTIC RAPID TRIAXIAL FREQUENCY SWEEP TESTING

Table B.1 Triaxial Frequency Sweep Test Results of Cement Stabilized Granular Materials applied on C.S. 15-11 (sample 1 and Sample 2)

Mix Type	Sample No.	Axial Traction (kPa)	Radial Traction (kPa)	Deviatoric Stress σ_D (kPa)	Freq. (Hz)	Dynamic Modulus (MPa)	Phase Angle (°)	RAMS	RRMS	Poisson's Ratio
cement	s1	450	250	200	10.0	1712	9.41	129.7	4.8	0.04
cement	s1	450	250	200	5.0	1700	5.71	122.2	5.9	0.05
cement	s1	450	250	200	1.0	1615	4.35	122.5	8.0	0.07
cement	s1	450	250	200	0.5	1631	3.95	120.9	8.8	0.07
cement	s1	650	250	400	10.0	1612	9.68	241.3	14.1	0.06
cement	s1	650	250	400	5.0	1694	6.11	233.8	13.8	0.06
cement	s1	650	250	400	1.0	1630	4.83	243.8	19.5	0.08
cement	s1	650	250	400	0.5	1653	4.74	239.9	19.0	0.08
cement	s1	650	100	550	10.0	1333	16.13	400.7	21.6	0.05
cement	s1	650	100	550	5.0	1581	6.13	343.4	29.7	0.09
cement	s1	650	100	550	1.0	1594	4.87	344.3	34.9	0.10
cement	s1	650	100	550	0.5	1612	4.81	339.8	36.7	0.11
cement	s1	450	250	200	10.0	1036	9.01	289.8	6.8	0.02
cement	s1	450	250	200	5.0	961	5.72	311.1	13.6	0.04
cement	s1	450	250	200	1.0	N/A	N/A	N/A	N/A	N/A
cement	s1	450	250	200	0.5	N/A	N/A	N/A	N/A	N/A
cement	s2	450	250	200	10.0	2067	10.91	94.3	7.3	0.08
cement	s2	450	250	200	5.0	2026	4.53	97.6	8.8	0.09
cement	s2	450	250	200	1.0	1696	5.89	116.4	11.6	0.10
cement	s2	450	250	200	0.5	1725	5.75	113.9	12.8	0.11
cement	s2	650	250	400	10.0	2288	11.68	169.6	13.7	0.08
cement	s2	650	250	400	5.0	2543	6.93	155.6	17.8	0.11
cement	s2	650	250	400	1.0	2341	5.72	170	17.5	0.10
cement	s2	650	250	400	0.5	2089	5.76	190.2	24.2	0.13
cement	s2	650	100	550	10.0	1678	18.36	317.9	18.9	0.06
cement	s2	650	100	550	5.0	2104	7.9	258	28.7	0.11
cement	s2	650	100	550	1.0	2076	5.99	264	31.8	0.12
cement	s2	650	100	550	0.5	2061	6.34	265.6	30.6	0.12
cement	s2	450	250	200	10.0	2178	9.79	137.3	8.5	0.06
cement	s2	450	250	200	5.0	2065	7.24	144.5	12.4	0.09
cement	s2	450	250	200	1.0	N/A	N/A	N/A	N/A	N/A
cement	s2	450	250	200	0.5	N/A	N/A	N/A	N/A	N/A

Table B.2Triaxial Frequency Sweep Test Results of Cement Stabilized Granular Materials applied on C.S. 15-11 (Sample 3 and Sample 4)

Mix Type	Sample No.	Axial Traction (kPa)	Radial Traction (kPa)	Deviatoric Stress σ_D (kPa)	Freq. (Hz)	Dynamic Modulus (MPa)	Phase Angle (°)	RAMS	RRMS	Poisson's Ratio
cement	s3	450	250	200	10.0	2132	6.25	91.9	8.8	0.10
cement	s3	450	250	200	5.0	1986	4.97	99.6	13.5	0.14
cement	s3	450	250	200	1.0	1899	4.79	104.2	13.0	0.12
cement	s3	450	250	200	0.5	1927	3.98	102.1	12.5	0.12
cement	s3	650	250	400	10.0	2131	7.4	181.9	24.2	0.13
cement	s3	650	250	400	5.0	1921	6.09	206	26.0	0.13
cement	s3	650	250	400	1.0	1779	5.28	223.7	30.9	0.14
cement	s3	650	250	400	0.5	1735	5.57	228.9	33.5	0.15
cement	s3	650	100	550	10.0	1832	7.37	291.1	45.4	0.16
cement	s3	650	100	550	5.0	1741	6.91	311.3	44.5	0.14
cement	s3	650	100	550	1.0	1720	6.1	319.1	43.9	0.14
cement	s3	650	100	550	0.5	1710	5.76	320.2	52.9	0.17
cement	s3	450	250	200	10.0	1497	8.06	199.5	24.8	0.12
cement	s3	450	250	200	5.0	1301	6.99	229.4	24.8	0.11
cement	s3	450	250	200	1.0	1073	173.93	276.4	29.1	0.11
cement	s3	450	250	200	0.5	1016	174.27	291.7	33.8	0.12
cement	s4	450	250	200	10.0	1784	6.5	116.7	11.0	0.09
cement	s4	450	250	200	5.0	1776	4.95	117.7	12.4	0.11
cement	s4	450	250	200	1.0	1712	4.49	115.5	12.2	0.11
cement	s4	450	250	200	0.5	1738	4.62	113.3	13.2	0.12
cement	s4	650	250	400	10.0	1769	7.61	219.4	27.3	0.12
cement	s4	650	250	400	5.0	1754	6.44	225.5	29.2	0.13
cement	s4	650	250	400	1.0	1756	5.54	226.9	27.3	0.12
cement	s4	650	250	400	0.5	1759	5.61	226	28.9	0.13
cement	s4	650	100	550	10.0	1748	8.46	305.9	45.7	0.15
cement	s4	650	100	550	5.0	1732	6.93	313.2	39.2	0.13
cement	s4	650	100	550	1.0	1737	6.01	315	40.6	0.13
cement	s4	650	100	550	0.5	1736	5.74	315.6	44.3	0.14
cement	s4	450	250	200	10.0	1020	8.6	293.3	22.4	0.08
cement	s4	450	250	200	5.0	1000	7.25	297.7	24.1	0.08
cement	s4	450	250	200	1.0	991	173.58	299.8	23.9	0.08
cement	s4	450	250	200	0.5	988	174.25	299.3	27.1	0.09

Table B.3Triaxial Frequency Sweep Test Results of Cement Stabilized Granular Materials applied on C.S. 15-11 (Sample 5 and Sample 6)

Mix Type	Sample No.	Axial Traction (kPa)	Radial Traction (kPa)	Deviatoric Stress σ_D (kPa)	Freq. (Hz)	Dynamic Modulus (MPa)	Phase Angle (°)	RAMS	RRMS	Poisson's Ratio
cement	s5	450	250	200	10.0	1370	7.35	142.4	11.5	0.08
cement	s5	450	250	200	5.0	1395	6.04	141.6	11.1	0.08
cement	s5	450	250	200	1.0	1433	4.78	137.5	14.4	0.10
cement	s5	450	250	200	0.5	1434	5.21	137	14.6	0.11
cement	s5	650	250	400	10.0	1443	8.61	269	35.9	0.13
cement	s5	650	250	400	5.0	1468	6.97	268.9	30.8	0.11
cement	s5	650	250	400	1.0	1457	5.91	273.2	34.8	0.13
cement	s5	650	250	400	0.5	1479	5.83	268.4	36.4	0.14
cement	s5	650	100	550	10.0	1481	9	359.6	49.2	0.14
cement	s5	650	100	550	5.0	1470	7.43	367.6	50.4	0.14
cement	s5	650	100	550	1.0	1458	6.49	376.1	54.0	0.14
cement	s5	650	100	550	0.5	1463	6.49	373.7	58.7	0.16
cement	s5	450	250	200	10.0	683	9.31	438.1	43.2	0.10
cement	s5	450	250	200	5.0	703	7.81	423.8	48.2	0.11
cement	s5	450	250	200	1.0	689	173.44	430.6	51.4	0.12
cement	s5	450	250	200	0.5	687	173.63	430.5	47.6	0.11
cement	s6	450	250	200	10.0	1284	7.72	152.3	4.2	0.03
cement	s6	450	250	200	5.0	1244	5.75	157.7	9.9	0.06
cement	s6	450	250	200	1.0	1246	4.11	158.5	11.5	0.07
cement	s6	450	250	200	0.5	1268	3.73	154.6	9.7	0.06
cement	s6	650	250	400	10.0	1623	7.97	239.1	16.5	0.07
cement	s6	650	250	400	5.0	1580	5.94	250.5	14.6	0.06
cement	s6	650	250	400	1.0	1665	6.26	239.3	20.1	0.08
cement	s6	650	250	400	0.5	1680	6.25	236.5	21.3	0.09
cement	s6	650	100	550	10.0	1678	10.73	318.1	36.3	0.11
cement	s6	650	100	550	5.0	1600	9.04	338.8	39.5	0.12
cement	s6	650	100	550	1.0	1582	8.1	346	46.1	0.13
cement	s6	650	100	550	0.5	1591	8.01	343.8	41.4	0.12
cement	s6	450	250	200	10.0	1356	11.27	220.3	20.7	0.09
cement	s6	450	250	200	5.0	1018	169.77	293	22.9	0.08
cement	s6	450	250	200	1.0	799	170.61	371.1	41.0	0.11
cement	s6	450	250	200	0.5	802	170.72	369.5	42.0	0.11

Table B.4 Triaxial Frequency Sweep Test Results of Cement and Asphalt Emulsion Stabilized Granular Materials applied on C.S. 15-11 (Sample 1 and Sample 2)

Mix Type	Sample No.	Axial Traction (kPa)	Radial Traction (kPa)	Deviatoric Stress σ_D (kPa)	Freq. (Hz)	Dynamic Modulus (MPa)	Phase Angle (°)	RAMS	RRMS	Poisson's Ratio
CE	s1	450	250	200	10.0	846	11.17	232	58.3	0.25
CE	s1	450	250	200	5.0	797	10.27	247.3	59.6	0.24
CE	s1	450	250	200	1.0	733	9.78	268.8	79.9	0.30
CE	s1	450	250	200	0.5	711	9.31	276.4	89.4	0.32
CE	s1	650	250	400	10.0	874	12.37	444.7	168.4	0.38
CE	s1	650	250	400	5.0	794	11.29	497.1	196.3	0.39
CE	s1	650	250	400	1.0	708	10.79	560.6	253.0	0.45
CE	s1	650	250	400	0.5	665	10.97	597.9	297.9	0.50
CE	s1	650	100	550	10.0	874	12.37	444.7	168.4	0.38
CE	s1	650	100	550	5.0	794	11.29	497.1	196.3	0.39
CE	s1	650	100	550	1.0	708	10.79	560.6	253.0	0.45
CE	s1	650	100	550	0.5	665	10.97	597.9	297.9	0.50
CE	s1	450	250	200	10.0	N/A	N/A	N/A	N/A	N/A
CE	s1	450	250	200	5.0	N/A	N/A	N/A	N/A	N/A
CE	s1	450	250	200	1.0	N/A	N/A	N/A	N/A	N/A
CE	s1	450	250	200	0.5	N/A	N/A	N/A	N/A	N/A
CE	s2	450	250	200	10.0	1090	10.71	180.5	46.2	0.26
CE	s2	450	250	200	5.0	1074	8.8	184.7	49.8	0.27
CE	s2	450	250	200	1.0	1039	8.12	190.9	45.6	0.24
CE	s2	450	250	200	0.5	1022	7.77	192.8	48.6	0.25
CE	s2	650	250	400	10.0	1033	11.75	376.4	115.7	0.31
CE	s2	650	250	400	5.0	1025	10.33	385.9	123.9	0.32
CE	s2	650	250	400	1.0	985	9.42	403.9	131.2	0.32
CE	s2	650	250	400	0.5	964	9.2	411.4	132.9	0.32
CE	s2	650	100	550	10.0	761	13.31	701.6	324.5	0.46
CE	s2	650	100	550	5.0	750	12	721.6	362.3	0.50
CE	s2	650	100	550	1.0	712	11.19	770.6	406.4	0.53
CE	s2	650	100	550	0.5	693	11.03	789.7	434.5	0.55
CE	s2	450	250	200	10.0	743	12.16	402.9	149.2	0.37
CE	s2	450	250	200	5.0	N/A	N/A	N/A	N/A	N/A
CE	s2	450	250	200	1.0	N/A	N/A	N/A	N/A	N/A
CE	s2	450	250	200	0.5	N/A	N/A	N/A	N/A	N/A

Table B.5 Triaxial Frequency Sweep Test Results of Cement and Asphalt Emulsion Stabilized Granular Materials applied on C.S. 15-11 (Sample 3 and Sample 4)

Mix Type	Sample No.	Axial Traction (kPa)	Radial Traction (kPa)	Deviatoric Stress σ_D (kPa)	Freq. (Hz)	Dynamic Modulus (MPa)	Phase Angle (°)	RAMS	RRMS	Poisson's Ratio
CE	s3	450	250	200	10.0	1183	10.3	166.5	20.3	0.12
CE	s3	450	250	200	5.0	1188	8.81	166.5	18.4	0.11
CE	s3	450	250	200	1.0	1139	8.32	173	21.4	0.12
CE	s3	450	250	200	0.5	1141	7.99	172.4	22.3	0.13
CE	s3	650	250	400	10.0	1166	11.8	333.5	60.7	0.18
CE	s3	650	250	400	5.0	1146	10.52	344.9	61.7	0.18
CE	s3	650	250	400	1.0	1093	9.75	364	63.3	0.17
CE	s3	650	250	400	0.5	1074	9.48	369.9	63.5	0.17
CE	s3	650	100	550	10.0	888	13.86	601.5	150.6	0.25
CE	s3	650	100	550	5.0	863	12.28	629.4	171.5	0.27
CE	s3	650	100	550	1.0	814	11.55	670.3	204.2	0.30
CE	s3	650	100	550	0.5	786	11.47	696.2	224.3	0.32
CE	s3	450	250	200	10.0	910	12.46	328.1	73.5	0.22
CE	s3	450	250	200	5.0	N/A	N/A	N/A	N/A	N/A
CE	s3	450	250	200	1.0	N/A	N/A	N/A	N/A	N/A
CE	s3	450	250	200	0.5	N/A	N/A	N/A	N/A	N/A
CE	s4	450	250	200	10.0	1165	10.35	167.8	19.7	0.12
CE	s4	450	250	200	5.0	1171	9.36	168.1	19.3	0.11
CE	s4	450	250	200	1.0	1135	8.25	173.2	23.6	0.14
CE	s4	450	250	200	0.5	1127	7.76	174	24.0	0.14
CE	s4	650	250	400	10.0	1154	11.87	336.2	63.3	0.19
CE	s4	650	250	400	5.0	1142	10.26	345.1	61.8	0.18
CE	s4	650	250	400	1.0	1097	9.72	362.5	69.0	0.19
CE	s4	650	250	400	0.5	1076	9.19	368.9	74.4	0.20
CE	s4	650	100	550	10.0	870	13.93	614.8	171.4	0.28
CE	s4	650	100	550	5.0	863	12.2	627.1	192.9	0.31
CE	s4	650	100	550	1.0	810	11.39	674.8	233.1	0.35
CE	s4	650	100	550	0.5	786	11.29	694.9	254.6	0.37
CE	s4	450	250	200	10.0	902	12.45	329.9	70.8	0.21
CE	s4	450	250	200	5.0	889	168.77	335	78.0	0.23
CE	s4	450	250	200	1.0	N/A	N/A	N/A	N/A	N/A
CE	s4	450	250	200	0.5	N/A	N/A	N/A	N/A	N/A

Table B.6 Triaxial Frequency Sweep Test Results of Cement and Asphalt Emulsion Stabilized Granular Materials applied on C.S. 15-11 (Sample 5 and Sample 6)

Mix Type	Sample No.	Axial Traction (kPa)	Radial Traction (kPa)	Deviatoric Stress σ_D (kPa)	Freq. (Hz)	Dynamic Modulus (MPa)	Phase Angle (°)	RAMS	RRMS	Poisson's Ratio
CE	s5	450	250	200	10.0	1071	10.76	183.1	26.4	0.14
CE	s5	450	250	200	5.0	1071	8.97	184.7	22.7	0.12
CE	s5	450	250	200	1.0	1047	7.71	187.8	26.0	0.14
CE	s5	450	250	200	0.5	1033	7.86	190	30.5	0.16
CE	s5	650	250	400	10.0	1051	11.43	370.6	77.1	0.21
CE	s5	650	250	400	5.0	1042	10.32	380.4	83.8	0.22
CE	s5	650	250	400	1.0	1010	9.33	394.8	90.9	0.23
CE	s5	650	250	400	0.5	991	9.14	400.8	95.6	0.24
CE	s5	650	100	550	10.0	796	13.42	670.5	225.5	0.34
CE	s5	650	100	550	5.0	785	12.09	689.6	252.2	0.37
CE	s5	650	100	550	1.0	745	11.09	735.2	295.0	0.40
CE	s5	650	100	550	0.5	731	11.02	747	315.8	0.42
CE	s5	450	250	200	10.0	796	13.42	670.5	225.5	0.34
CE	s5	450	250	200	5.0	785	12.09	689.6	252.2	0.37
CE	s5	450	250	200	1.0	N/A	N/A	N/A	N/A	N/A
CE	s5	450	250	200	0.5	N/A	N/A	N/A	N/A	N/A
CE	s6	450	250	200	10.0	1160	10.08	169.3	26.6	0.16
CE	s6	450	250	200	5.0	1124	8.86	174.8	25.5	0.15
CE	s6	450	250	200	1.0	1078	7.45	182.1	32.7	0.18
CE	s6	450	250	200	0.5	1052	7.88	186.2	28.9	0.16
CE	s6	650	250	400	10.0	1115	11.09	348.8	66.7	0.19
CE	s6	650	250	400	5.0	1065	10.06	371.4	68.7	0.18
CE	s6	650	250	400	1.0	1011	9.08	392.4	74.0	0.19
CE	s6	650	250	400	0.5	988	8.84	400.9	84.2	0.21
CE	s6	650	100	550	10.0	793	13.06	672.7	198.7	0.30
CE	s6	650	100	550	5.0	781	11.99	693.8	222.4	0.32
CE	s6	650	100	550	1.0	732	10.98	746.7	269.0	0.36
CE	s6	650	100	550	0.5	707	11.01	773.6	301.6	0.39
CE	s6	450	250	200	10.0	789	12.09	377.2	86.4	0.23
CE	s6	450	250	200	5.0	N/A	N/A	N/A	N/A	N/A
CE	s6	450	250	200	1.0	N/A	N/A	N/A	N/A	N/A
CE	s6	450	250	200	0.5	N/A	N/A	N/A	N/A	N/A

Table B.7 Triaxial Frequency Sweep Test Results of Unstabilized Granular Materials applied on C.S. 15-11 (Sample 1 and Sample 2)

Mix Type	Sample No.	Axial Traction (kPa)	Radial Traction (kPa)	Deviatoric Stress σ_D (kPa)	Freq. (Hz)	Dynamic Modulus (MPa)	Phase Angle (°)	RAMS	RRMS	Poisson's Ratio
Unstabilized	s1	450	250	200	10.0	578	11.17	329.84	146.1	0.44
Unstabilized	s1	450	250	200	5.0	576	10.27	333.68	151.9	0.46
Unstabilized	s1	450	250	200	1.0	576	9.78	333.04	151.4	0.45
Unstabilized	s1	450	250	200	0.5	570	9.31	333.28	152.2	0.46
Unstabilized	s2	450	250	200	10.0	475	10.66	412.3	169.9	0.41
Unstabilized	s2	450	250	200	5.0	473	8.58	417.1	176.6	0.42
Unstabilized	s2	450	250	200	1.0	473	7.31	416.3	176.1	0.42
Unstabilized	s2	450	250	200	0.5	471	6.76	416.6	177.0	0.42

APPENDIX C. PAVEMENT RESPONSE CALCULATION RESULTS

Table C.1 Max Shear Stress in Cement and Emulsion Stabilized Base on the C.S. 15-11

Depth from Surface (m)	Absolute Values of Maximum Shear Stress (Kpa)	
	Tire Edge	Tire Centre
0.04	240	148
0.08	206	177
0.12	178	178
0.16	148	185
0.19	157	213
Maximum Value (Kpa)	240	213

Maximum shear stress at a point equals to half of the differences of principal stresses at the same point.

Table C. 2 Max Shear Stress in Unstabilized Base on the C.S. 15-11

Depth from Surface (m)	Absolute Values of Maximum Shear Stress (Kpa)	
	Tire Outside Edge	Tire Centre
0.04	177	108
0.08	172	154
0.12	155	160
0.16	133	159
0.19	123	167
Maximum Value (Kpa)	177	167

Maximum shear stress at a point equals to half of the differences of principal stresses at the same point.

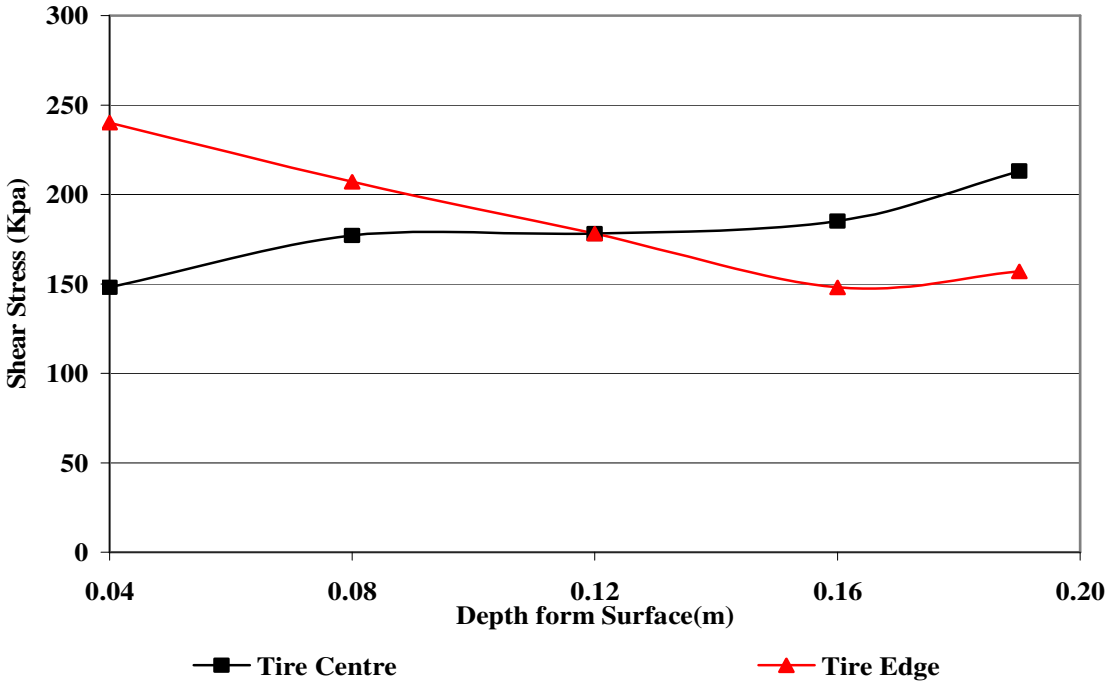

Figure C.1 Max Shear Stress in Cement and Emulsion Stabilized Base on the C.S. 15-11

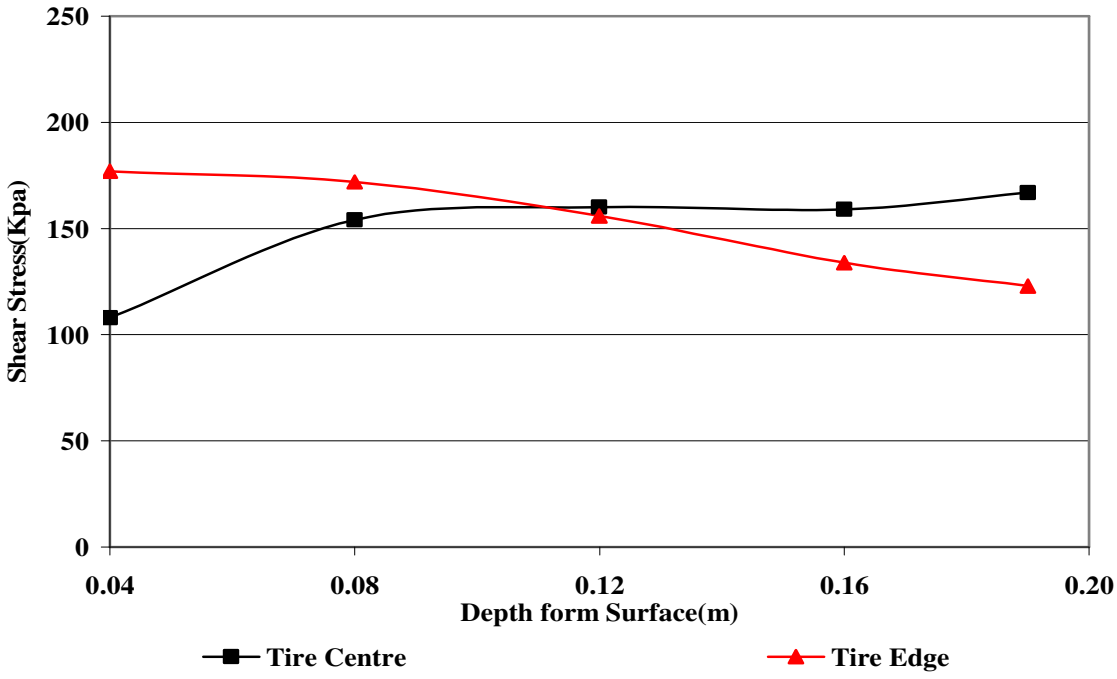

Figure C.2 Max Shear Stress in Unstabilized Base on the C.S. 15-11